Exploring the sustainable production of biobased building blocks for chemically recyclable aromatic polymers

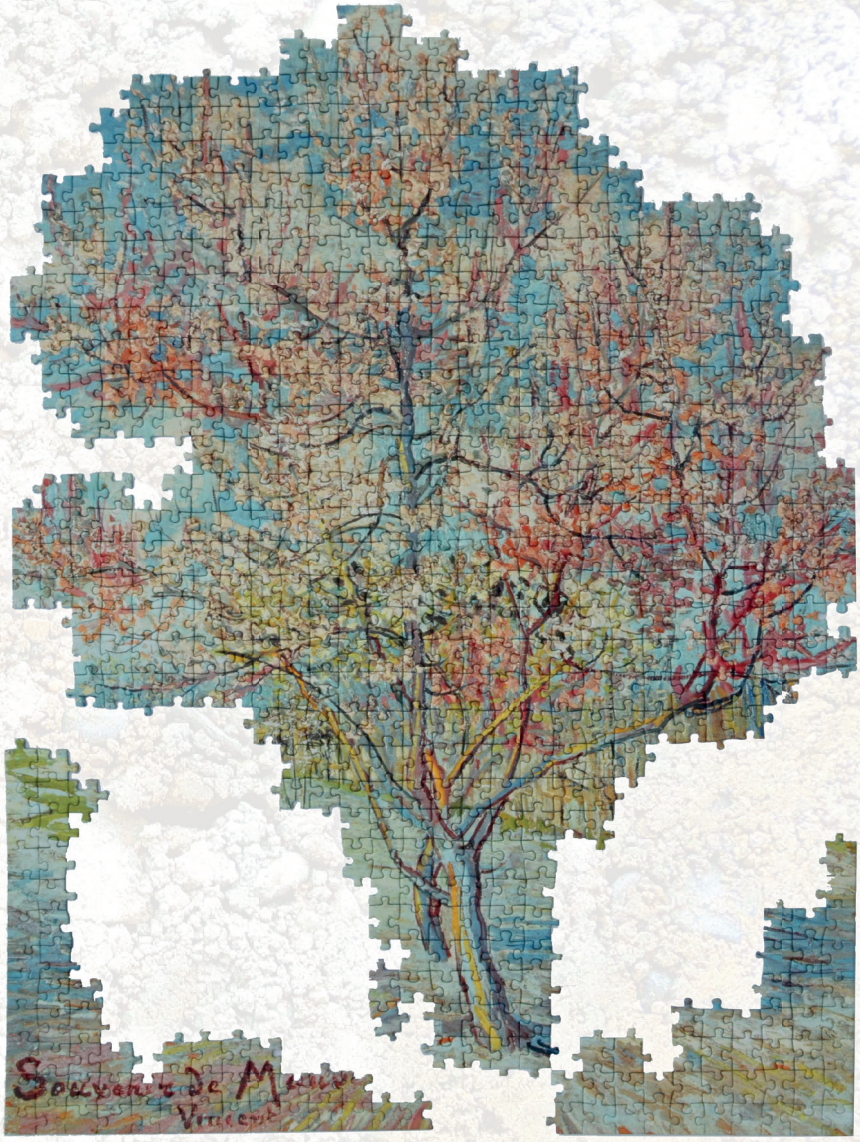

Jack van Schijndel

Exploring the sustainable production of biobased building blocks for chemically recyclable aromatic polymers

Proefschrift

ter verkrijging van de graad van doctor aan de Technische Universiteit Eindhoven, op gezag van de rector magnificus prof.dr.ir. F.P.T. Baaijens, voor een commissie aangewezen door het College voor Promoties, in het openbaar te verdedigen op woensdag 1 april 2020 om 16:00 uur

door

Jacobus Adam Maria van Schijndel

geboren te Terheijden

Dit proefschrift is goedgekeurd door de promotoren en de samenstelling van de promotiecommissie is als volgt:

voorzitter:	prof.dr. F. Gallucci
1e promotor:	prof.dr. J. Meuldijk
2e promotor:	dr. T. Noël
leden:	prof.dr. C.E. Koning (RUG)
	prof.dr. J.H. Bitter (WUR)
	prof.dr.ir. A.R.A. Palmans
	prof.dr.ir. M. van Sint Annaland
adviseur:	dr.ir. B.A.J. Noordover (Allnex)

Het onderzoek of ontwerp dat in dit proefschrift wordt beschreven is uitgevoerd in overeenstemming met de TU/e Gedragscode Wetenschapsbeoefening.

...The paths of research rarely lead in straight forward fashion from starting point to the desired goal. Although intention predisposes the route, chance or occurrences along the way often enforce a change of course.

Georg Wittig
Two Organic Chemists Share Nobel Prize
(Chem. Eng. News, **1979**, 57, 6–7)

Printed by Proefschriftmaken.nl

© Jack van Schijndel, 2020

Cover design by Enny van Schijndel

Jack van Schijndel

Exploring the sustainable production of biobased building blocks for chemically recyclable aromatic polymers, Eindhoven University of Technology, 2020

This research has received funding from Netherlands Organization for Scientific Research (NWO) (grant 023.007.020 awarded to Jack van Schijndel).



Table of contents

Glossary **7**

Summary **9**

Samenvatting voor geïnteresseerden **11**

1 Introduction **13**

1.1 A toolkit in Green Chemistry 14
1.2 Safer solvents 16
1.3 Use of renewable feedstocks 17
1.4 Design for degradation 21
1.5 Aim and scope of this thesis 22
1.6 Outline of this thesis 23
1.7 References 25

2 A global kinetic model of the Knoevenagel-Doebner reaction applied to the synthesis of sinapinic acid **29**

2.1 Introduction 31
2.2 Results and discussion 32
2.3 Conclusions 38
2.4 Experimental section 39
2.5 References 41

3 The Green Knoevenagel condensation: solvent-free condensation of benzaldehydes **43**

3.1 Introduction 45
3.2 Results and discussion 47
3.3 Conclusions 54
3.4 Experimental section 54
3.5 References 61

4 Mechanistic considerations and characterization of catalytic active intermediates of the Green Knoevenagel reaction of various benzaldehydes **63**

4.1 Introduction 65
4.2 Results and discussion 66
4.3 Conclusions 75
4.4 Experimental section 76
4.5 References 85

5 Repeatable molecularly recyclable semi-aromatic polyesters derived from lignin 87

5.1 Introduction 89
5.2 Results and discussion 90
5.3 Conclusions 100
5.4 Experimental section 100
5.5 References 105

6 Molecularly recyclable poly(ethylene terephtalate) versus semi-aromatic polyesters 107

6.1 Introduction 109
6.2 Results and discussion 111
6.3 Conclusions 120
6.4 Experimental section 121
6.5 References 127

7 Preparation of biobased styrene alternatives and their free radical polymerization 129

7.1 Introduction 131
7.2 Results and discussion 132
7.3 Conclusions 142
7.4 Experimental section 142
7.5 References 151

8 Epilogue 153

8.1 Highlights 153
8.2 Technology assessment 156
8.3 Outlook 159
8.4 References 160

Dankwoord 161

List of publications 165

About the Author 166

Glossary



AIBN		azobisisobutylnitrile
AS		4-acetoxystyrene
AMS		4-acetoxy-3-methoxystyrene
ADMS		4-acetoxy-3,5-dimethoxystyrene
δ	[ppm]	chemical shift
$CDCl_3$		deuterated chloroform
$D_{½}$		temperature when 50 wt.% is decomposed with TGA
DHCA		*p*-dihydrocoumaric acid
DHFA		dihydroferulic acid
DHSA		dihydrosinapinic acid
DMF		N,N-dimethylformamide
DMSO		dimethyl sulfoxide
DMSO-*d6*		deuterated dimethyl sulfoxide
DSC		Differential Scanning Calorimetry
E_a	[kJ]	activation energy
EWG		electron withdrawing groups
FTIR		Fourier Transformed Infra-Red
GC		Gas Chromatography
HFIP		1,1,1,3,3,3-hexafluro-2-propanol
HS		4-hydroxystyrene
HMS		4-hydroxy-3-methoxystyrene
HMDS		4-hydroxy-3,5-dimethoxystyrene
MFI		Melt Flow Index
MS (ESI)		ElectroSpray Ionization Mass Spectrometry
MW	[g mol^{-1}]	molecular weight
M_n	[g mol^{-1}]	number average molecular weight
M_w	[g mol^{-1}]	weight average molecular weight
^1H NMR		H-1 Nuclear Magnetic Resonance (spectroscopy)
^{13}C NMR		C-13 Nuclear Magnetic Resonance (spectroscopy)
PAS		poly(4-acetoxystyrene)
PAMS		poly(4-acetoxy-3-methoxystyrene)

PADMS		poly(4-acetoxy-3,5-dimethoxystyrene)
PBS		phosphate buffered solution
PDI		polydispersity index
PET		Poly(ethylene terephthalate)
Poly-H		poly(phloretic acid)
Poly-G		poly(dihydroferulic acid)
Poly-S		poly(dihydrosinapinic acid)
PS		poly(styrene)
SAXS		Small-Angle X-ray Scattering
SEC		Size Exclusion Chromatography
SSPC		solid-state post-condensation
T_g	[° C]	glass transition temperature
TGA		ThermoGravimetric Analysis
THF		tetrahydrofuran
T_m	[° C]	melting temperature
x_i		number of segments *i* in a polymer chain
WAXS		Wide-Angle X-ray Scattering



Summary

Oil, gas, and coal are hardly renewable on the scale of product lifetime, and excessive use of these fossil-based sources leads to global environmental concern. So it is of utmost importance to look for renewable sources as well as to recycling products towards their original building blocks, i.e., material circulation. Most important is the awareness that after product usage, waste can be seen as a resource. Selective depolymerization of redesigned new polymeric materials can be a significant driver towards the development of renewable and sustainable polymer materials. Chemical recycling, or even more precise, molecular recycling of materials reshape product life cycles. This thesis describes the design and synthesis of molecularly recyclable aromatic polyesters that demonstrate under certain conditions selective and reversible hydrolytic depolymerization.

The polyesters studied typically contain aliphatic ester groups because, for electronic reasons, derivatives of aliphatic carboxylic acids are more electrophilic than the analogous derivatives of aromatic carboxylic acids. Therefore, polyesters derived from aromatic carboxylic acids, e.g., polyethylene terephthalate (PET), are much less electrophilic and, therefore, far less sensitive to hydrolysis than aliphatic polyesters, e.g., polylactic acid (PLA). However, aromatic polyesters are of high technical relevance because of their excellent material properties. Hence, a combination of both is evident and, by taking nature as a guide, could be found in the building blocks of lignin.

The first part of the thesis describes how these building blocks (monomers) are synthesized in a more sustainable way than previously reported. A greener version of the Knoevenagel reaction, which is one of the most important methodologies for carbon-carbon double-bound formation in synthetic organic chemistry, has been developed. The direct use of piperidine, pyridine, or other harmful amines is avoided, and the use of a solvent can be limited or even excluded. The developed method with ammonium bicarbonate as a catalyst provides high yields of the products in this carbon-carbon formation reaction. Understanding the fundamental steps of the reaction is necessary to gain more insight into the role of different reactants and to be able to control the reaction. Ammonia plays a role as a precursor for this Green Knoevenagel reaction. A closed

catalytic cycle demonstrates how starting reactants and ammonia form “in situ” catalytic intermediates, that catalyze the carbon-carbon coupling. Besides, it is demonstrated that the in situ formed intermediates play a second catalytic role in the consecutive decarboxylation reaction resulting after hydrogenation in the building blocks, as mentioned above.

A procedure has been developed to synthesize various highly crystalline homopolyesters successfully (e.g., poly(phloretic acid), poly(dihydroferulic acid), and poly(dihydrosinapinic acid)) that could be depolymerized with minimal loss of material after separations. Because these PET analogs are composed of only one type of monomer, this cycle of polymerizing and depolymerizing can be applied several times, which is a significant advantage compared to PET. Because economic factors primarily motivate the recycling of plastics, molecular recycling has proven to be attractive, as long as the depolymerization conditions include catalysts that can be easily separated after use or subsequently used with the recovered building blocks.

Finally, it has been shown that a second decarboxylation of the formerly used building blocks is possible in a quantitative way, and so preparing biobased styrene alternatives. With these styrene alternatives, free radical polymerization can be applied to produce polymer materials based on these styrene alternatives.

The result of the work described in the thesis demonstrates that it is possible to synthesize the building blocks sustainably and to characterize the obtained molecularly recyclable aromatic polyesters. These polymers can be returned to their building blocks under relatively favorable conditions and can be repolymerized over and over again with minimal material loss.



Samenvatting voor geïnteresseerden

Het dringt steeds meer tot ons door dat onze verslaving aan fossiele brandstoffen (olie, gas en kolen) leidt tot wereldwijde problemen en bezorgdheid over de gevolgen voor het milieu. Met dit besef komt ook de aandacht voor het relatief kortstondig gebruik van veel materialen in onze eendimensionale wegwerpmaatschappij. Indien we materialen na hun gebruiksfase opnieuw in productie kunnen nemen als grondstof, volgen we niet alleen het voorbeeld van de natuur maar zal de afhankelijkheid van grondstoffen (fossiel én biobased) ook minder zijn. Voor polymeren en plastics is het van belang dat we op een eenvoudige manier terug kunnen keren naar de oorspronkelijke bouwstenen hiervan. Selectieve depolymerisatie van intelligenter ontworpen nieuwe polymere materialen kan een belangrijke motor zijn voor de ontwikkeling van hernieuwbare en meer duurzame polymere materialen. Chemische recycling, of nog beter omschreven moleculaire recycling van polymeren, verandert sterk de levenscyclus van deze producten. Dit proefschrift beschrijft het ontwerp en de synthese van moleculair recyclebare semi-aromatische polyesters die onder de gekozen omstandigheden meerdere keren selectieve en omkeerbare depolymerisatie en re-polymerisatie ondergaan.

De ontworpen en gesynthetiseerde polyesters bevatten alifatische estergroepen doordat deze meer reactief zijn dan de aromatische carbonzuren. Aromatische polyesters afgeleid van aromatische carbonzuren, zoals polyethyleentereftalaat (PET), zijn veel minder reactief en minder geschikt voor depolymerisatie in vergelijking tot alifatische polyesters, zoals polymelkzuur (PLA). Aromatische polyesters zijn echter vaak van groot belang vanwege hun uitstekende materiaaleigenschappen. Een combinatie van beide kan in de bouwstenen van lignine worden gevonden, een belangrijk onderdeel van hout en staat centraal in dit onderzoek.

Het eerste deel van dit proefschrift beschrijft hoe de benodigde bouwstenen (chemici noemen dit monomeren) voor de moleculair recyclebare polyesters op een meer milieuvriendelijke manier kunnen worden gesynthetiseerd. De al eeuwenoude Knoevenagel-reactie is zodanig aangepast dat het gebruik van piperidine, pyridine of andere schadelijke amines niet meer nodig is en het gebruik van een oplosmiddel beperkt of zelfs weggelaten kan worden. Het doorgronden

van een chemische reactie is belangrijk om meer inzicht te krijgen in de rol van verschillende reactanten en om de reactie in de gewenste richting te kunnen sturen. In dit onderzoek wordt aangetoond dat in deze Groene Knoevenagel ammoniak, afkomstig van een ammoniumzout of als ammonia toegediend, een belangrijke rol speelt. Een door ons opgestelde gesloten katalytische cyclus toont aan hoe de reactanten en ammoniak "in situ" (“ter plekke”) zogenaamde katalytische tussenproducten vormen, die de koolstof-koolstofkoppeling daadwerkelijk tot stand brengt. Verder is aangetoond dat de in situ gevormde tussenproducten nog een tweede katalytische rol spelen in de decarboxyleringsreactie die nodig is om de bouwstenen (monomeren) voor de polyesters te krijgen.

Er is een polymerisatieproces ontwikkeld om succesvol verschillende hoog kristallijne homopolyesters te synthetiseren, deze te identificeren en daarna weer terug te laten keren naar de bouwstenen. Dit met minimaal materiaalverlies van ongeveer 5% per generatie. Doordat deze polyesters uit slechts één type monomeer bestaan, kan deze cyclus van polymerisatie, depolymerisatie en re-polymerisatie relatief eenvoudig worden toegepast, wat een aanzienlijk voordeel is in vergelijking tot bijvoorbeeld PET. Het is verder van belang dat bij moleculaire recycling de hulpstoffen, zoals katalysatoren en kleurstoffen, niet moeilijk te scheiden zijn van de teruggewonnen bouwstenen. Dat lijkt bij de gesynthetiseerde polyesters ook van toepassing te zijn.

Ten slotte is ook nog aangetoond dat met een tweede decarboxylering van de gebruikte bouwstenen ook styreen-alternatieven gemaakt kunnen worden. Met deze styreen-alternatieven kunnen op een meer milieuvriendelijke en omgevingsvriendelijke manier verschillende polymerisatietechnieken worden toegepast, bijvoorbeeld in het hbo-onderwijs.

Het resultaat van het werk dat beschreven is in dit proefschrift toont aan dat het mogelijk is om de bouwstenen voor de nieuwe polyesters op een meer duurzame manier te synthetiseren en de gesynthetiseerde polyesters te karakteriseren. Deze polyesters kunnen onder relatief gunstige omstandigheden worden teruggebracht naar de oorspronkelijke bouwstenen en kunnen worden ge-repolymeriseerd met minimaal materiaalverlies. Hierbij is de 10^{e} generatie polyesters, wat betreft de onderzochte fysisch-chemische eigenschappen, nog steeds gelijk aan de 1^{e} generatie polyesters.



1 Introduction

The current production and disposal of polymeric materials are generally unsustainable.[1] A sustainable process is one with the proper resources management while still leaving sufficient reserves for future generations.[2] At this moment, the polymeric material is predominantly based on fossil-based resources, which are being rapidly depleted by our increasing energy demand. Biobased polymers have the potential to decouple economic growth from fossil-based resource depletion and environmental impact. Moreover, the vast majority of synthetic polymeric materials is designed for performance and durability and certainly not for degradability and recyclability. The result is a tremendous growth of widely spread polymeric wastes over the past few decades.[3]

Selective polymer depolymerization and repolymerization of monomers offer a sustainable route to the recycling of polymeric materials.[4] This not only solves the end-of-product life issue of polymeric material but also provides a pathway to develop an approximately circular materials economy. A circular materials economy is described as an economy that is "*restorative and regenerative by design and aims to keep products, components, and materials at their highest utility and value at all times*".[5]

Green Chemistry is crucial to realize an approximately circular materials economy. Green Chemistry and environmentally-friendly chemical engineering is an opportunity for reducing negative human impact on the earth, and, acting also related to cost efficiency, an opportunity for economic development.[6,7] Chemists and chemical engineers use the concepts of the E-factor and atom economy for comparing reaction alternatives, but the most important subject is to minimize "waste".[8-10] Catalytic methodologies developed by chemists and chemical engineers have been a major contributing factor in reducing the E-factors of processes in the industrial applications.[11-13] The main advantages of catalysis and catalysis engineering improved selectivity towards the desired product and by using less auxiliary substances. [14-18] The consequence of these novel sustainable catalytic processes reduce consumption of resources and generate less waste.[19-22]

1.1 A toolkit in Green Chemistry

For almost three decades, Green Chemistry has been recognized as a scientific discipline within the field of chemistry. In 1998 Anastas and Warner provided a concise and comprehensive definition:

Green Chemistry is the utilization of a set of principles that eliminates or reduces the generation or use of hazardous substances in the design, manufacture, and application of chemical products. [6]

Those well-defined "12 Principles of Green Chemistry" are list as follows:



1. Prevention
It is better to prevent waste than to treat or clean up waste.

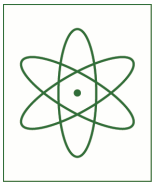

2. Atom Economy
Chemists design synthetic methods to maximize the incorporation of all materials used in the process into the final product.



3. Less Hazardous Chemical Syntheses
Chemists develop synthetic methods to use and to generate substances with little or no toxicity and causing no environmental burden.



4. Designing Safer Chemicals
Chemists design chemical products with optimal performance and no toxicity.



5. Safer Solvents and Auxiliaries

The use of auxiliary substances (e.g., solvents, separation agents) should be prevented or limited as much as possible.

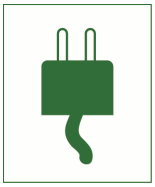

6. Design for Energy Efficiency

Chemists design synthetic procedures for operation at ambient temperature and pressure.



7. Use of Renewable Feedstocks

A raw material or feedstock should be renewable rather than depleting whenever technically and economically practicable.

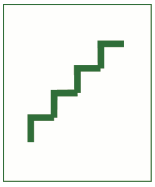

8. Reduce Derivatives

Unnecessary derivatization (temporary modification of physical/ chemical processes) should be minimized or avoided if possible because such steps require additional reagents and can generate waste.



9. Catalysis

Catalysts improve selectivity and should be used to avoid the use of stoichiometric reagents.



10. Design for Degradation

Chemists design chemical products which at the end of their technical or economic lifetime, are transformed into building blocks for the same product or other valuable chemicals.



11. Real-time analysis for Pollution Prevention
Analytical methodologies need to be further developed to allow for real-time, in-process monitoring, and control before the formation of hazardous substances.



12. Inherently Safer Chemistry for Accident Prevention
Substances and the form of a substance used in a chemical process should be chosen to minimize the potential for chemical accidents, including releases, explosions, and fires.

Over the past few decades, Green Chemistry has reached almost all the frontiers of chemical research and education. The principles of Green Chemistry are now well accepted and becoming a regular thinking basis for chemists and chemical engineers to design chemical processes. Of course, no chemical process will fulfill all of these twelve principles. However, processes that meet some of these criteria would already be more favorable than processes that do not meet them. In this introduction, not all of the principles will be discussed on the same level of detail. The focus will be specifically put on Principle 5: Safer Solvents, Principle 7: Use of Renewable Feedstocks, and Principle 10: Design for Degradation.

1.2 Safer solvents

Solvents constitute about 80% of the total volume of chemicals used in a process.[23] Up to now, the most commonly used solvents in industrial applications have a petrochemical origin. However, over the past 30 years, environmental and health concerns initiated several drivers, which stimulated efforts to modify the field of industrial solvents. Chemists are continuously searching for innovative and safe solvent systems intending to maximize the sustainability and safety of chemical processes.[24]

Capello[25] et al. have used the term "green solvent" to "*express the goal to minimize the environmental impact resulting from the use of solvents in chemical production*." Alternatively, Moity[26] et al. proposed that a "*green solvent*" has to bear some environmental, health, and safety characteristics that differentiate it from existing "*hazardous solvents*." Although the general idea is to minimize risks

for health and environment, there is a lack of agreement concerning the exact definition of what a green solvent is.

Because the "greenness" of a solvent is related to very diverse parameters and considerations, there is no general rule in the search for a green solvent. A universal green solvent does not exist, and the green aspect of a solvent firmly depends on the reaction considered.[27,28] Nowadays, the so-called: "green solvents" described in the current literature are water, ionic liquids[29,30], deep eutectic solvents[31,32], biobased solvents, and supercritical fluids[33]. However, although it is hypothetical in many cases: "the best solution is no solution".[34-37]

1.3 Use of renewable feedstocks

Undoubtedly, in the last few decades, there is an increasing interest in one of the crucial principles of green chemistry; the substitution of non-renewable fossil resources (crude oil, coal, and natural gas) by renewable biomass as a sustainable feedstock for the production of chemical products. There are many advantages to using biomass as a chemical feedstock.[38]

1. The use of biomass could be a way to moderate the buildup of CO_2 in the atmosphere because the use of biomass as a feedstock results in no net increase in the atmospheric CO_2 content.[39]
2. Increased use of biomass would increase the lifetime of diminishing crude oil reserves.
3. Biomass is available practically worldwide, on varying scales.[40]
4. A vast array of diverse materials is available from biomass, frequently stereochemical, and enantiomerically defined, giving the chemist and other users many novel structural features to utilize.[41]
5. Biomass is already highly oxygenated and could be used to reduce problems with oxidation.[42]

The estimated global production of biomass amounts for about 10^{11} tonnes per annum, which is divided into ca. 60% terrestrial and 40% aquatic biomass.[43] Figure 1.1 shows the global steps which have to be taken to convert biomass into specific substances. Noteworthy, humans use only 3-4% of these compounds for food and non-food purposes.

Carbohydrates and lignin are roughly the main constituents of biomass, respectively, 75 wt.% and 20 wt.%. The remaining 5 wt.% are triglycerides (oils and fats), proteins, and terpenes.[44]

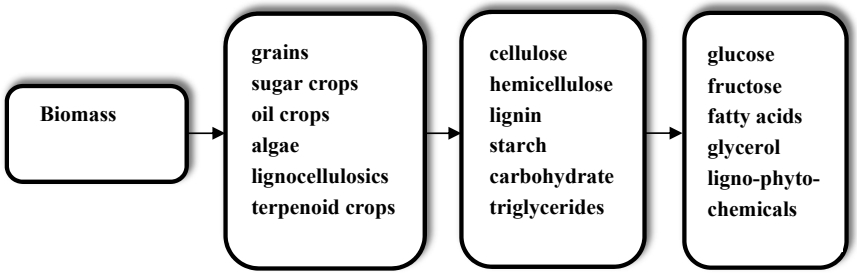

Figure 1.1: Biomass refining.[45]

Lignin is a complicated three-dimensional amorphous polymer. Its role in woody biomass is providing rigidity, strength, and resistance against degradation. Chemically expressed: lignin is a highly complex polyphenol-derived resin, consisting of various methoxylated phenylpropane structures. There are three primary constituents: *p*-hydroxyphenyl (**H**), guaiacyl (**G**), syringyl (**S**), derived from the monolignols *p*-coumaryl-, coniferyl-, and sinapyl-alcohols as shown in Figure 1.2.[46] The composition of lignin, and the ratio of the three units vary with the cell and plant type. Lignin from grasses is built up by the three monomeric units (H, G, and S). Softwood lignins mainly consist out of G units and hardwood lignins contains roughly equal amounts of G and S units. The typical lignin content is 24–33 wt.% in softwoods, 19–28 wt.% in hardwoods depending on the sources, and 15–25 wt.% in cereal straws, bamboo, or bagasse. About one decade ago, "cracking" the recalcitrant lignin structure appeared to be a challenging task. Owing to the remarkable achievements in catalysis research, it is now possible to isolate well-defined compounds from lignin in acceptable quantities. Among these compounds, several structures emerge as future lignin-derived platform chemicals.[47]

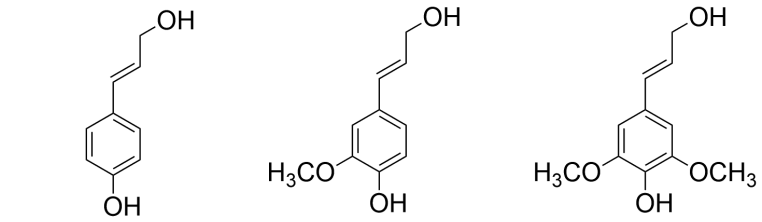

Figure 1.2: The three main monomer building blocks of lignin.

In general, two routes are known to isolate the aromatic products from lignin, as shown in Figure 1.3. The first route involves the non-selective degradation of lignin resulting in breaking C-C as well as C-O bonds. Sometimes also partial cleavage of the aromatic rings occurs.[48-51] The second route involves the selective degradation of lignin (as white-rot fungi break down the lignin in wood), which yields aromatics, derived from 4-hydroxyphenyl (red), guaiacyl (blue), or syringyl (green) moieties with various functional groups, see Figure 1.3.[52,53] Examples of these aromatics are 4-hydroxy benzaldehyde, vanillin, and syringaldehyde. Due to their inherent structure and natural origin, these aromatics are preferable, starting materials for the synthesis of natural aromatic products (e.g., ferulic acid, sinapinic acid, monolignols). These natural aromatic products, however, are not directly obtained by lignin degradation methods. Therefore sustainable and scalable additional reactions are needed and well valued. Figure 1.3 also shows examples of aromatic hydroxycarboxylic acid monomers and styrene analogs, obtained via additional reactions. In this thesis, these aromatic hydroxycarboxylic acid monomers and styrene analogs are employed as lignin-derived renewable aromatic monomers for the development of novel polymers.

At this moment, Borregaard in Norway is the only industrial producer of vanillin from the lignosulfonate oxidation path.[54] Here, 90% of the woody biomass input exits as marketable products. The refinery separates the biomass into cellulose specialty fibers (dissolving cellulose) and lignosulfonates. Part of the latter is then converted into vanillin, while the dissolved carbohydrates produce 2nd-generation bioethanol. Vanillin is the world's most used flavoring agent with a production of about 20 ktpa (with vanillin from vanilla beans represents only 1% of that and vanillin from lignin around 15%).[55,56] Interestingly, the conversion of

lignin into aromatics was once more common in the industry, but today vanillin is the only commercial aromatic product of lignin. However, more and more lignin is available as degradation and separation technologies continuously improve. Novel and efficient defunctionalization methods hold the promise of producing simpler drop-in molecules (e.g., BTX, phenol, catechol, and cyclohexane), which have enormous market potential. The advantage of producing compounds equivalent to those obtained from petrochemicals is that these structures are fully compatible with existing infrastructure.[57,58] Presumably, these technologies generate as well chemicals with more added value likewise 4-hydroxy benzaldehyde, vanillin, and syringaldehyde from the lignin in the nearby future.

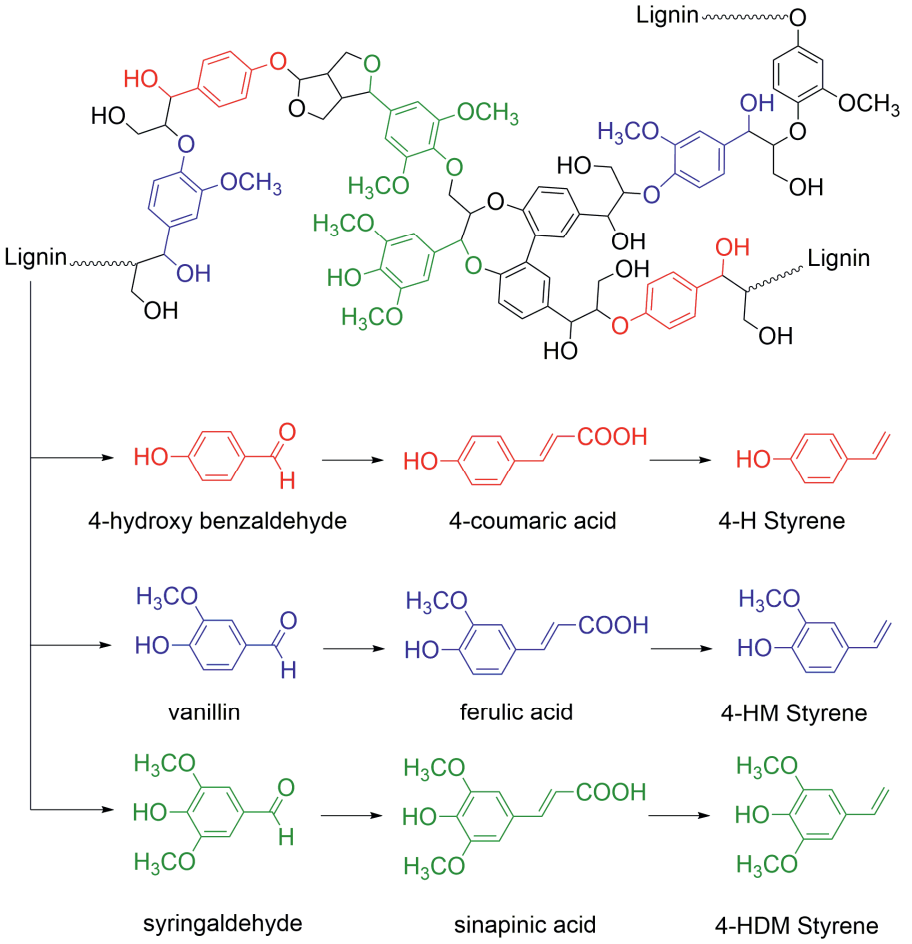

Figure 1.3: Various aromatic hydroxycarboxylic acid monomers and styrene analogs that can be obtained from lignin. A representative chemical structure of lignin is shown in this figure since the composition of lignin varies from species to species.[59]

1.4 Design for degradation

Environmental organizations sometimes nominate renewable and biodegradable polymeric material as sustainable. However, the fact that a product can be left in the environment promotes littering. Another issue regularly overlooked is that microplastics and polymers partially degraded from a plastic bottle cause more harm to the environment than the original bottle. The Green Chemistry principle to design materials for degradation does not automatically lead to an increase in sustainability. Therefore with polymers, it is often more preferable to collect waste streams and recycle them in dedicated plants into value-added materials rather than aiming for product degradation.[60]

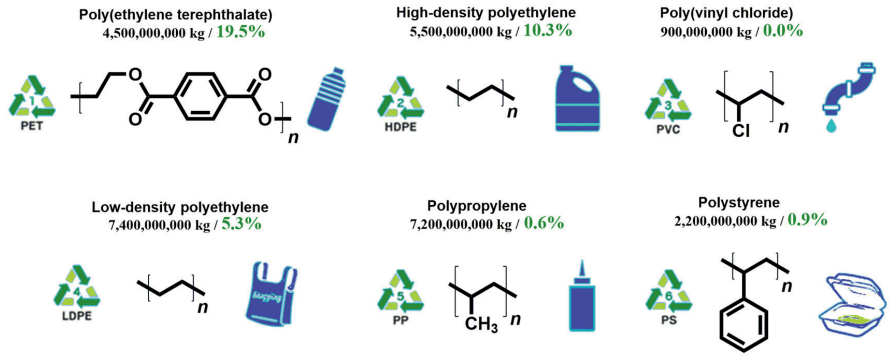

Figure 1.4: Municipal solid waste generation, mechanical recycling, and disposal in the United States: Facts and Figures for 2012, with their resin identification codes (RIC's) in the recycling symbol.[61]

Four main recycling techniques are implemented in the polymer producing/processing industry: primary recycling, mechanical recycling, chemical recycling, and energy recovery. Primary recycling involves the reuse of clean polymer with either the addition of virgin material to reprocess into products using the same processing method as used to produce from the virgin resin. With mechanical recycling (secondary recycling), the polymer is separated from its contaminants before it is molten and reformed. The main drawback of secondary recycling is the deterioration of the product properties, increasing with every cycle. Secondary recycling is the most used route for the recycling of PET, high-density polyethylene (HDPE), and low-density polyethylene (LDPE), as shown in Figure 1.4. The lower molecular weight recycled PET is used for fiber production. The comparatively high thermal stability of polyethylene allows HDPE and LDPE to

be processed through several melts and remold cycles. Guardrail posts made from mixed polyolefins is a perfect example of secondary recycling.

The third recycling technique, which is the only acceptable one according to sustainability prospects, is chemical recycling. An example of chemical recycling is pyrolysis, in which plastics are subjected to high temperatures in the presence of a catalyst to give a mixture of products that are generally difficult to separate. Gasification can process unsorted, uncleaned plastic waste and turn it into syngas, which can be used to build bigger building blocks for new polymers. A unique form of chemical recycling is molecular recycling, in which polymers are de-polymerized to its monomer units. Re-polymerization of the obtained monomers results in a polymer with the same properties as the virgin material. This method involves no addition of new polymeric material, and material properties are retained. Up to now, chemical recycling is not practiced to a large extent on an industrial scale because the present methods require considerable energy input and the lack of potential candidates.[62] Molecular recycling could be a significant driver towards the development of more innovative renewable plastics.

The fourth method, energy recovery recycling, is executed when either the other recycling methods are not economically viable, or the waste is toxic and hazardous to handle. In that case, the energy content of the plastic waste is recovered by incineration. The plastic waste is burned in air presence, hydrocarbons are converted to carbon dioxide and water, the chemical identity is lost, but the chemical energy is recovered as thermal energy.

1.5 Aim and scope of this thesis

The fundamental motivation for the work presented in this thesis is the scientific curiosity to redesign innovative polymers using carbon-neutral building blocks as monomers. The objective of this work is to demonstrate the applicability of a set of renewable, semi-aromatic monomers in molecularly recyclable semi-aromatic polyesters. These polymers should be returned to their building blocks under relatively favorable conditions and can be re-polymerized with material losses as small as possible. Monomer synthesis, as well as polymer synthesis, must obey the principles of Green Chemistry.

Therefore, a chain-of-knowledge approach was adopted, comprising the following steps:

- ✓ Set up and development of sustainable production of the monomer
- ✓ Elucidating the mechanism of the developed green synthesis route
- ✓ Monomer preparation and purification
- ✓ Design and preparation of the molecularly recyclable semi-aromatic polyesters
- ✓ Physico/chemical characterization of the molecularly recyclable semi-aromatic polyesters
- ✓ Multiple molecular recycling and re-polymerization of the semi-aromatic polyesters producing several generations of polymer

The results obtained within the framework of this project are summarized in this thesis.

1.6 Outline of this thesis

This thesis consists of eight chapters describing the application of the Green Knoevenagel reaction to obtain several monomers. With these isolated monomers, various molecularly recyclable semi-aromatic polyesters are synthesized and re-polymerized for numerous generations. **Chapter 2** and **chapter 3** describe how these building blocks (monomers) could be synthesized in a more environmentally friendly way than previously reported.

In education and research, in many cases, only the starting materials and the end products are presented, and the reaction path between them remains unknown. Understanding the detailed mechanism is necessary to gain insight into the role of the different reactants play. This knowledge is a prerequisite to control a reaction and to allow safe upscaling. **Chapter 4** explains how ammonia plays a catalytic role in the conversion of benzaldehydes to cinnamic acid derivatives. In the proposed mechanism, starting benzaldehyde reacts with the precursor ammonia released from ammonium salts to form a catalytically active double Schiff base. A closed catalytic cycle shows how these "in situ" intermediates catalyze the carbon-carbon coupling with malonic acid and generates the end products and ammonia after their catalytic action. It is also demonstrated that the in situ formed intermediates can play a second catalytic role in decarboxylation.

Chapter 5 reports the development of a route to successfully synthesize thermotropic polyesters up to a 50-gram scale via solvent-assisted polycondensation. Three different homopolymers poly(phloretic acid) (poly-H), poly(dihydroferulic acid) (poly-G), and poly(dihydrosinapinic acid) (poly-S) have been synthesized. The products could be depolymerized and re-polymerized several times without only a limited loss of material. In **chapter 6**, the three homopolymers (poly-H, poly-G, and poly-S) are compared to PET concerning molecular recyclability.

Chapter 7 demonstrates that an additional decarboxylation of the monomers previously synthesized with the "Green Knoevenagel" is possible, thereby offering the opportunity to produce biobased styrene derivatives. With these styrene-derivatives, radical polymerization can be applied in education and research, taking into account the principles of Green Chemistry.

In **chapter 8**, the main conclusions are summarized, and future technological possibilities for recyclable semi-aromatic polyesters are discussed.

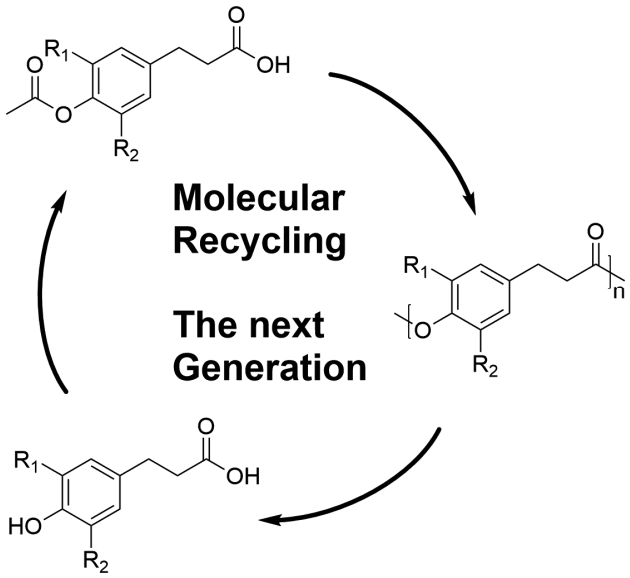

Scheme 1.1: Molecular recycling process for poly(phloretic acid) (poly-H, $R_1 = R_2 = H$), poly(dihydroferulic acid) (poly-G, $R_1 = OCH_3$ and $R_2 = H$), and poly(dihydrosinapinic acid) (poly-S, $R_1 = R_2 = OCH_3$).

1.7 References

1. Hong, M.; Chen, E. Y. Future Directions for Sustainable Polymers. *Trends in Chemistry* **2019**, *1*, 148-151.
2. Sheldon, R. A. Fundamentals of green chemistry: efficiency in reaction design. *Chemical Society reviews* **2012**, *41*, 1437-1451.
3. Luzi, F.; Torre, L.; Kenny, M. J.; Puglia, D. Bio- and Fossil-Based Polymeric Blends and Nanocomposites for Packaging: Structure-Property Relationship. *Materials* **2019**, *12,* 471.
4. Hong, M.; Chen, E. Y. Chemically recyclable polymers: a circular economy approach to sustainability. *Green Chemistry* **2017**, *19*, 3692-3706
5. MacArthur, E. Towards the circular economy, economic and business rationale for an accelerated transition. *Ellen MacArthur Foundation: Cowes, UK* **2013**.
6. Anastas, P. T., Warner, J. C. *Green chemistry: theory and practice;* Oxford University Press: New York, **1998**.
7. Cue, B. W.; Zhang, J. Green process chemistry in the pharmaceutical industry. *Green Chemistry Letters and Reviews* **2009**, *2*, 193-211.
8. Sheldon, R. A. The E factor 25 years on the rise of green chemistry and sustainability. *Green Chemistry* **2017**, *19*, 18-43.
9. Dichiarante, V.; Ravelli, D.; Albini, A. Green chemistry: state of the art through an analysis of the literature. *Green Chemistry Letters and Reviews* **2010**, *3*, 105-113.
10. van Schijndel, J.; Molendijk, D.; Canalle, L. A.; Rump, E. T.; Meuldijk, J. Temperature Dependent Green Synthesis of 3-Carboxycoumarins and 3,4-unsubstituted Coumarins. *Current Organic Synthesis* **2019**, *16*, 130-135.
11. Alfonsi, K.; Colberg, J.; Dunn, P. J.; Fevig, T.; Jennings, S.; Johnson, T. A.; Kleine, H. P.; Knight, C.; Nagy, M. A.; Perry, D. A.; Stefaniak, M. Green chemistry tools to influence a medicinal chemistry and research chemistry based organisation. *Green Chemistry* **2008**, *10*, 31-36.
12. Climent, M. J.; Corma, A.; Iborra, S.; Mifsud, M.; Velty, A. New one-pot multistep process with multifunctional catalysts: decreasing the E factor in the synthesis of fine chemicals. *Green Chemistry* **2010**, *12*, 99-107.
13. Ma, S. K.; Gruber, J.; Davis, C.; Newman, L.; Gray, D.; Wang, A.; Grate, J.; Huisman, G. W.; Sheldon, R. A. A green-by-design biocatalytic process for atorvastatin intermediate. *Green Chemistry* **2010**, *12*, 81-86.
14. Anastas, P. T.; Lankey, R. L. Life cycle assessment and green chemistry: the yin and yang of industrial ecology. *Green Chemistry* **2000**, *2*, 289-295.
15. Dawes, G. J. S.; Scott, E. L.; Le Notre, J. E. L.; Sanders, J. P. M.; Bitter, J. H. Deoxygenation of biobased molecules by decarboxylation and decarbonylation - a review on the role of heterogeneous, homogeneous and bio-catalysis. *Green Chemistry* **2015**, *17*, 3231-3250.
16. van Schijndel, J.; Canalle, L. A.; Molendijk, D.; Meuldijk, J. Exploration of the Role of Double Schiff Bases as Catalytic Intermediates in the Knoevenagel Reaction of Furanic Aldehydes: Mechanistic Considerations. *Synlett* **2018**, *29*, 1983-1988.
17. van Schijndel, J.; Molendijk, D.; Spakman, H.; Knaven, E.; Canalle, L. A.; Meuldijk, J. Mechanistic considerations and characterization of ammonia-based catalytic active intermediates of the green Knoevenagel reaction of various benzaldehydes. *Green Chemistry Letters and Reviews* **2019**, *12*, 323-331.
18. Fu, H.; Dencic, I.; Tibhe, J.; Sanchez Pedraza, C. A.; Wang, Q.; Noël, T.; Meuldijk, J.; de Croon, M.; Hessel, V.; Weizenmann, N.; Oeser, T.; Kinkeade, T.; Hyatt, D.; Van Roy, S.; Dejonghe, W.; Diels, L. Threonine aldolase immobilization on different supports for engineering of productive, cost-efficient enzymatic microreactors. *Chemical Engineering Journal* **2012**, *207-208*, 564-576.
19. Hessel, V.; Noël, T. Heterocat, homocat and biocat: what does better flow? *Chimica Oggi* **2015**, *33*, 4-8

20. Liu, Y.; Pujals, S.; Stals, P. J. M.; Pauloehrl, T.; Presolski, S. I.; Meijer, E. W.; Albertazzi, L.; Palmans, A. R. A. Catalytically Active Single-Chain Polymeric Nanoparticles: Exploring Their Functions in Complex Biological Media. *Journal of the American Chemical Society* **2018**, *140*, 3423-3433.
21. Lefferts, L.; Hanefeld, U.; Bitter, J. H. Introduction. *Catalysis* **2017**.
22. Gustini, L.; Lavilla Aguilar, C.; Janssen, W. T. J.; Martinez de Ilarduya, A.; Muñoz-Guerra, S.; Koning, C. E. Green and selective polycondensation methods toward linear sorbitol-based polyesters:enzymatic versus organic and metal-based catalysis. *ChemSusChem* **2016**, *9*, 2250-2260.
23. Häckl, K.; Kunz, W. Some aspects of green solvents. *Comptes Rendus Chimie* **2018**, *21*, 572-580.
24. Marion, P.; Bernela, B.; Piccirilli, A.; Estrine, B.; Patouillard, N.; Guilbot, J.; Jérôme, F. Sustainable chemistry: how to produce better and more from less? *Green Chemistry* **2017**, *19*, 4973-4989.
25. Capello, C.; Fischer, U.; Hungerbühler, K. What is a green solvent? A comprehensive framework for the environmental assessment of solvents. *Green Chemistry* **2007**, *9*, 927-934.
26. Moity, L.; Durand, M.; Benazzouz, A.; Pierlot, C.; Molinier, V.; Aubry, J. Panorama of sustainable solvents using the COSMO-RS approach. *Green Chemistry* **2012**, *14*, 1132-1145.
27. Lafleur, R. P. M.; Lou, X.; Pavan, G. M.; Palmans, A. R. A.; Meijer, E. W. Consequences of a cosolvent on the structure and molecular dynamics of supramolecular polymers in water. *Chemical science* **2018**, *9*, 6199-6209.
28. Leenders, C. M. A.; Baker, M. B.; Pijpers, I. A. B.; Lafleur, R. P. M.; Albertazzi, L.; Palmans, A. R. A.; Meijer, E. W. Supramolecular polymerisation in water; Elucidating the role of hydrophobic and hydrogen-bond interactions. *Soft Matter* **2016**, *12*, 2887-2893.
29. Hangarge, R. V.; Jarikote, D. V.; Shingare, M. S. Knoevenagel condensation reactions in an ionic liquid. *Green Chemistry* **2002**, *4*, 266-268.
30. Ranu, B. C.; Jana, R. Ionic Liquid as Catalyst and Reaction Medium - A Simple, Efficient and Green Procedure for Knoevenagel Condensation of Aliphatic and Aromatic Carbonyl Compounds Using a Task-Specific Basic Ionic Liquid. *European Journal of Organic Chemistry* **2006**, *2006*, 3767-3770.
31. Dietz, C. H. J. T; Creemers, J. T.; Meuleman, M. A.; Held, C.; Sadowski, G.; van Sint Annaland, M.; Gallucci, F.; Kroon, M. C. Determination of the Total Vapor Pressure of Hydrophobic Deep Eutectic Solvents: Experiments and Perturbed-Chain Statistical Associating Fluid Theory Modeling. *ACS Sustainable Chemistry & Engineering* **2019**, *7*, 4047-4057.
32. van Osch, D. J. G. P; Dietz, C. H. J. T; van Spronsen, J.; Kroon, M. C.; Gallucci, F.; van Sint Annaland, M.; Tuinier, R. A Search for Natural Hydrophobic Deep Eutectic Solvents Based on Natural Components. *ACS Sustainable Chemistry & Engineering* **2019**, *7*, 2933-2942.
33. Marcus, Y. *Supercritical Carbon Dioxide;* Chemistry research and applications; Nova Science Publishers, Incorporated: New York, **2019**.
34. van Schijndel, J.; Canalle, L. A.; Molendijk, D.; Meuldijk, J. The green Knoevenagel condensation: solvent-free condensation of benzaldehydes. *Green Chemistry Letters and Reviews* **2017**, *10*, 404-411.
35. Jawor, M. L.; Ahmed, B. M.; Mezei, G. Solvent- and catalyst-free, quantitative protection of hydroxyl, thiol, carboxylic acid, amide and heterocyclic amino functional groups. *Green Chemistry* **2016**, *18*, 6209-6214.
36. Martins, M. A. P.; Frizzo, C. P.; Moreira, D. N.; Buriol, L.; Machado, P. Solvent-free heterocyclic synthesis. *Chemical reviews* **2009**, *109*, 4140-4182.
37. Pinxterhuis, E. B.; Giannerini, M.; Hornillos, V.; Feringa, B. L. Fast, greener and scalable direct coupling of organolithium compounds with no additional solvents. *Nature communications* **2016**, *7*, 11698.

38. Höfer, R.; Bigorra, J. Biomass-based green chemistry: sustainable solutions for modern economies. *Green Chemistry Letters and Reviews* **2008**, *1*, 79-97.
39. Velthoven, van, J. L. J.; Noordover, B. A. J.; Meuldijk, J. Amorphous polyamide coating resins from sugar-derived monomers. *J Coat Technol Res* **2016**, *13*, 613-622.
40. Noordover, B. A. J.; Staalduinen, van, V. G.; Duchateau, R.; Koning, C. E.; Benthem, van, R. A. T. M.; Mak, M.; Heise, A.; Frissen, A. E.; Haveren, van, J. Co- and terpolyesters based on isosorbide and succinic acid for coating applications: Synthesis and Characterization. *Biomacromolecules* **2006**, *7*, 3406-3416.
41. Wu, J.; Eduard, P.; Thiyagarajan, S.; Haveren, van, J; Es, van, D. S; Koning, C. E.; Lutz, M.; Fonesca Guerra, C. Isohexide Derivatives from Renewable Resources as Chiral Building Blocks. *ChemSusChem* **2011**, *4*, 599-603.
42. Laudadio, G.; Straathof, N. J. W.; Lanting, M. D.; Knoops, B.; Hessel, V.; Noël, T. An environmentally benign and selective electrochemical oxidation of sulfides and thiols in a continuous-flow microreactor. *Green Chemistry* **2017**, *19*, 4061-4066.
43. Field, C. B.; Behrenfeld, M. J.; Randerson, J. T.; Falkowski, P. Primary Production of the Biosphere: Integrating Terrestrial and Oceanic Components. *Science* **1998**, *281*, 237-240.
44. Tursi, A. A review on biomass: importance, chemistry, classification, and conversion. *Biofuel Research Journal* **2019**, *6*, 962-979.
45. Ahorsu, R.; Medina, F.; Constantí, M. Significance and Challenges of Biomass as a Suitable Feedstock for Bioenergy and Biochemical Production: A Review. *Energies* **2018**, *11*, 3366.
46. Dorrestijn, E.; Laarhoven, L. J. J.; Arends, I. W. C. E.; Mulder, P. The occurrence and reactivity of phenoxyl linkages in lignin and low rank coal. *Journal of Analytical and Applied Pyrolysis* **2000**, *54*, 153-192.
47. Strassberger, Z.; Tanase, S.; Rothenberg, G. The pros and cons of lignin valorisation in an integrated biorefinery. *RSC ADVANCES* **2014**, *4*, 25310-25318.
48. Parkhurst, H. J. J.; Huibers, D. T. A.; Jones, M. W. In *In Production of phenol from lignin;* United States, **1980**.
49. Fernandes, M. R. C.; Huang, X.; Abbenhuis, H. C. L.; Hensen, E. J. M. Lignin oxidation with an organic peroxide and subsequent aromatic ring opening. *International Journal of Biological Macromolecules* **2019**, *123*, 1044-1051.
50. Huang, X.; Ludenhoff, J. M.; Dirks, M.; Ouyang, X.; Boot, M. D.; Hensen, E. J. M. Selective Production of Biobased Phenol from Lignocellulose-Derived Alkylmethoxyphenols. *ACS catalysis* **2018**, *8*, 11184-11190.
51. Ouyang, X.; Huang, X.; Zhu, J.; Boot, M. D.; Hensen, E. J. M. Catalytic Conversion of Lignin in Woody Biomass into Phenolic Monomers in Methanol/Water Mixtures without External Hydrogen. *ACS Sustainable Chemistry & Engineering* **2019**, *7*, 13764-13773.
52. Mota, M. I. F.; Mota, M. I. F.; Rodrigues Pinto, P. C.; Rodrigues Pinto, P. C.; Loureiro, J. M.; Rodrigues, A. E. Recovery of Vanillin and Syringaldehyde from Lignin Oxidation: A Review of Separation and Purification Processes. *Separation & Purification Reviews* **2016**, *45*, 227-259.
53. Sun, Z.; Fridrich, B.; de Santi, A.; Elangovan, S.; Barta, K. Bright Side of Lignin Depolymerization: Toward New Platform Chemicals. *Chemical reviews* **2018**, *118*, 614-678.
54. Rødsrud, G.; Lersch, M.; Sjöde, A. History and future of world's most advanced biorefinery in operation. *Biomass and Bioenergy* **2012**, *46*, 46-59.
55. Winter, R. T.; van Beek, H. L.; Fraaije, M. W. The Nose Knows: Biotechnological Production of Vanillin. *Journal of Chemical Education* **2012**, *89*, 258-261.
56. Fache, M.; Boutevin, B.; Caillol, S. Vanillin Production from Lignin and Its Use as a Renewable Chemical. *ACS Sustainable Chemistry & Engineering* **2016**, *4*, 35-46.
57. Zhang, L.; Hu, G. Supply chain design and operational planning models for biomass to drop-in fuel production. *Biomass and Bioenergy* **2013**, *58*, 238-250.
58. Sheldon, R. A. Green and sustainable manufacture of chemicals from biomass: state of the art. *Green Chemistry* **2014**, *16*, 950-963.

59. Vanholme, R.; Demedts, B.; Morreel, K.; Ralph, J.; Boerjan, W. Lignin Biosynthesis and Structure. *Plant Physiol.* **2010***, 153*, 895-905.
60. Meulen, van de, I; Li, Y.; Deumens, R.; Joosten, E. A. J.; Koning, C. E.; Heise, A. Copolymers from unsaturated macrolactones: toward the design of cross-linked biodegradable polyesters. *Biomacromolecules* **2011***, 12*, 837-843.
61. U.S. Environmental Protection Agency (EPA) Municipal Solid Waste Generation, Recycling, and Disposal in the United States: Facts and Figures for **2012**.
62. Ragaert, K.; Delva, L.; Van Geem, K. Mechanical and chemical recycling of solid plastic waste. *Waste Management* **2017***, 69*, 24-58.

2 A global kinetic model of the Knoevenagel-Doebner reaction applied to the synthesis of sinapinic acid

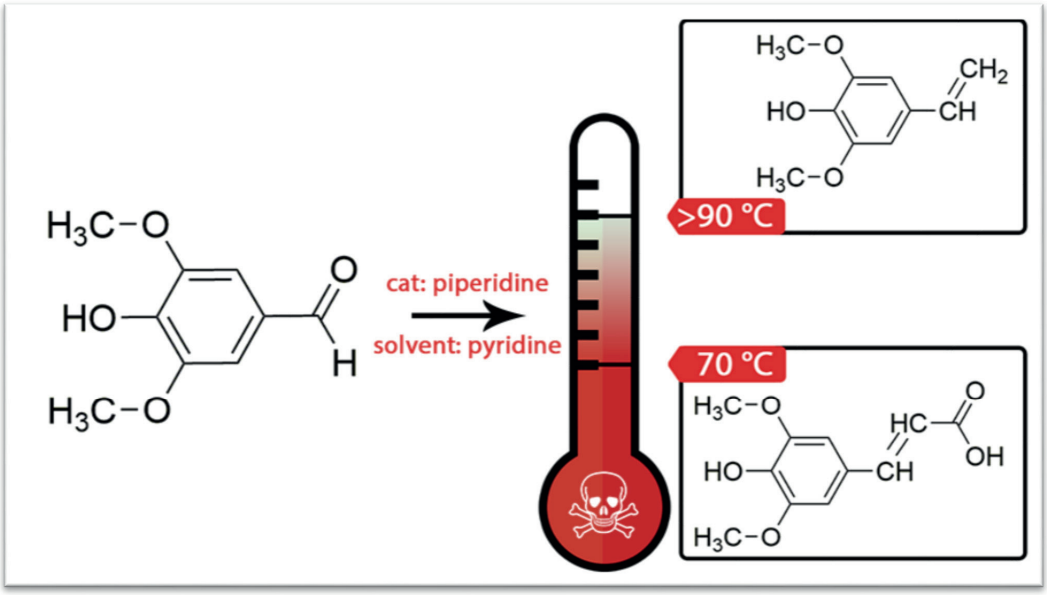

This chapter is partially based on:

van Schijndel, J.; Open Journal of Physical Chemistry **2016**, *6*, 101-108. (DOI:10.4236/ojpc.2016.64010)

Abstract

This chapter describes the application of the original Knoevenagel-Doebner reaction. This method covers reactions of carbonyl compounds (aldehydes and ketones) with active methylene compounds in the presence of an amine, leading to alkylidene- or benzylidene-dicarbonyls or analogous compounds (Knoevenagel products).

Sinapinic acid is a widespread compound in vegetable material and is as such common in the human diet. Sinapinic acid is synthesized by reacting syringaldehyde and malonic acid, a typical example of the Knoevenagel-Doebner reaction. However, a consecutive decarboxylation of sinapinic acid leading to 4-hydroxy-3,5-dimethoxy styrene limits the yield of sinapinic acid. The concentration-time history of syringaldehyde and the reaction products have been monitored to increase the insight in this reaction. Also, this chapter describes a global kinetic model of which the rate coefficients of the three separated steps were estimated. The optimal conversion for the production of sinapinic acid from syringaldehyde was 78% after 2.5 hours of reaction at 70 °C.

2.1 Introduction

The Knoevenagel-Doebner reaction has always been an important and reliable method for the formation of carbon-carbon bonds and is frequently used in industry.[1-3] The condensation of aldehydes or ketones with an activated methylene compound is not only a fundamental organic reaction by itself but may be considered biomimetic insofar as numerous biosynthetic pathways and aldolase enzymes use similar intermediates.[4] In an activated methylene compound, the methylene group is situated between two strong electron-withdrawing groups (EWG) such as nitro-, carbonyl- or nitrile groups.[5,6]

Two principal mechanisms have been proposed for the Knoevenagel-Doebner reaction. The first is based on Knoevenagel's original mechanistic investigation, in which he attempted to obtain possible intermediates in the reaction and to cause these to react further.[7-10] After it was shown that pyridine was a useful catalyst in the so-called Knoevenagel-Doebner reaction, Hann and Lapworth proposed an alternative mechanism in which the role of the base was to remove a proton from the activated methylene compound. The formed carbanion reacts with the carbon atom of the aldehyde.[11,12] The Knoevenagel reaction was considered to be a modification of the aldol condensation with amongst others, for example, an amine as a Lewis base catalyst.[13-17]

Aldabalde[18] et al. and Simpson[19] et al. proposed a mechanism for the Knoevenagel-Doebner reaction of aromatic aldehydes and malonic acid using pyridine and piperidine as organocatalysts. The mechanism suggested reactive intermediates, which was illustrated by the conversion of vanillin to ferulic acid. During the reaction, 4-hydroxy-3-methoxy styrene was observed as a second product as a result of an extra decarboxylation step.

4-Hydroxybenzaldehydes can react with malonic acid in a Knoevenagel-Doebner reaction to give the corresponding α,β-unsaturated carboxylic acids known as hydroxycinnamic acids. In nature, hydroxycinnamic acids can be found in the vegetable kingdom as secondary metabolites.[20] There are three familiar members of these so-called ligno-phytochemicals of which ferulic acid has been studied extensively, primarily due to its antioxidant properties.[21-23]

Sinapinic acid is another member of the hydroxycinnamic acid family. Its effectiveness as an antioxidant is considered to be superior over that of ferulic acid. Moreover, sinapinic acid shows anti-microbial, anti-inflammatory, anti-cancer, and anti-anxiety activities.[24] In this study, the transformation of syringaldehyde (**1**) to sinapinic acid (**5**) with the Knoevenagel-Doebner reaction was investigated in

more detail. A global kinetic model has been developed, and the rate coefficients of the global reactions have been estimated. This model achieves a better understanding of the mechanism of the Knoevenagel-Doebner reaction of syringaldehyde and other 4-hydroxy aldehydes.

2.2 Results and discussion

Aldabalde et al. previously reported the conversion of vanillin to ferulic acid using the Knoevenagel-Doebner reaction. In their study, the reaction was performed in refluxing pyridine (115 °C), which served as the solvent. Piperidine served as organocatalyst in both the carbon-carbon bond formation and the consecutive decarboxylation. The use of organocatalysts in organic synthesis is environmentally beneficial, as stated by the Green Chemistry principles.[25] In the research of Aldabalde, however, the 4-vinylphenolic product 4-hydroxy, 3-methoxy-styrene (HMS), was the main product. For the Knoevenagel-Doebner reaction of syringaldehyde **1** and malonic acid **2** towards sinapinic acid **5**, we, therefore, decreased the temperature in the range of 50 to 90 °C to suppress the formation of the 4-vinylphenolic product HDMS **7** (Scheme 2.1). We moreover used smaller amounts of the organocatalyst piperidine to limit further the environmental impact (0.2 eq instead of 0.4 eq as used before).

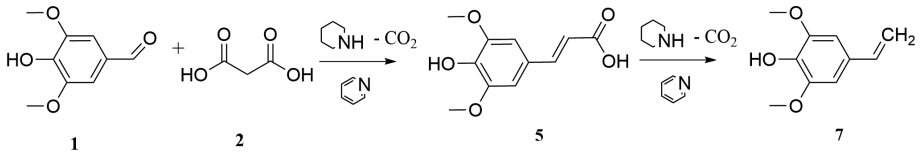

Scheme 2.1: Knoevenagel-Doebner reaction of syringaldehyde **1** with malonic acid **2** towards sinapinic acid **5** in the solvent pyridine, followed by a second decarboxylation leading to 4-hydroxy-3,5-dimethoxy styrene (HDMS) **7**.

From the results obtained, it is evident that the conversion rate of syringaldehyde **1** increases with temperature (Figure 2.1a). It was observed that sinapinic dicarboxylic acid **3** was initially formed to a limited extent (Figure 2.1b), followed by a decarboxylation resulting in sinapinic acid **5**. A moderate conversion to sinapinic acid **5** was obtained, and there seems to be an optimum between 70 and 80 °C (Figure 2.1c).

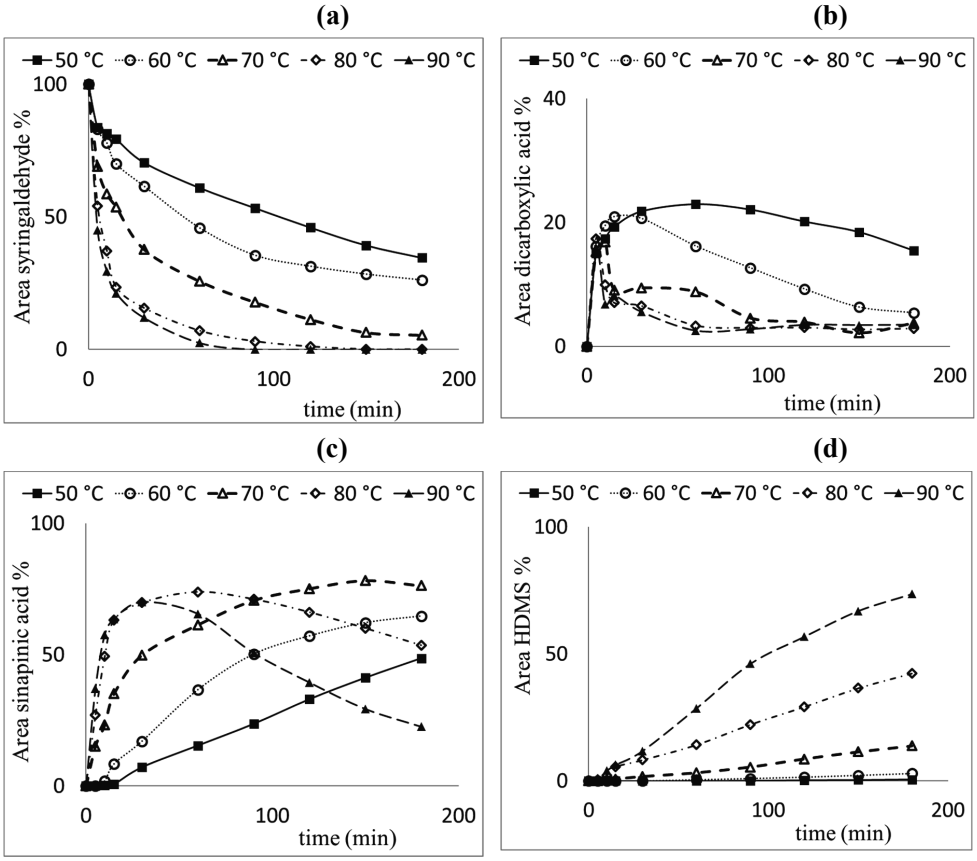

Figure 2.1: Concentration-time profiles of (a) syringaldehyde **1**, (b) sinapinic dicarboxylic acid **3**, (c) sinapinic acid **5**, and (d) 4-hydroxy-3,5-dimethoxy styrene (HDMS) **7** at various temperatures between 50 °C and 90 °C.

For temperatures above 70°C, the formation of 4-hydroxy-3,5-dimethoxy styrene (HDMS) **7** as a side product is observed (Figure 2.1d) in the solvent pyridine following a second decarboxylation step. HPLC can separate HDMS **7** and sinapinic acid **5**, and their structures have been confirmed with ^{1}H NMR and mass spectrometry. Furthermore, it should be noted that the formation of HDMS

7 complicates the isolation of sinapinic acid **5** using precipitation. Pure sinapinic acid **5** forms a free-flowing powder, while an HDMS **7** contamination changes the morphology of the product into an oily, viscous material. The optimal conversion for the production of sinapinic acid **5** from syringaldehyde **1** was 78% after 2.5 hours at 70 °C.

The Knoevenagel-Doebner reaction of syringaldehyde follows the reaction scheme, as shown in Scheme 2.2, and can be subdivided into three separate global reactions. To improve the understanding of the mechanism of the Knoevenagel-Doebner reaction of syringaldehyde, a global kinetic model has been developed. The differential equations [4, 5, 6, and 7] derived from mass balances of the compounds **1**, **2**, **3**, **5,** and **7** for a batch process have been solved numerically using Matlab©. So the rate coefficients of the global reactions have been "estimated."

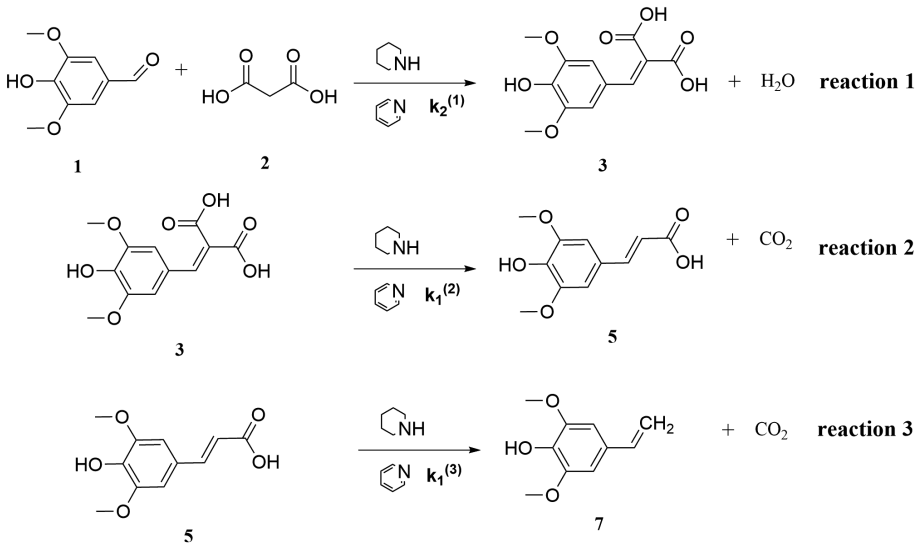

Scheme 2.2: Knoevenagel-Doebner condensation of syringaldehyde **1** with malonic acid **2** towards sinapinic dicarboxylic acid **3** and water, followed by the first decarboxylation towards sinapinic acid **5** and CO_2. Also, a second decarboxylation occurs leading to HDMS **7** and CO_2.

The Knoevenagel-Doebner reaction of syringaldehyde can be rewritten in the following general reactions:

$1 + 2 \rightarrow 3 + H_2O$ (reaction 1)

$3 \rightarrow 5 + CO_2$ (reaction 2)

$5 \rightarrow 7 + CO_2$ (reaction 3)

The Runge-Kutta method[26] is a frequently used numerical method to solve sets of ordinary differential equations. The set of differential equations [4, 5, 6, and 7] has been solved by Matlab© with a second-order Runge-Kutta method, by giving an initial guess for $k_2^{(1)}$, $k_1^{(2)}$ and $k_1^{(3)}$ and minimizing the residual sum of squares as shown in Figure 2.2.

$$\frac{dC_1}{dt} = \frac{dC_2}{dt} = -k_2^{(1)} \times C_1 \times C_2 \quad [4]$$

$$\frac{dC_3}{dt} = k_2^{(1)} \times C_1 \times C_2 - k_1^{(2)} \times C_3 \quad [5]$$

$$\frac{dC_5}{dt} = k_1^{(2)} \times C_3 - k_1^{(3)} \times C_5 \quad [6]$$

$$\frac{dC_7}{dt} = k_1^{(3)} \times C_5 \quad [7]$$

Boundary conditions at t=0 are: $C_1=C_2=1.5625 \times 10^3$ mol/m^3 and $C_3=C_5=C_7=0$ mol/m^3. Here it is assumed that CO_2 directly leaves the reaction mixture as a gas, and all the other components in this system are perfectly mixed. In Table 2.1, the values for $k_2^{(1)}$, $k_1^{(2)}$, and $k_1^{(3)}$ for each temperature are collected together with the correlation coefficient (R^2) for each temperature.

Table 2.1: Global rate coefficients for the Knoevenagel-Doebner condensation reactions of syringaldehyde towards sinapinic acid at different temperatures.

T (°C)	**$k_2^{(1)}$ (10^{-3}·m^3/mol·s)**	**$k_1^{(2)}$ (s^{-1})**	**$k_1^{(3)}$ (10^{-3}·s^{-1})**	**R^2 (-)**
50	6.6	0.013	0.5	0.994
60	12	0.029	0.7	0.995
70	32	0.15	1.2	0.992
80	94	0.26	3.3	0.996
90	128	0.31	7.7	0.996

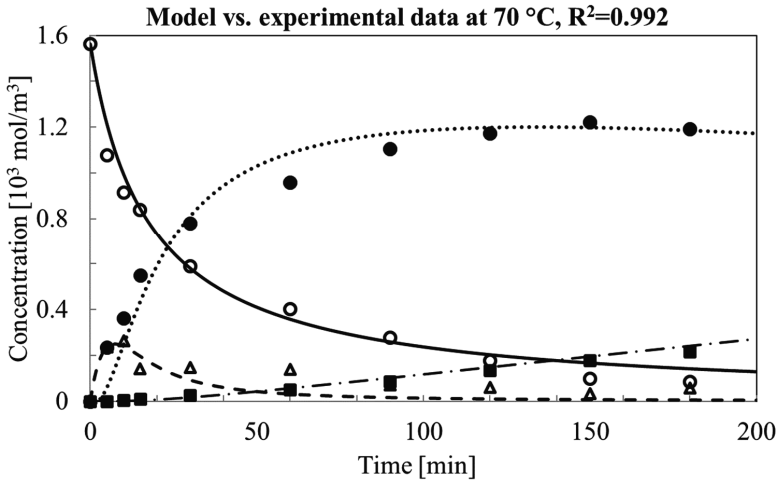

Figure 2.2: Concentration-time history of syringaldehyde **1** (○), sinapinic dicarboxylic acid **3** (Δ), sinapinic acid **5** (●), and HDMS **7** (■) at the optimal temperature of 70 °C. Malonic acid **2** could not be measured at a wavelength of 300 nm. Lines represent the best fit using equations [4-7] and the rate coefficients collected in Table 2.1.

As shown in Table 2.1, the reaction rate constants increase with increasing temperature, according to the Arrhenius equation, see equation [8].

$$k = A \cdot \exp\left(\frac{-E_a}{RT}\right) \qquad [8]$$

As a rule of thumb in most biological and chemical reactions, the reaction rate doubles when the temperature increases every 10 degrees Celsius. When plotting ln(k) against 1/T, as shown in Figure 2.3, the values for the activation energy (E_a) and the pre-exponential factor (A) can be determined.

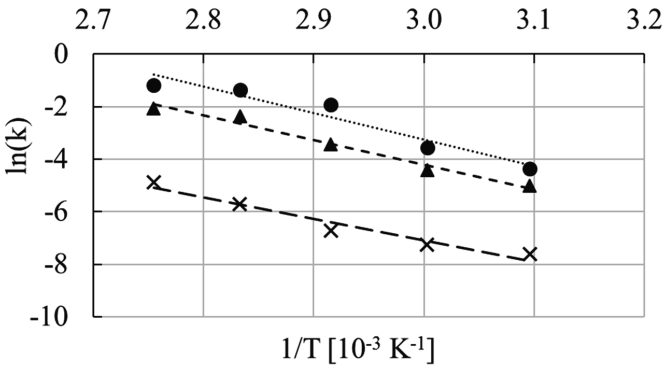

Figure 2.3: Global estimated rate coefficients $k_2^{(1)}$ (▲), $k_1^{(2)}$ (●), and $k_1^{(3)}$ (×) for the Knoevenagel-Doebner condensation of syringaldehyde **1** with malonic acid **2** towards sinapinic acid **5**, followed by a second decarboxylation leading to HDMS **7**.

The values for the activation energy (E_a) and the pre-exponential factor (A) of the three separate reactions are presented in Table 2.2.

Table 2.2: The activation energies and pre-exponential factors for reaction rate constant temperature dependency for the Knoevenagel-Doebner reaction of syringaldehyde.

Reaction	**E_a (kJ/mol)**	**A**	**R^2**
1 = condensation step	78.0	23×10^9 [m^3/(mol·s)]	0.98
2 = first decarboxylation	84.4	0.64×10^{12} [1/s]	0.94
3 = second decarboxylation	68.6	46×10^6 [1/s]	0.96

It has to be emphasized, however, that the first reaction step (condensation step 1) in this global kinetic model, comprises various fundamental reaction steps such as the carbon-carbon coupling and dehydration step (and probably the formation of catalytic intermediates). The condensation step 1 covers the principal difference between the mechanism of Hann and Lapworth[11] (often with an excess of the catalyst) and the mechanism of Knoevenagel[9,10] (with catalytic quantities). This first condensation step demands further investigations in additional research to unravel the detailed mechanism.

2.3 Conclusions

This study supports the mechanism for the Knoevenagel-Doebner reaction of syringaldehyde and malonic acid, as proposed by Aldabalde *et al*.[18] The formation of the 4-vinylphenolic product HDMS **7** via a second decarboxylation step was found to be inhibited by performing the reaction at a temperature of 80 °C or lower. On this experience, the Knoevenagel-Doebner reaction is optimized for the production of sinapinic acid **5**. The optimal conversion for sinapinic acid **5** was 78% after 2.5 hours at 70 °C. To gain more insight into the mechanism of the Knoevenagel-Doebner condensation of syringaldehyde, we developed a global kinetic model for the complete set of reactions. In the present protocol, pyridine is mainly used as a solvent. Because of the environmental impact of pyridine, it would be worthwhile to reduce or eliminate its use and investigate alternatives.

2.4 Experimental section

2.4.1 General remarks

Reagents: Syringaldehyde (**1**), and all other chemicals (99% purity) were purchased from Sigma-Aldrich and were used as received. DMSO-*d6* was purchased from Cambridge Isotope, with 99 atom% deuterated.

Instrumentation: ^{1}H NMR spectroscopy measurements were performed on an Agilent 400-MHz NMR system with DMSO-*d6* as a solvent. Chemical shifts are reported in ppm, relative to tetramethylsilane (TMS).

HPLC analysis was carried out using a reversed-phase liquid chromatographic system (Agilent 1100 series) equipped with a diode array detector operating at 300 nm (Agilent 1100 series) and an autosampler injector with a 20 µL loop (Agilent 1100 series G1316A). The system was equipped with a Grace Alltima C18 5 µm column (250 mm × 4.6 mm). The determination of the concentration of the components in the reaction mixtures was carried out by the external standard method and was based on peak areas. HPLC measurements were made with the following settings: Flowrate 1.0 mL/min at a temperature of 25 °C, eluent A = methanol, eluent B = acetic acid buffer (99% milliQ, 1% acetic acid). The samples were eluted using the following gradient: 40% A and 60% B set for 6 min, gradient to 100% A and 0% B in subsequent 10 min, 100% A and 0% B set for 5 min, followed by 40% A and 60% B set for 8 min.

LC-MS analysis was performed using a liquid chromatographic system (Agilent 1100 series) equipped with a Luna 3 µm C18 column (200 × 2.0 mm) and an ion trap (Agilent 6300 series).

Melting points were determined on a Büchi Melting Point B-540 apparatus.

2.4.2 Experimental procedures

Protocol for the Knoevenagel-Doebner condensation: Malonic acid (1.0 g, 10 mmol) was dissolved in pyridine (3.0 mL, 37 mmol). Syringaldehyde (**1**, 0.90 g, 5 mmol) and piperidine (0.10 mL, 1 mmol) were subsequently added. The reaction was heated to the desired temperature and 50.0 µL samples were taken for reversed-phase HPLC analysis. The samples were immediately diluted in 7.5 mL methanol, filtered, and analyzed using the method described in section 2.4.1. The calculated percentage of the peak area of the component of interest is in relation to the total area of peaks.

After 3 hours, the reaction was stopped, and pyridine was removed in vacuo. The residue was dissolved in a small amount of a saturated aqueous $NaHCO_3$-solution and acidified to a pH of 2 with 6 M HCl. The resulting precipitate was separated by filtration and washed with water. After recrystallization in a mixture of water and ethanol (v/v) (3:1), the crystals were separated by filtration and dried in a nitrogen atmosphere. 4-Hydroxy-3,5-dimethoxy styrene **7** was purified with column chromatography with ethyl acetate as eluent and silica gel as the stationary phase.

2.4.3 Characterization

2-[(4-hydroxy-3,5 dimethoxyphenyl) methylene]-propanedioic acid (3)

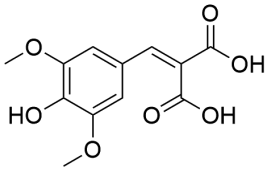

Light yellow solid, decomposes at 174 °C.
^{1}H NMR (400 MHz, DMSO) δ (ppm) = 13.09 (s, 2H), 9.10 (s, 1H), 7.43 (s, 1H), 6.95 (s, 2H), 3.74 (s, 6H)
MS (ESI) M calculated: 268.22 g/mol; *m/z* observed $[M-H]^-$: 266.8

3-(4-hydroxy-3,5-dimethoxyphenyl) prop-2-enoic acid (5)

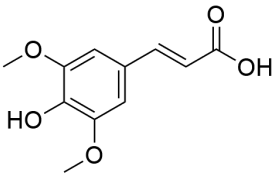

Light yellow solid, m.p. = 198-199 °C.
^{1}H NMR (400 MHz, DMSO) δ (ppm) = 12.10 (s, 1H), 8.88 (s, 1H), 7.47 (d, J = 15.9 Hz, 1H), 6.97 (s, 2H), 6.40 (d, J = 15.9 Hz, 1H), 3.78 (s, 6H)
^{13}C NMR (101 MHz, DMSO) δ (ppm) = 168.50, 148.50, 145.32, 138.52, 125.11, 116.53, 106.48, 56.49.
MS (ESI) M calculated: 224.21 g/mol; *m/z* observed $[M+H]^+$: 225 $[M-H]^-$: 223

4-hydroxy-3,5-dimethoxy styrene (7)

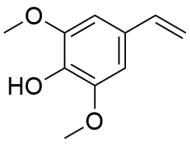

Isolated as a brown liquid.
^{1}H NMR (400 MHz, DMSO) δ (ppm) = 6.72 (s, 2H), 6.63 (d, 1H), 5.61 (dd, 1H), 5.35 (s, 1H), 5.18 (dd, 1H), 3.85 (s, 6H).
MS (ESI) M calculated: 180.20 g/mol; *m/z* observed $[M-H]^-$: 178.8

2.5 References

1. Mase, N.; Horibe, T. Organocatalytic Knoevenagel condensations by means of carbamic acid ammonium salts. *Organic letters* **2013***, 15*, 1854-1857.
2. Pawar, H. S.; Wagh, A. S.; Lali, A. M. Triethylamine: a potential N-base surrogate for pyridine in Knoevenagel condensation of aromatic aldehydes and malonic acid. *New J. Chem* **2016***, 40*, 4962-4968.
3. Khare, R.; Pandey, J.; Smriti, S.; Ruchi, R. The Importance and Applications of Knoevenagel Reaction. *Oriental Journal of Chemistry* **2019***, 35*, 423-429.
4. List, B. Emil Knoevenagel and the Roots of Aminocatalysis. *Angewandte Chemie (International ed. in English)* **2010***, 49*, 1730-1734.
5. Kwak, G.; Fujiki, M. Colored and Luminous Aliphatic Polyester via One-Pot Intra- and Intermolecular Knoevenagel Reactions. *Macromolecules* **2004***, 37*, 2021-2025.
6. Ranu, B. C.; Jana, R. Ionic Liquid as Catalyst and Reaction Medium - A Simple, Efficient and Green Procedure for Knoevenagel Condensation of Aliphatic and Aromatic Carbonyl Compounds Using a Task-Specific Basic Ionic Liquid. *European Journal of Organic Chemistry* **2006***, 2006*, 3767-3770.
7. Lu, J.; Toy, P. Organocatalytic Decarboxylative Doebner-Knoevenagel Reactions between Arylaldehydes and Monoethyl Malonate Mediated by a Bifunctional Polymeric Catalyst. *Synlett* **2011***, 2011*, 1723-1726.
8. Rodionow, W. M. The mechanism of Knoevenagel's synthesis of cinnamic acids. *Journal of the American Chemical Society* **1929***, 51*, 847-852.
9. Knoevenagel, E. Condensation von Malonsäure mit aromatischen Aldehyden durch Ammoniak und Amine. *Berichte der deutschen chemischen Gesellschaft* **1898***, 31*, 2596-2619.
10. Knoevenagel, E. Condensation zwischen Malonester und Aldehyden unter dem Einfluss von Ammoniak und organischen Aminen. *Berichte der deutschen chemischen Gesellschaft* **1898***, 31*, 2585-2595.
11. Hann, A. C. O.; Lapworth, A. VII. Optically active esters of β-ketonic and β-aldehydic acids. Part IV. Condensation of aldehydes with menthyl acetoacetate. *Journal of the Chemical Society, Transactions* **1904***, 85*, 46-56.
12. Doebner, O. Synthese der Sorbinsäure. *Berichte der deutschen chemischen Gesellschaft* **1900***, 33*, 2140-2142.
13. Trotzki, R.; Hoffmann, M. M.; Ondruschka, B. Studies on the solvent-free and waste-free Knoevenagel condensation. *Green Chemistry* **2008***, 1*, 767-772.
14. Gupta, M.; Wakhloo, B. P. Tetrabutylammoniumbromide mediated Knoevenagel condensation in water: synthesis of cinnamic acids. *Coordination Chemistry Reviews* **2008**, *252*, 1420-1450.
15. Leelavathi, P.; Kumar, S. R. Niobium (V) chloride catalyzed Knoevenagel condensation: An efficient protocol for the preparation of electrophilic alkenes. *Journal of Molecular Catalysis. A, Chemical* **2005***, 240*, 99-102.
16. Nokami, J.; Kataoka, K.; Shiraishi, K.; Osafune, M.; Hussain, I.; Sumida, S. Convenient formation of 4-hydroxyalk-2-en-1-one functionality via A knoevenagel-type carbon chain elongation reaction of aldehyde with 1-arylsulfinylalkan-2-one. *The Journal of organic chemistry* **2001***, 66*, 1228-1232.
17. Ogiwara, Y.; Takahashi, K.; Kitazawa, T.; Sakai, N. Indium(III)-catalyzed knoevenagel condensation of aldehydes and activated methylenes using acetic anhydride as a promoter. *The Journal of organic chemistry* **2015***, 80*, 3101-3110.
18. Aldabalde, V. Organocatalyzed Decarboxylation of Naturally Occurring Cinnamic Acids: Potential Role in Flavoring Chemicals Production. *Open Journal of Physical Chemistry* **2011***, 1*, 85-93.
19. Simpson, C. J.; Fitzhenry, M. J.; Stamford, N. P. J. Preparation of vinylphenols from 2- and 4-hydroxybenzaldehydes. *Tetrahedron Letters* **2005***, 46*, 6893-6896.

20. FitzPatrick, M.; Champagne, P.; Cunningham, M. F.; Whitney, R. A. A biorefinery processing perspective: Treatment of lignocellulosic materials for the production of value-added products. *Bioresource Technology* **2010***, 101*, 8915-8922.
21. Ou, S.; Kwok, K. Ferulic acid: pharmaceutical functions, preparation and applications in foods. *Journal of the Science of Food and Agriculture* **2004***, 84*, 1261-1269.
22. De, P.; Koumba Yoya, G.; Constant, P.; Bedos-Belval, F.; Duran, H.; Saffon, N.; Daffé, M.; Baltas, M. Design, synthesis, and biological evaluation of new cinnamic derivatives as antituberculosis agents. *Journal of medicinal chemistry* **2011***, 54*, 1449-1461.
23. Cuvelier, M.; Richard, H.; Berset, C. Comparison of the Antioxidative Activity of Some Acid-phenols: Structure-Activity Relationship. *Bioscience, Biotechnology, and Biochemistry* **1992***, 56*, 324-325.
24. Nićiforović, N.; Abramovič, H. Sinapic Acid and Its Derivatives: Natural Sources and Bioactivity. *Comprehensive Reviews in Food Science and Food Safety* **2014***, 13*, 34-51.
25. Anastas, P. T., Warner, J. C. *Green chemistry: theory and practice;* Oxford University Press: New York, 1998; .
26. Yang, X.; Shen, Y. Runge-Kutta Method for Solving Uncertain Differential Equations. *J. Uncertain. Anal. Appl* **2015***, 3*, 1-12.

3 The Green Knoevenagel condensation: solvent-free condensation of benzaldehydes

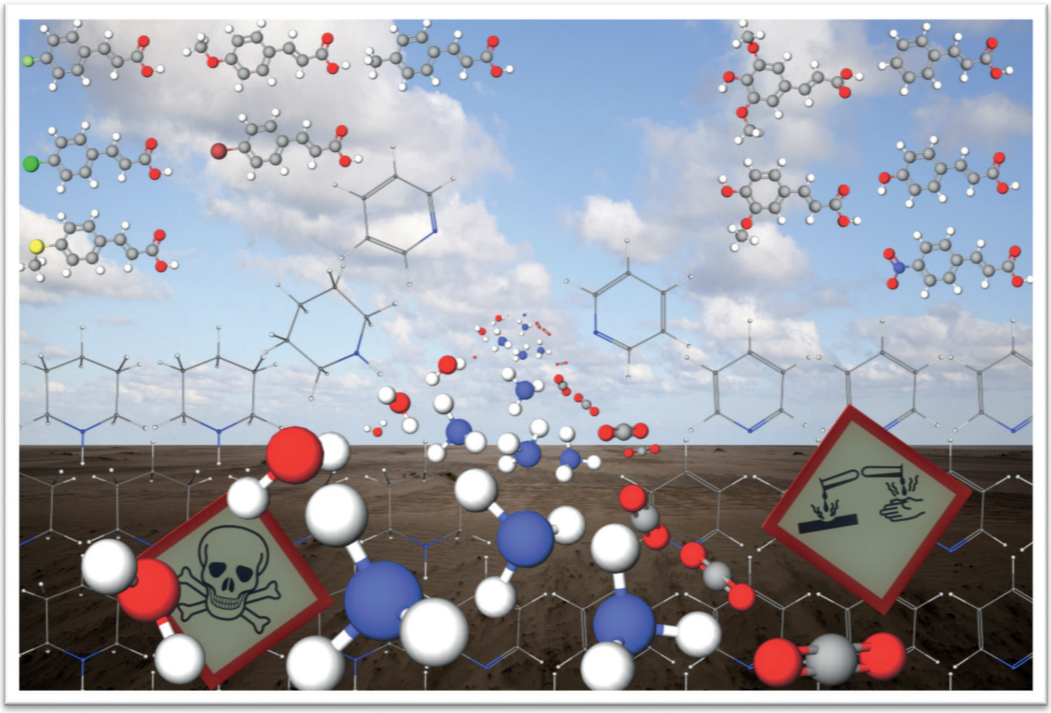

This chapter is based on:

van Schijndel, J.; Current Organic Synthesis **2019**, *16*, 130-135.
(DOI: 10.2174/1570179415666180924124134)

van Schijndel, J.; Green Chemistry Letters and Reviews **2017**, *10*, 404-411.
(DOI:10.1080/17518253.2017.1391881)

Abstract

In this chapter, a novel, Green Knoevenagel procedure for the chemical transformation of benzaldehydes into their corresponding α,β-unsaturated acids, is presented. The essential part of this procedure is a solvent-free reaction that uses environmentally benign amines or ammonium salts as catalysts instead of pyridine and piperidine as used in the traditional Knoevenagel-Doebner reaction. The condensation step is followed by a decarboxylation in the solid phase, resulting in high overall yields and purity. The influence of temperature and catalyst type on the yield of sinapinic acid was monitored for the reaction between syringaldehyde and malonic acid. After optimization of this reaction, its scope was explored for various types of benzaldehydes, demonstrating the broad applicability of this procedure. The developed method provides good to an excellent conversion of various benzaldehydes and high selectivity to the respective α,β-unsaturated acids in an environmentally friendly and efficient way.

3.1 Introduction

The Knoevenagel condensation is one of the most important methodologies for carbon-carbon double-bond formation in synthetic organic chemistry. It is the most commonly used method for the production of various α,β-unsaturated acids, usually referred to as cinnamic acids.[1] These cinnamic acids are essential intermediates for the synthesis of natural and therapeutic drugs, polymers, cosmetics and perfumes.[2-5] Knoevenagel found that primary and secondary amines, as well as their salts, catalyze the aldol condensation of β-ketoesters or malonates with aldehydes. Generally, the Knoevenagel-Doebner reactions are carried out by the condensation of an active methylene compound with an aldehyde using large amounts of pyridine as solvent and piperidine as organocatalyst (Scheme 3.1).[6]

For a variety of reasons, the use of pyridine as a solvent is not acceptable and should be significantly reduced or eliminated.[7,8] Pyridine is toxic and represents a significant health risk above a vapor concentration of 3500 ppm.[9] The use of ionic liquids has been examined as an alternative because of their unique properties, e.g., excellent solubility, non-flammability, negligible vapor pressure, and recyclability.[10] However, their industrial application is limited due to their high cost.[11] Another possibility is to exclude the solvent completely from the reaction medium.[12] These so-called solvent-free conditions can lead to additional improvements such as the reduced amount of catalyst needed, increased reaction rate, and higher yield.[13] It is believed that solvent-free organic transformations are industrially useful and fit well with the principles of Green Chemistry.[14,15]

Various examples limit the exposure to the catalyst piperidine by coupling piperidine to a solid support[16] or by applying alternative organocatalysts such as dimethylamino pyridine and 1,2-diaminoethane.[17-19] Strikingly enough, "Knoevenagel protocols" have been developed that use Lewis acids such as LiOH, $ZnCl_2$, $InCl_3$, $TiCl_4$, $NbCl_5$,[20-22] and various heterogeneous solid bases as a catalyst.[23] Knoevenagel only used primary and secondary amines, and the use of heavy metals for the synthesis of food and pharmaceutical products is not desirable because of their toxicity.[24]

The current procedure of the Knoevenagel-Doebner reaction can be improved further, directed towards an environmentally friendly, efficient, and operationally simple reaction. Often microwave reactions are used, but these also have their limitations on scalability, applicability, and energy use.[25-28]

In this chapter, therefore, the possibilities are explored to conduct the Knoevenagel-Doebner reaction of syringaldehyde, and malonic acid without pyridine and piperidine using a solvent-free condensation which employs environmentally benign amines and ammonium salts as catalysts.[29] After the reaction has been optimized for syringaldehyde, the scope of the method will be explored using various benzaldehydes with different electron-donating or electron-withdrawing groups, see Scheme 3.1.

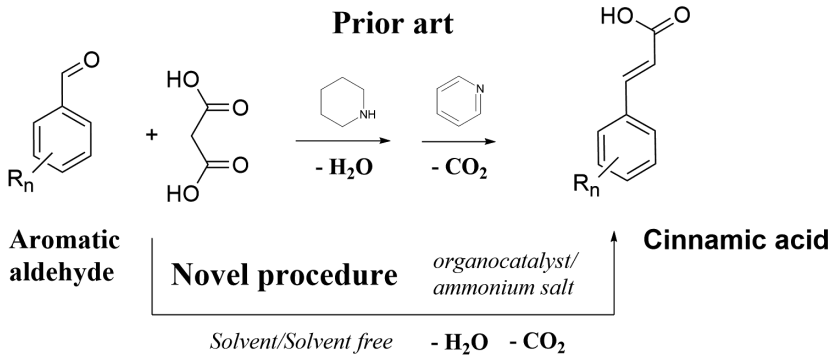

Scheme 3.1: General reaction scheme for the pyridine-free synthesis of cinnamic acids.

3.2 Results and discussion

As stated before, the Knoevenagel-Doebner reaction is traditionally carried out using pyridine as solvent and piperidine as an organocatalyst. In our initial efforts to develop an environmentally friendly procedure, we explored the possibility of performing a pyridine-free condensation between syringaldehyde **1a** and malonic acid using piperidine as a catalyst in refluxing water, ethanol and ethyl acetate (Scheme 3.2). The concentration of syringaldehyde in solution at different times was monitored using HPLC analysis. We observed that sinapinic dicarboxylic acid **2a** was initially formed to a limited extent, followed by a quick decarboxylation resulting in sinapinic acid **3a**. As previously reported by our research group,[30] the formation of 4-hydroxy-3,5-dimethoxy styrene (HDMS) **4a** was avoided at this relatively low temperature. High conversion towards sinapinic acid (>97%) was obtained after 7 hours in refluxing ethyl acetate (Figure 3.1).

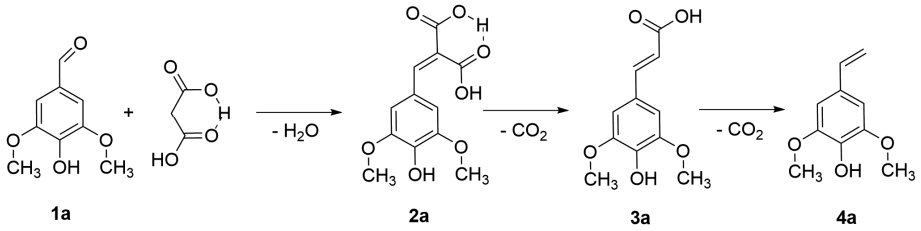

Scheme 3.2: Reaction scheme of syringaldehyde with malonic acid.

When sinapinic acid was subsequently isolated from the different HPLC samples by evaporation of the solvent, much higher yields were obtained compared to the conversions from the HPLC measurements in solution. This observation gave rise to the idea that the evaporation of the solvent itself might promote the conversion of syringaldehyde towards sinapinic acid or that the reaction might proceed after the solvent has been removed.

In order to test this hypothesis, a new protocol was performed where syringaldehyde, malonic acid, and piperidine were dissolved in ethyl acetate, and the mixture was immediately concentrated in vacuo at 40 °C to obtain an adequate mixing of the solids. After ethyl acetate had been removed, the resulting solvent-free mixture was placed at 77 °C, and the conversion of syringaldehyde was measured using HPLC, as demonstrated in Figure 3.1. Immediately after removal of the solvent (t=0 h), the conversion of syringaldehyde was negligible. Once the solvent-free mixture was placed at 77 °C, however, we observed a much faster

conversion of syringaldehyde towards sinapinic acid than what was observed in the solution. The step in which the reactants are mixed in solution preceding the solvent-free reaction can be skipped when working on a small scale. When working with larger badges, however, sufficient mixing in the solid-state could not be accomplished, resulting in varying conversions and yields. Therefore, all subsequent reactions are first mixed properly in ethyl acetate before the solvent-free reaction step.

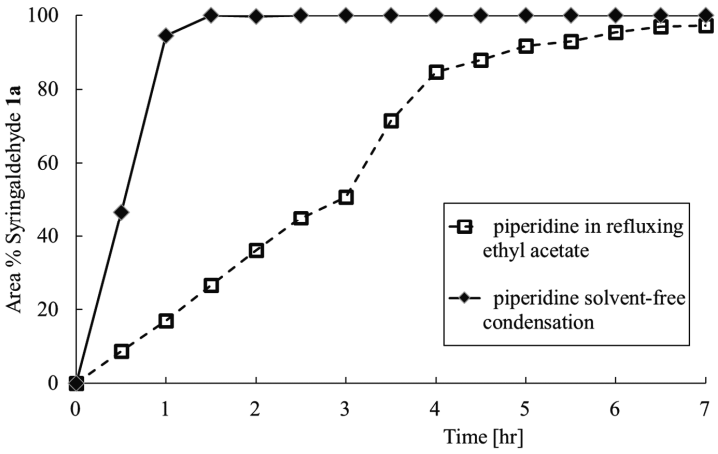

Figure 3.1: Conversion of syringaldehyde **1a** in time in the solution and the solid-state. Reagents and conditions in solution: syringaldehyde **1a**, 2 eq. malonic acid, and 0.4 eq. piperidine in ethyl acetate at 77 °C. Reagents and conditions in the solid-state: mixture, as mentioned above, was concentrated in vacuo at 40 °C; the resulting solvent-free mixture was heated at 77 °C. Reported conversions are based on the ratio of peaks of the HPLC chromatogram.

To investigate the influence of the temperature after the removal of the solvent, the temperature at which the solvent-free mixture was kept, was varied between 40 °C and 130 °C as demonstrated in Figure 3.2. Higher temperatures increased the conversion rate of syringaldehyde **1a**. At temperatures below 50 °C, a low syringaldehyde conversion resulted only in sinapinic dicarboxylic acid **2a**. At 90 °C, complete conversion of syringaldehyde is reached after 120 minutes with almost 100% selectivity towards sinapinic acid **3a**. At higher temperatures, the yield of sinapinic acid decreases because of a second decarboxylation reaction resulting in the also valuable 4-hydroxy-3,5-dimethoxy styrene (HDMS) **4a**, which in turn is followed by the formation of its dimers and trimers of this by-product.

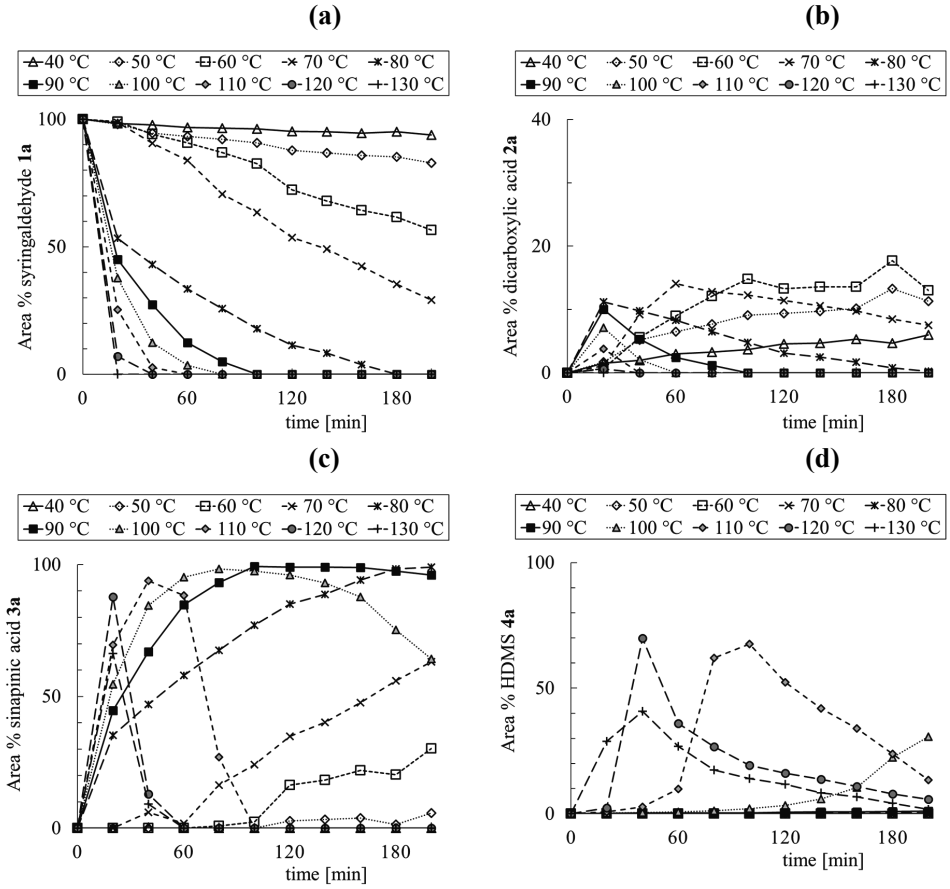

Figure 3.2: Concentration-time profiles of (a) syringaldehyde **1a**, (b) sinapinic dicarboxylic acid **2a**, (c) sinapinic acid **3a**, and (d) 4-hydroxy-3,5-dimethoxy styrene **4a** as a function of time at various reaction temperatures. Reagents and conditions: syringaldehyde, 2 eq. malonic acid, and 0.4 eq. piperidine in ethyl acetate; concentrated in vacuo at 40 °C; resulting solvent-free mixture was heated at specified temperatures. Reported conversions and yields are based on the ratio of peaks of the HPLC chromatogram at 300 nm.

This fast and straightforward solvent-free procedure demonstrates that pyridine is no longer necessary as a solvent in this novel Knoevenagel condensation. Subsequently, we investigated also the possibility of replacing piperidine as the catalyst while using the optimized conditions from Figure 3.2, i.e., 90 °C and 2 hours. The outright omission of piperidine resulted in a much lower reaction rate and yield of sinapinic acid (Table 3.1), demonstrating the role of piperidine as the catalyst. Next, a variety of amines and ammonium salts were tested as an alternative catalyst.

Table 3.1: Conversion of syringaldehyde **1a** and yield of sinapinic acid **3a** with different catalysts. Reagents and conditions: syringaldehyde, 2 eq. malonic acid and 0.4 eq. of the specified catalyst in ethyl acetate; concentrated in vacuo at 40 °C; resulting solvent-free mixture is heated at 90 °C for 2h. Reported conversions and yields are based on the ratio of peaks of the HPLC chromatogram at 300 nm.

	Decarboxylation (2h; 90 °C)	
Catalyst	**Conversion (%)**	**HPLC area yield (%)**
no catalyst*	43	15
piperidine	**100**	**99**
n-butylamine	88	85
dibutylamine	72	84
triethylamine	87	77
1,2-diaminoethane	**100**	**100**
2-amino-ethanol	**95**	**94**
TRIS	60	15
pyridine	88	87
benzylamine	**100**	**99**
urea	99	22
glycine	57	39
ammonium iodide	60	33
ammonium sulphate	**98**	**96**
ammonium chloride	**100**	**92**
ammonium bicarbonate	**100**	**100**

** After 23 hours a conversion of 91% is achieved and a 61% yield of sinapinic acid is reached (and 22% of sinapinic dicarboxylic acid)*

The first replacements for piperidine, which were tested, were other aliphatic amines. No apparent differences were observed between primary (butylamine), secondary (dibutyl amine), and tertiary amines (triethylamine). The diamine (1,2-diaminoethane) gave very high conversion and yields of sinapinic acid but is very toxic. However, it can successfully be replaced by the less toxic 2-amino-ethanol. The commonly used hydroxylamine TRIS (2-amino-2-hydroxymethyl-propane-1,3-diol), on the other hand, performed relatively poorly.

There are several claims in the literature [1,9,18,28] that pyridine is not only a solvent in the traditional Knoevenagel-Doebner reaction but also acts as a catalyst. In the case of the solvent-free procedure, this was confirmed. Besides pyridine, benzylamine was taken as an alternative aromatic amine, which gave better results compared to pyridine. Urea and glycine were also screened as benign alternatives to piperidine but showed lower activity than the preceding amines.

Because these results suggested that the presence of nitrogen is the only essential prerequisite for the catalyst in the condensation reaction of the Knoevenagel reaction, several ammonium salts were screened. It was striking that these benign ammonium salts also gave high conversion and yields of sinapinic acid. We expect that the dissociation of the ammonium salts at higher temperatures results in the formation of ammonia, which serves as a nitrogen-based catalyst. Based on these observations, ammonium bicarbonate (NH_4HCO_3) was selected as the catalyst for further optimization of the reaction.

The traditional Knoevenagel-Doebner reaction in solution requires a substantial molar excess of malonic acid to obtain high yields. As a final step in the optimization of this new solvent-free procedure, a reduction of the amount of malonic acid used for the reaction was attempted. Reducing the amount of malonic acid from 2.0 equivalents to 1.2 equivalents had no adverse effect on the reaction rate, conversion, or yield. When the amount of malonic acid was reduced further to 1.0 equivalent, a drop in the reaction rate was observed. Therefore, the molar ratio of syringaldehyde and malonic acid was set at 1.2 for larger-scale experiments and the application of the solvent-free condensation reaction on other benzaldehydes.

Solvent-free reactions can be hard to scale-up because of poor heat transfer and insufficient mixing. However, this green solvent-free Knoevenagel condensation did not show a drop in performance on 100 mmol (18 gram) of syringaldehyde. Furthermore, we were able to obtain sinapinic acid with a yield of 90% yield after recrystallization. It is noteworthy that this two-step procedure, composed of a Green Knoevenagel condensation, followed by decarboxylation results in an E-factor below 1 for the crude sinapinic acid. The E-factor is an indication of waste production where a higher number means more substantial waste. It can be calculated by taking the total material input, subtracting the amount of the desired product, and dividing the whole by the amount of the desired product. Because this synthesis doesn't use any solvent (the mixing-step with ethyl acetate can be omitted) and because the condensation reaction is atom-efficient the E-factor equals ((18 g + 12 g + 1.58 g) – 20.2 g) / 20.2 g = 0.56.

This E-factor is exceptionally low for a transformation that produces fine chemicals that typically have an E-factor in the range of 5-100.[13,31] The environmental impact of waste is not only determined by its amount, however, but also by its nature. NH_4HCO_3 can be considered as a solid which decomposes in three different components CO_2, H_2O, and NH_3 above 60 °C.[32] Because the environmental impact of these three components is relatively low, the unfriendliness quotient Q[33] is probably also low but needs further investigation.

To investigate the scope of the solvent-free Knoevenagel condensation, various derivatives of benzaldehydes were screened using the optimized reaction conditions of syringaldehyde (Table 3.2). Overall, high conversion of the aromatic aldehydes was achieved at 90 °C after 2 hours, and there was no apparent difference between electron-withdrawing and electron-donating groups at the para-position of the benzaldehyde. In most cases, the corresponding cinnamic dicarboxylic acid (**2**) was the main product. The temperature of the reaction was therefore raised to 140 °C, promoting the required decarboxylation leading to the respective cinnamic acids. For entries 1b-1i, this resulted in the formation of the proper cinnamic acids (**3**). For the entries with a hydroxyl group on the para-position (**3a**, **3j**, and **3k**), this resulted in a second decarboxylation leading to the corresponding styrene-analogs (**4**) (and their dimers and trimers). The second decarboxylation (and polymerization) is probably accelerated by the formation of the transient quinone-like structures of **3a**, **3j**, and **3k** and seems to depend on the amount number of methoxy-groups on the aromatic ring.[34]

Furthermore, it was remarkable that **3l** was already fully converted to the styrene-variant at 90 °C. The second decarboxylation, in this case, is probably accelerated by the formation of the transient iminium ion-like structure of **3l**. The benzaldehydes missing a hydroxyl or amine group on the para-position are less susceptible to a second decarboxylation and are therefore very suitable to be converted by this procedure to their corresponding cinnamic acids.

Table 3.2: Conversion of various benzaldehydes. Conversions and yields are based on the ratio of peaks of the HPLC chromatogram at 300 nm. Reagents and conditions: syringaldehyde, 1.2 eq. malonic acid, and 0.4 eq. ammonium bicarbonate in minimum amount ethyl acetate; concentrated in vacuo at 40 °C; resulting solvent-free mixture was heated at either 90 °C or 140 °C for 2h.

Entry	Aldehyde	Conversion (2h, 90 °C)	HPLC area % towards 2 (2h, 90 °C)	HPLC area % towards 3 (2h, 90 °C)	HPLC area % towards 4 (2h, 90 °C)	HPLC area% towards 2 (2h, 140 °C)	HPLC area% towards 3 (2h, 140 °C)	HPLC area% towards 4 (2h, 140 °C)	Isolated yield towards 3 %
1a	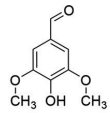	99	1	**98**	0	0	0	98	**91**
1b		99	61	36	0	0	**92**	0	**86**
1c	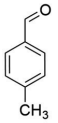	100	88	12	0	0	**96**	0	**85**
1d	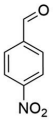	89	83	6	0	1	**82**	0	**75**
1e	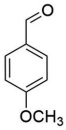	100	86	12	0	0	**71**	0	**65**
1f	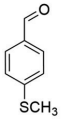	87	33	50	0	0	**85**	0	**81**
1g	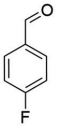	100	64	36	0	0	**99**	0	**91**
1h	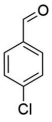	100	62	38	0	1	**95**	0	**89**
1i	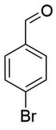	99	66	34	0	0	**95**	0	**85**
1j	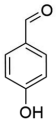	91	42	**47**	0	0	0	97	**88***
1k	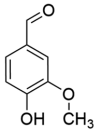	93	12	**77**	0	0	0	98	**89***
1l	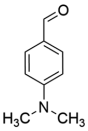	97	0	3	**94**	0	0	99	-

*After optimization of the reaction conditions at 120 °C and 105 °C respectively

In summary, it was found that a wide array of benzaldehydes can be used in this solvent-free Knoevenagel condensation with ammonium bicarbonate, although differences in reactivity are observed. However, the selectivity of the reaction can be controlled by optimizing the reaction time and temperature. The benzaldehydes missing a hydroxyl or amine group on the para-position are less susceptible to a second decarboxylation and are therefore very suitable to be converted by this procedure to their corresponding cinnamic acids.

3.3 Conclusions

This chapter reports the development of a greener version of the Knoevenagel-Doebner reaction using benign amines or ammonium salts as the catalysts. The use of pyridine and piperidine is avoided, and the required excess of malonic acid is limited. The developed method with ammonium bicarbonate as catalyst provides good to an excellent conversion of various benzaldehydes and high yields of the corresponding cinnamic acids in an efficient, rapid, and environmentally friendly way.

3.4 Experimental section

3.4.1 General remarks

Reagents: Syringaldehyde (**1**), and all other chemicals (99% purity) were purchased from Sigma-Aldrich and were used as received. DMSO-*d6* was purchased from Cambridge Isotope, with 99 atom% deuterated.

Instrumentation: ^{1}H NMR spectroscopy measurements were performed on an Agilent 400-MHz NMR system with DMSO-*d6* as a solvent. Chemical shifts are reported in ppm, relative to tetramethylsilane (TMS).

HPLC analysis was carried out using a reversed-phase liquid chromatographic system (Agilent 1100 series) equipped with a diode array detector operating at 300 nm (Agilent 1100 series) and an autosampler injector with a 20 µL loop (Agilent 1100 series G1316A). The system was equipped with a Grace Alltima C18 5 µm column (250 mm × 4.6 mm). The determination of the concentration of the components in the reaction mixtures was carried out by the external standard method and was based on peak areas. HPLC measurements were made with the following settings: Flowrate 1.0 mL/min at a temperature of 25 °C, eluent A = methanol, eluent B = acetic acid buffer (99% milliQ, 1% acetic acid). The samples were eluted using the following gradient: 40% A and 60% B set for 6 min, gradient

to 100% A and 0% B in subsequent 10 min, 100% A and 0% B set for 5 min, followed by 40% A and 60% B set for 8 min.

LC-MS analysis was performed using a liquid chromatographic system (Agilent 1100 series) equipped with a Luna 3 µm C18 column (200 × 2.0 mm) and an ion trap (Agilent 6300 series).

Thermogravimetric analysis (TGA) was performed on a Q50 TA Instruments TGA, using nitrogen as a purge gas, at a heating rate of 20 °C/min in the range of 0-600 °C.

Melting points were determined with the Hanon Automatic Video Melting Point apparatus MP450.

3.4.2 Experimental procedures

Protocol for optimized Knoevenagel reaction: Malonic acid (1.0 g, 10 mmol) was dissolved in a minimum amount (e.g., 2.5 mL) of solvent (often ethyl acetate although ethanol and water were also used). Syringaldehyde (**1a**, 0.90 g, 5 mmol) and piperidine (0.20 mL, 2 mmol) were subsequently added. Then the solvent (ethyl acetate) was removed by distillation under reduced pressure at 40°C. The solid was kept for 2 hours at 90°C for complete conversion. Samples were taken for reversed-phase HPLC analysis and diluted in 7.5 mL methanol, filtered, and analyzed using the method described in section 2.2. The calculated percentage of the peak area of the component of interest is in relation to the total area of peaks. In the workup to sinapinic acid, the residue was dissolved in 10 mL of a saturated aqueous $NaHCO_3$-solution and subsequently acidified to a pH of 2 by using 6 M HCl. The resulting precipitate was separated by filtration and washed with (demineralized) water. After recrystallization in a mixture of water-ethanol (4:1, v/v), the crystals were separated by filtration, dried using a suction pump, and dried at 60°C in a vacuum oven.

3.4.3 Characterization

2-[(4-hydroxy-3,5 dimethoxyphenyl) methylene]-propanedioic acid (2a)

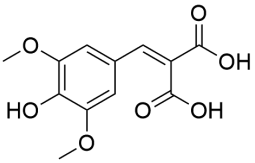

Light yellow solid, decomposes at 174 °C.

^{1}H NMR (400 MHz, DMSO) δ (ppm) = 13.09 (s, 2H), 9.10 (s, 1H), 7.43 (s, 1H), 6.95 (s, 2H), 3.74 (s, 6H)

^{13}C NMR (101 MHz, DMSO) δ (ppm) = 169.18, 166.08, 148.32, 139.99, 138.86, 125.46, 123.34, 108.04, 56.43.

MS (ESI) M calculated: 268.22 g/mol; *m/z* observed $[M+H]^{+}$: 269 $[M-H]^{-}$: 267

3-(4-hydroxy-3,5-dimethoxyphenyl) prop-2-enoic acid (3a)

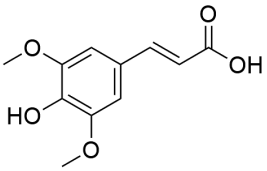

Light yellow solid, m.p. = 198-199 °C.

^{1}H NMR (400 MHz, DMSO) δ (ppm) = 12.10 (s, 1H), 8.88 (s, 1H), 7.47 (d, J = 15.9 Hz, 1H), 6.97 (s, 2H), 6.40 (d, J = 15.9 Hz, 1H), 3.78 (s, 6H)

^{13}C NMR (101 MHz, DMSO) δ (ppm) = 168.50, 148.50, 145.32, 138.52, 125.11, 116.53, 106.48, 56.49.

MS (ESI) M calculated: 224.21 g/mol; *m/z* observed $[M+H]^{+}$: 225 $[M-H]^{-}$: 223

(2E)-3-phenylprop-2-enoic acid (3b)

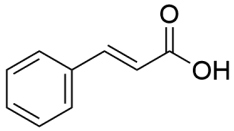

White solid, m.p. = 133-134 °C.

^{1}H NMR (400 MHz, DMSO) δ (ppm) = 12.41 (s, 1H), 7.74 – 7.64 (m, 2H), 7.60 (d, J = 16.0 Hz, 1H), 7.47 – 7.37 (m, 3H), 6.54 (d, J = 16.0 Hz, 1H).

^{13}C NMR (101 MHz, DMSO) δ (ppm) = 168.07, 144.38, 134.71, 130.63, 129.33, 128.62, 119.70.

MS (ESI) M calculated: 148.16 g/mol; *m/z* observed $[M+H]^{+}$: 149 $[M-H]^{-}$: 147

(E)-3-(4-methylphenyl)prop-2-enoic acid (3c)

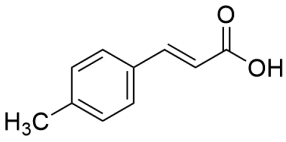

White solid, m.p. = 196 – 198 °C.

^{1}H NMR (400 MHz, DMSO) δ (ppm) = 12.30 (s, 1H), 7.56 (dd, J = 12.0, 8.4 Hz, 3H), 7.23 (d, J = 8.0 Hz, 2H), 6.46 (d, J = 16.0 Hz, 1H), 2.33 (s, 3H).

^{13}C NMR (101 MHz, DMSO) δ (ppm) = 168.16, 144.36, 140.58, 131.97, 129.96, 128.63, 118.58, 21.44.

MS (ESI) M calculated: 162.19 g/mol; *m/z* observed $[M+H]^+$: 163 $[M-H]^-$: 161

(E)-3-(4-nitrophenyl)prop-2-enoic acid (3d)

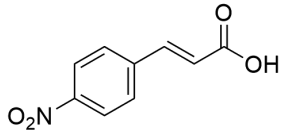

Yellow solid, decomposes at 274 °C.

^{1}H NMR (400 MHz, DMSO) δ (ppm) = 12.59 (s, 1H), 8.30 – 8.19 (m, 3H), 8.03 – 7.95 (m, 2H), 7.69 (dd, J = 13.4, 6.7 Hz, 2H), 6.76 (d, J = 16.1 Hz, 1H).

^{13}C NMR (101 MHz, DMSO) δ (ppm) = 167.58, 148.34, 141.56, 141.27, 129.69, 124.36.

MS (ESI) M calculated: 193.16 g/mol; *m/z* observed $[M+H]^+$: 194 $[M-H]^-$: 192

(E)-3-(4-methoxyphenyl)prop-2-enoic acid (3e)

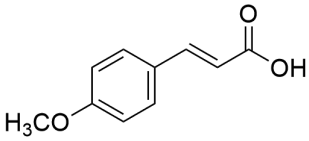

White solid, m.p. = 170-172 °C. **^{1}H NMR** (400 MHz, DMSO) δ (ppm) = 12.22 (s, 1H), 7.69 – 7.60 (m, 2H), 7.55 (d, J = 16.0 Hz, 1H), 7.01 – 6.94 (m, 2H), 6.38 (d, J = 16.0 Hz, 1H), 3.80 (s, 3H). **^{13}C NMR** (101 MHz, DMSO) δ (ppm) = 168.29, 161.39, 144.17, 130.37, 127.29, 116.99, 114.80, 55.73.

MS (ESI) M calculated: 178.18 g/mol; *m/z* observed $[M+H]^+$: 179 $[M-H]^-$: 177

(E)-3-(4-methylthiophenyl)prop-2-enoic acid (3f)

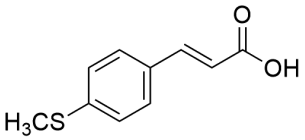

Light yellow solid, m.p. = 174 – 175 °C.

^{1}H NMR (400 MHz, DMSO) δ (ppm) = 12.32 (s, 1H), 7.62 (d, J = 8.4 Hz, 2H), 7.55 (d, J = 16.0 Hz, 1H), 7.27 (d, J = 8.4 Hz, 2H), 6.48 (d, J = 16.0 Hz, 1H), 2.54 – 2.48 (m, 3H).

^{13}C NMR (101 MHz, DMSO) δ (ppm) = 168.14, 143.91, 141.79, 129.13, 126.07, 118.52, 14.66.

MS (ESI) M calculated: 194.25 g/mol; *m/z* observed $[M+H]^+$: 195 $[M-H]^-$: 193

(E)-3-(4-fluorophenyl)prop-2-enoic acid (3g)

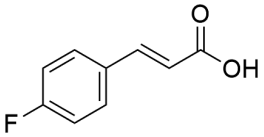

White solid, m.p. = 207 – 209 °C.

^{1}H NMR (400 MHz, DMSO) δ (ppm) = 12.39 (s, 1H), 7.83 – 7.72 (m, 2H), 7.59 (d, J = 16.0 Hz, 1H), 7.30 – 7.18 (m, 2H), 6.50 (d, J = 16.0 Hz, 1H).

^{13}C NMR (101 MHz, DMSO) δ (ppm) = 168.01, 164.84, 162.37, 143.14, 131.35 (d, J = 3.1 Hz), 130.92 (d, J = 8.6 Hz), 119.58 (d, J = 2.3 Hz), 116.31 (d, J = 21.7 Hz).

MS (ESI) M calculated: 166.15 g/mol; *m/z* observed $[M+H]^+$: 167 $[M-H]^-$: 165

(E)-3-(4-chlorophenyl)prop-2-enoic acid (3h)

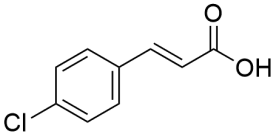

White solid, m.p. = 236 – 238 °C.

^{1}H NMR (400 MHz, DMSO) δ (ppm) = 12.42 (s, 1H), 7.73 (d, J = 8.5 Hz, 2H), 7.62 – 7.53 (m, 1H), 7.47 (d, J = 8.5 Hz, 2H), 6.56 (d, J = 16.0 Hz, 1H).

^{13}C NMR (101 MHz, DMSO) δ (ppm) = 167.86, 142.89, 135.15, 133.67, 130.34, 129.36, 120.59.

MS (ESI) M calculated: 181.9 and 183.9 g/mol; *m/z* observed $[M-Cl^{\bullet}]^+$ *m/z* 148 $[M-Cl]^-$: 183 and 185

(E)-3-(4-bromophenyl)prop-2-enoic acid (3i)

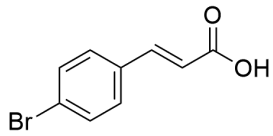

Light yellow solid, m.p. = 248 – 251 °C.

^{1}H NMR (400 MHz, DMSO) δ (ppm) = 10.87 (s, 1H), 7.59 – 7.55 (m, 2H), 7.55 – 7.51 (m, 2H), 7.51 – 7.45 (m, 1H), 6.50 (d, J = 16.0 Hz, 1H).

^{13}C NMR (101 MHz, DMSO) δ (ppm) = 167.85, 143.00, 133.98, 132.29, 130.55, 123.97, 120.62.

MS (ESI) M calculated: 226.1 and 228.1 g/mol; *m/z* observed $[M\text{-}Br^{\bullet}]^{+}$ *m/z* 148 $[M\text{-}Br]^{-}$: 225 and 227

(E)-3-(4-hydroxyphenyl)prop-2-enoic acid (3j)

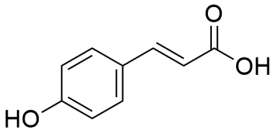

White solid, m.p. = 212 – 214 °C.

^{1}H NMR (400 MHz, DMSO) δ (ppm) = 12.11 (s, 1H), 10.02 (s, 1H), 7.59 – 7.47 (m, 3H), 6.82 (d, J = 8.5 Hz, 2H), 6.32 (d, J = 16.0 Hz, 1H).

^{13}C NMR (101 MHz, DMSO) δ (ppm) = 168.47, 160.06, 144.66, 130.53, 125.75, 116.23, 115.80.

MS (ESI) M calculated: 164.16 g/mol; *m/z* observed $[M+H]^{+}$: 165 $[M-H]^{-}$: 163

(E)-3-(4-hydroxy-3-methoxy-phenyl)prop-2-enoic acid (3k)

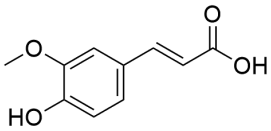

Light yellow solid, m.p. = 171 – 173 °C.

^{1}H NMR (400 MHz, DMSO) δ (ppm) = 12.12 (s, 1H), 9.54 (s, 1H), 7.49 (d, J = 15.9 Hz, 1H), 7.28 (d, J = 1.9 Hz, 1H), 7.08 (dd, J = 8.2, 1.9 Hz, 1H), 6.83 – 6.76 (m, 1H), 6.36 (d, J = 15.9 Hz, 1H), 3.82 (s, 3H).

^{13}C NMR (101 MHz, DMSO)

δ (ppm) = 168.49, 149.54, 148.37, 144.99, 126.25, 123.28, 116.05, 111.59, 56.12.

MS (ESI) M calculated: 194.18 g/mol; *m/z* observed $[M+H]^{+}$: 195 $[M-H]^{-}$: 193

4-hydroxy-3,5-dimethoxy styrene (4a)

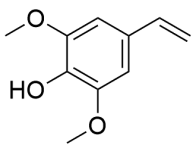

White solid, m.p. = 53 – 54 °C.

^{1}H NMR (400 MHz, DMSO) δ (ppm) = 8.44 (s, 1H), 6.73 (s, 1H), 6.66 – 6.53 (m, 1H), 5.67 (dd, J = 17.6, 0.9 Hz, 1H), 5.09 (dd, J = 10.9, 0.8 Hz, 1H), 3.77 (s, 6H).

^{13}C NMR (101 MHz, DMSO) δ (ppm) = 148.51, 137.45, 136.29, 128.21, 111.78, 104.24, 56.40.

MS (ESI) M calculated: 180.20 g/mol; *m/z* observed $[M+H]^+$: 181 $[M-H]^-$: 179

3.5 References

1. List, B. Emil Knoevenagel and the roots of aminocatalysis. *Angewandte Chemie (International ed. in English)* **2010**, *49*, 1730-1734.
2. Cho, H.; Ueda, M.; Tamaoka, M.; Hamaguchi, M.; Aisaka, K.; Kiso, Y.; Inoue, T.; Ogino, R.; Tatsuoka, T.; Ishihara, T. Novel caffeic acid derivatives: extremely potent inhibitors of 12-lipoxygenase. *Journal of medicinal chemistry* **1991**, *34*, 1503-1505.
3. Kwak, G.; Fujiki, M. Colored and Luminous Aliphatic Polyester via One-Pot Intra- and Intermolecular Knoevenagel Reactions. *Macromolecules* **2004**, *37*, 2021-2025.
4. Nokami, J.; Kataoka, K.; Shiraishi, K.; Osafune, M.; Hussain, I.; Sumida, S. Convenient formation of 4-hydroxyalk-2-en-1-one functionality via A knoevenagel-type carbon chain elongation reaction of aldehyde with 1-arylsulfinylalkan-2-one. *The Journal of organic chemistry* **2001**, *66*, 1228-1232.
5. De, P.; Koumba Yoya, G.; Constant, P.; Bedos-Belval, F.; Duran, H.; Saffon, N.; Daffé, M.; Baltas, M. Design, synthesis, and biological evaluation of new cinnamic derivatives as antituberculosis agents. *Journal of medicinal chemistry* **2011**, *54*, 1449-1461.
6. Knoevenagel, E. Ueber eine Darstellungsweise der Glutarsäure. *Berichte der deutschen chemischen Gesellschaft* **1894**, *27*, 2345-2346.
7. Alfonsi, K.; Colberg, J.; Dunn, P. J.; Fevig, T.; Jennings, S.; Johnson, T. A.; Kleine, H. P.; Knight, C.; Nagy, M. A.; Stefaniak, M. Green chemistry tools to influence a medicinal chemistry and research chemistry based organisation. *Green Chemistry* **2008**, *10*, 31-36.
8. Kerton, F.; Marriott, R.; Clark, J. H.; Seidl, P.; Clark, J. H. *Alternative Solvents for Green Chemistry;* Green Chemistry Series; Royal Society of Chemistry: Cambridge, **2013**
9. Pawar, H. S.; Wagh, A. S.; Lali, A. M. Triethylamine: a potential N-base surrogate for pyridine in Knoevenagel condensation of aromatic aldehydes and malonic acid. *New Journal Chem* **2016**, *40*, 4962-4968.
10. Ranu, B. C.; Jana, R. Ionic Liquid as Catalyst and Reaction Medium – A Simple, Efficient and Green Procedure for Knoevenagel Condensation of Aliphatic and Aromatic Carbonyl Compounds Using a Task-Specific Basic Ionic Liquid. *European Journal of Organic Chemistry* **2006**, *2006*, 3767-3770.
11. Hangarge, R. V.; Jarikote, D. V.; Shingare, M. S. Knoevenagel condensation reactions in an ionic liquid. *Green Chemistry* **2002**, *4*, 266-268.
12. Kaupp, G.; Reza Naimi-Jamal, M.; Schmeyers, J. Solvent-free Knoevenagel condensations and Michael additions in the solid state and in the melt with quantitative yield. *Tetrahedron* **2003**, *59*, 3753-3760.
13. Pinxterhuis, E. B.; Giannerini, M.; Hornillos, V.; Feringa, B. L. Fast, greener and scalable direct coupling of organolithium compounds with no additional solvents. *Nature communications* **2016**, *7*, 11698.
14. Martins, M. A. P.; Frizzo, C. P.; Moreira, D. N.; Buriol, L.; Machado, P. Solvent-free heterocyclic synthesis. *Chemical reviews* **2009**, *109*, 4140-4182.
15. Jawor, M. L.; Ahmed, B. M.; Mezei, G. Solvent- and catalyst-free, quantitative protection of hydroxyl, thiol, carboxylic acid, amide and heterocyclic amino functional groups. *Green Chemistry* **2016**, *18*, 6209-6214.
16. Lu, J.; Toy, P. Organocatalytic Decarboxylative Doebner-Knoevenagel Reactions between Arylaldehydes and Monoethyl Malonate Mediated by a Bifunctional Polymeric Catalyst. *Synlett* **2011**, *2011*, 1723-1726.
17. Kasinathan, P.; Seo, Y.; Shim, K.; Hwang, Y.; Lee, U.; Hwang, D.; Hong, D.; Halligudi, S. B.; Chang, J. Effect of Diamine in Amine-Functionalized MIL-101 for Knoevenagel Condensation. *Bulletin of the Korean Chemical Society* **2011**, *32*, 2073-2075.
18. Gu, X.; Tang, Y.; Zhang, X.; Luo, Z.; Lu, H. Organocatalytic Knoevenagel condensation by chiral C2-symmetric tertiary diamines. *New Journal Chem* **2016**, *40*, 6580-6583.
19. Hoskins, T. J. C. Carbon-carbon bond forming reactions of biomass derived aldehydes, Georgia Institute of Technology, **2008**

20. Pasha, M. A.; Manjula, K. Lithium hydroxide: A simple and an efficient catalyst for Knoevenagel condensation under solvent-free Grindstone method. *Journal of Saudi Chemical Society* **2011***, 15*, 283-286.
21. Leelavathi, P.; Kumar, S. R. Niobium (V) chloride catalyzed Knoevenagel condensation: An efficient protocol for the preparation of electrophilic alkenes. *Journal of Molecular Catalysis. A, Chemical* **2005***, 240*, 99-102.
22. Ogiwara, Y.; Takahashi, K.; Kitazawa, T.; Sakai, N. Indium(III)-catalyzed knoevenagel condensation of aldehydes and activated methylenes using acetic anhydride as a promoter. *The Journal of organic chemistry* **2015***, 80*, 3101-3110.
23. Jackson, T.; Clark, J. H.; Macquarrie, D. J.; Brophy, J. H. Base catalysts immobilised on silica coated reactor walls for use in continuous flow systems. *Green Chemistry* **2004***, 6*, 193-195.
24. Nageswara Rao, R.; Kumar Talluri, M. V. N. An overview of recent applications of inductively coupled plasma-mass spectrometry (ICP-MS) in determination of inorganic impurities in drugs and pharmaceuticals. *Journal of Pharmaceutical and Biomedical Analysis* **2007***, 43*, 1-13.
25. Gupta, M.; Wakhloo, B. P. Tetrabutylammoniumbromide mediated Knoevenagel condensation in water: synthesis of cinnamic acids. *Arkivoc* **2007**, 94-98.
26. M.M.H. Bhuiyan; M.I. Hossain; M. Ashraful Alam; M.M. Mahmud Microwave Assisted Knoevenagel Condensation: Synthesis and Antimicrobial Activities of Some Arylidene-malononitriles. *Chemistry Journal* **2012***, 02*, 31-37
27. Moseley, J. D.; Kappe, C. O. A critical assessment of the greenness and energy efficiency of microwave-assisted organic synthesis. *Green Chemistry* **2011***, 13*, 794-806.
28. Trotzki, R.; Hoffmann, M. M.; Ondruschka, B. Studies on the solvent-free and waste-free Knoevenagel condensation. *Green Chemistry* **2008***, 1*, 767-772.
29. Mase, N.; Horibe, T. Organocatalytic Knoevenagel condensations by means of carbamic acid ammonium salts. *Organic letters* **2013***, 15*, 1854-1857.
30. van Schijndel, J.; Canalle, L. A.; Smid, J.; Meuldijk, J. Conversion of Syringaldehyde to Sinapinic Acid through Knoevenagel-Doebner Condensation. *Open Journal of Physical Chemistry* **2016***, 6*, 101-108.
31. Sheldon, R. A. Fundamentals of green chemistry: efficiency in reaction design. *Chemical Society reviews* **2012***, 41*, 1437-1451.
32. Kiyama, R.; Minomura, S. A note on the stability of ammonium bicarbonate tablets. *The Review of Physical Chemistry of Japan* **1952***, 22*, 43-45.
33. Sheldon, R. A. The E factor 25 years on: the rise of green chemistry and sustainability. *Green Chemistry***2017***, 19*, 18-43.
34. Aldabalde, V. Organocatalyzed Decarboxylation of Naturally Occurring Cinnamic Acids: Potential Role in Flavoring Chemicals Production. *Open Journal of Physical Chemistry* **2011***, 1*, 85-93.

4 Mechanistic considerations and characterization of catalytic active intermediates of the Green Knoevenagel reaction of various benzaldehydes

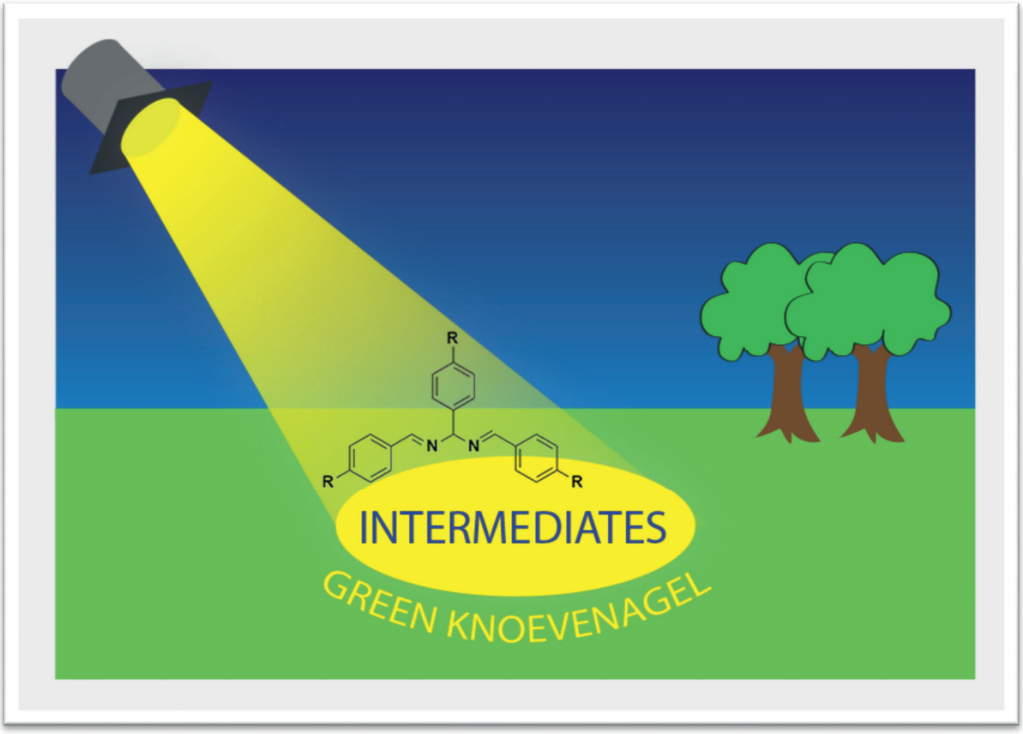

This chapter is based on:

van Schijndel, J.; SynLett **2018**, *29*, 1983-1988.
(DOI: 10.1055/s-0037-1610235)

van Schijndel, J.; Green Chemistry Letters and Reviews **2019**, *12*, 323-331.
(DOI: 10.1080/17518253.2019.1643931)

Abstract

In this chapter, a mechanism for the Green Knoevenagel reaction has been proposed. In the proposed mechanism, benzaldehyde reacts with the precursor ammonia released from ammonium salts to form a catalytically active double Schiff base. A closed catalytic cycle explains why various ammonium salts, including ammonium bicarbonate, have been correctly reported as catalysts in Knoevenagel-like reactions. Several catalytically active intermediates from derivatives of benzaldehyde were isolated and characterized. Unfortunately, it was not possible to isolate or characterize the benzaldehyde derivatives with a phenolic-group at the para position of benzaldehyde. However, the results of mass spectrometry points to the existence of these putative in situ formed catalytic intermediates. In addition to malonic acid **3**, other keto compounds were tested as reaction partners for benzaldehyde. The acidity of the α-hydrogen in the keto compounds appears to play a major role in the interaction between the keto compound and the double Schiff base **2a**. Furthermore, these in situ formed double Schiff bases play another catalytic role in the consecutive decarboxylation reaction to various cinnamic acids.

4.1 Introduction

Catalysis is a major specialism of chemistry, and this is emphasized by the chemical industry where catalytic processes produce 85-90% of all products.[1] The start of industrial catalysis was by the end of the 19th century and the beginning of the 20th century.[2] One of the most important catalytic processes developed industrially is the Haber-Bosch process, which uses a simple iron catalyst to make ammonia and other nitrogen-containing compounds from nitrogen and hydrogen.[3] The significant influence of the Haber-Bosch process on sustainability is that ammonia production made inexpensive fertilizers available to the world, allowing many people to grow a steady abundance of food for the first time.[4]

Catalytically promoted aldol condensations are important in organic synthesis as they provide an efficient way to form carbon-carbon bonds, which are the basis of organic chemistry.[5] The aldol condensation can either be acid-catalyzed or base-catalyzed. A base-catalyzed aldol condensation in the presence of an amine is called a Knoevenagel condensation. In 1898 Emil Knoevenagel was the first who realized that amines were truly catalytic ("Contactsubstanz"). He isolated catalytic intermediates and as a result of this laid the fundamentals of "organocatalysis".[6,7] Unfortunately, the impact of his research has not yet been valued by everyone.[8-11] Organocatalysis is the catalysis of reactions with small organic molecules and generally seen as a more environmentally friendly form of catalysis contrasted to (toxic) transition metal catalysts.[12,13]

It is well known for a long time that benzaldehyde and ammonia react together to form hydrobenzamide which is a double Schiff base.[14-19] Schiff bases have been playing vital roles in, e.g., pharmaceuticals, as a protective group, and in liquid crystals.[20-23] In combination with various metals but never alone, it has further been shown that hydrobenzamide exhibits catalytic activity in the field of interactions with biogenic macromolecules such as DNA, RNA, and peptides.[24]

In the pursuit to develop eco-friendly Knoevenagel condensation reactions to produce ligno-phytochemicals, we reported earlier about a Green Knoevenagel method with ammonium bicarbonate as a catalyst and source of ammonia.[25] This method provides good to an excellent conversion of various benzaldehydes and high yields of the corresponding cinnamic acids in an efficient, rapid, scalable, and environmentally friendly way. The question arose to what extent hydrobenzamide-like intermediates could be isolated and whether these intermediates could be identified as catalytically active.[25,26]

The study presented in this chapter investigates the organocatalytic activity of various "in situ formed" hydrobenzamides in the Green Knoevenagel reaction.

4.2 Results and discussion

4.2.1 Catalytical activity of hydrobenzamide

The double Schiff base hydrobenzamide **2a** (1-[(phenyl)]-N,N'-bis [(phenyl)methylene] methanediamine) synthesized from benzaldehyde and ammonium bicarbonate was isolated with a high yield (>95%) as reported before.[27] In order to prove the catalytical activity of hydrobenzamide **2a**, various amounts of hydrobenzamide **2a** were added to a mixture of benzaldehyde and malonic acid at 60 °C. Figure 4.1 shows cinnamic dicarboxylic acid **4a** formed as a function of time. Under these conditions, benzaldehyde **1a** is both reagent to the product cinnamic dicarboxylic acid **4a** (Scheme 4.1) and also a continuously incorporated part of the catalytic intermediate **2a**. In the design of the experiment, it was therefore decided that the reported mol percentages of hydrobenzamide **2a** were calculated relative to malonic acid and the total molar amount of benzaldehyde (free and incorporated in **2a**) was kept equal to the molar amount of malonic acid **3**.

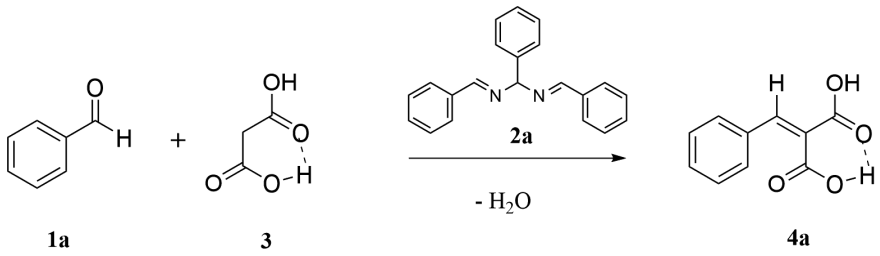

Scheme 4.1: Knoevenagel condensation of benzaldehyde **1a** with malonic acid **3** with hydrobenzamide **2a** as a catalyst towards cinnamic dicarboxylic acid **4a**.

Figure 4.1 clearly shows that hydrobenzamide **2a** accelerates the conversion of benzaldehyde **1a** towards its corresponding cinnamic dicarboxylic acid **4a**. Using 10 mol% hydrobenzamide **2a** full conversion towards cinnamic dicarboxylic acid is reached within 1 hour. To emphasize the impact of the catalytic intermediate hydrobenzamide: with a catalytic amount of only 1.25 mol% of hydrobenzamide **2a**, complete conversion of benzaldehyde **1a** towards cinnamic dicarboxylic acid **4a** is reached within 2 hours! Note that without the addition of hydrobenzamide **2a**, the product cinnamic dicarboxylic acid **4a** is also formed because of the carboxylic groups of malonic acid **3** also have acid catalytic activity in the condensation reaction. However, the results collected in Figure 4.1 reveals that this contribution is much smaller in comparison to the catalytic activity of hydrobenzamide **2a**.

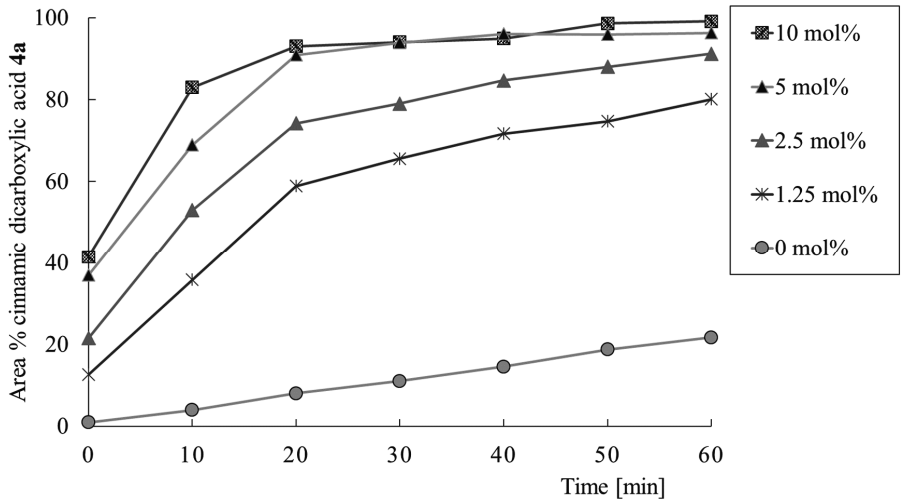

Figure 4.1: Concentration-time history of cinnamic dicarboxylic acid **4a** formed using various amounts of hydrobenzamide **2a** in a mixture with an equal total amount of benzaldehyde **1a** and malonic acid **3** at 60 °C. Reported conversions are based on the ratio of peaks of the HPLC chromatogram measured with a UV detector operating at 300 nm.

4.2.2 Mechanism condensation step

Now hydrobenzamide **2a** has been demonstrated to play a catalytic role in the reaction from benzaldehyde **1a** to cinnamic dicarboxylic acid **4a**, a mechanism is proposed in Scheme 4.2 with hydrobenzamide **2a** as a catalytic intermediate. On top of Scheme 4.2, the build-up is shown: precursor ammonia originated from and formed after decomposition of NH_4HCO_3, reacts with benzaldehyde **1a**, and results in benzyl imine **I** (step i). Benzyl imine **I** could not be isolated, due to its high reactivity but could be identified in the reaction mixture using MS. Two molecules of benzyl imine **I** can subsequently combine into intermediate **II**, which also has been identified in the reaction mixture using MS (step ii). Finally, a third benzaldehyde **1a** is incorporated into intermediate **II**, resulting in the production of hydrobenzamide **2a**, which forms the basis of the catalytic cycle marked by the green circle at the lower part of Scheme 4.2 (step iii).

First, a proton from the α-carbon of the reactant malonic acid **3** is transferred to an imine in hydrobenzamide **2a** (step iv). The ion-pair created, reacts to form a carbon-carbon bond (step v) into Intermediate **III**. Intermediate **III** could also be identified with MS measurements. A second proton from the α-carbon of the malonic acid moiety is removed by the former imine nitrogen atom (step vi), and the desired product cinnamic dicarboxylic acid **4a** is formed in step vii. Intermediate **II** is formed as an accompanying product and regenerates hydrobenzamide **2a** again after coupling with benzaldehyde **1a** (step iii) closing the catalytic cycle.

4.2.3 Catalytically active hydrobenzamide analogs

Also, other catalytically active hydrobenzamide analogs without a phenolic group were isolated successfully, and to the best of our knowledge, some of these catalytic intermediates are characterized for the first time, as demonstrated by the results collected in Table 4.1. Many other catalytic intermediates still are to be explored because each benzaldehyde derivative generates its catalytic intermediate. Purification of the double Schiff bases of the non-phenolic derivatives was possible by suspending the obtained precipitate in 30% ammonia solution and subsequently removing the liquid by filtration. Noteworthy, the synthesized and purified hydrobenzamides were not only catalytically active for the corresponding benzaldehyde but also catalytically active for a different type of benzaldehyde.

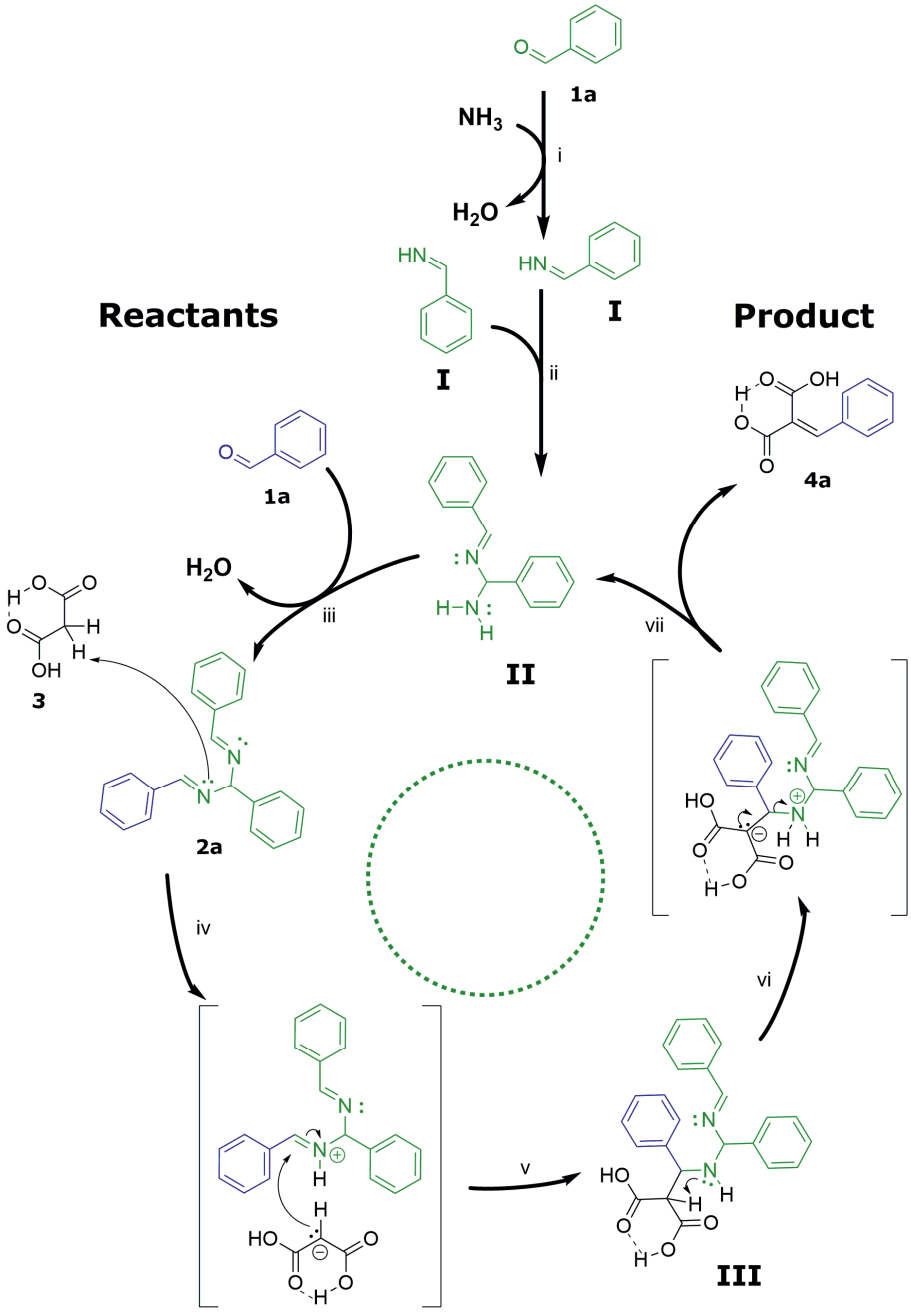

Scheme 4.2: Proposed mechanism of the reaction between the reactants benzaldehyde **1a** and malonic acid **3** towards the product cinnamic dicarboxylic acid **4a** catalyzed by in situ formed hydrobenzamide **2a**.

For instance, with equal amounts of benzaldehyde **1a** and malonic acid **3** and 10 mol% of the catalytically active hydrobenzamide **2a** at 60 °C, cinnamic dicarboxylic acid **4a** was formed. However, after the addition of equal amounts of 4-methyl benzaldehyde **1b** and malonic acid **3** to the former reaction mixture, also a 4-methyl cinnamic dicarboxylic acid **4b** was produced. Other combinations of catalysts and benzaldehydes derivatives could be carried out interchangeably. The catalytic intermediates of non-phenolic benzaldehydes derivatives were synthesized, purified, characterized by ^{1}H NMR, ^{13}C NMR, MS, TGA, and they all showed the expected catalytic activity in the condensation reaction with their corresponding benzaldehyde **1** and malonic acid **3**. The range of melting points is broad and is of no importance in the condensation reaction because all these intermediates are formed in situ during the Green Knoevenagel reaction and do not show up isolated.

Unfortunately, we were not able to isolate and characterize the putative catalytic intermediates from benzaldehydes with a phenolic group at the para position, e.g., 4-hydroxy benzaldehyde **1j**, vanillin **1k**, and syringaldehyde **1l**. The results of the indirect analysis of the fragments in the reaction mixture using MS points to the presence of the in situ formed catalytic double Schiff bases. Due to the absence of the phenolic group on the para position, the acetylated intermediates are more stable, and the melting points of all three acetylated benzaldehydes could be determined and presented in Table 4.1. However, only the double Schiff base of 4-acetoxy-syringaldehyde **2o** could be characterized by ^{1}H NMR. Characterization of the double Schiff base of 4-acetoxy-benzaldehyde **2m** and 4-acetoxy-vanillin **2n** with NMR proved to be impossible due to instability in various solvents. All three of these derivatized hydrobenzamides showed catalytic activity in the Knoevenagel condensation reaction with the corresponding benzaldehyde **1** and malonic acid **3**. Also, the same catalytic activity was shown with benzaldehyde **1a** and malonic acid **3** underlying that the catalytic intermediates are interchangeable.

Table 4.1: Various hydrobenzamides **2** obtained from benzaldehyde derivatives **1**.

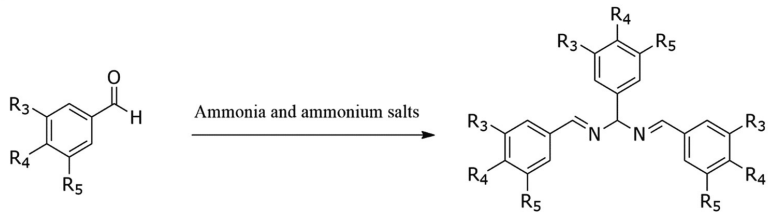

1 **2**

Entry	Hydrobenzamide	R_3	R_4	R_5	mp (°C)	mp (°C) ref	ref.
2a	Hydrobenzamide	H	H	H	104.9 - 105.2	101.8-102.5	Nishiyama[16]
2b	Hydro-4-methyl-benzamide	H	CH_3	H	92.2 - 93.6	95.8 - 96.4	Nishiyama[16]
2c	Hydroanisamide	H	OCH_3	H	127.0 - 129.1	125 - 126	Kamal[15]
2d	Hydro-4-methylthio-benzamide	H	SCH_3	H	99.2 - 101.9	unknown	
2e	Hydro-4-fluoro-benzamide	H	F	H	70.6 - 71.3	unknown	
2f	Hydro-4-chloro-benzamide	H	Cl	H	86.2 - 87.7	84.5 - 85.5	Sim[17]
2g	Hydro-4-bromo-benzamide	H	Br	H	117.4 - 118.8	unknown	
2h	Hydro-4-dimethylamino-benzamide	H	$N(CH_3)_2$	H	192.8-194.7	194-196	Crowell[14]
2i	Hydro-4-phenyl-benzamide	H	Ph	H	132.1 - 133.9	unknown	
2m	Hydro-4-acetoxy-benzamide	H	$OC(O)CH_3$	H	76.2 - 77.3	unknown	
2n	Hydro-4-acetoxy-vanillinamide	OCH_3	$OC(O)CH_3$	H	57.0 - 58.9	unknown	
2o	Hydro-4-acetoxy-syringamide	OCH_3	$OC(O)CH_3$	OCH_3	151.3-154.3	unknown	

4.2.4 Other β–keto compounds

In addition to malonic acid **3**, other β–keto compounds were tested as reaction partners for benzaldehyde. The β–keto compounds show varying reactivity towards benzaldehyde at a temperature of 80 °C, as presented in Table 4.2. The acidity of the α-hydrogen in the β–keto compounds appears to play a significant role in the interaction between the β–keto compound and the double Schiff base **2a**. More acidic α-hydrogens[28] corresponded with higher conversion to the α, β-unsaturated products after 1 hour. These observations seem to underline the importance of the hydrogen transfer between the α-carbon of diethyl malonate and the imine nitrogen of hydrobenzamide **2a** in the catalytic mechanism.

Table 4.2: Green Knoevenagel condensation of benzaldehyde **1a** with various β-keto compounds **3**.

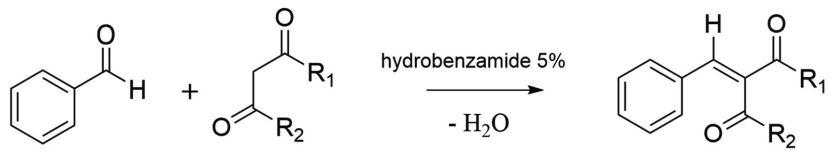

1a **3** **4**

Entry	β keto compound	name	R_1	R_2	pKa (DMSO) (Bordwell)	Product	Yield % HPLC
1	3a	malonic acid	OH	OH	12.30	5a	100
2	3b	acetylacetone	CH_3	CH_3	13.30	4b	53
3	3c	ethyl acetoacetate	OC_2H_5	CH_3	14.20	4c	66
4	3e	di-methyl malonate	OCH_3	OCH_3	15.87	4e	45
5	3f	di-ethyl malonate	OC_2H_5	OC_2H_5	16.40	4f	18
6	3d	di-benzyl malonate	$OCH_2C_6H_5$	$OCH_2C_6H_5$		4d	12

Reaction conditions: benzaldehyde **1a**, 1.0 eq. β-keto compound **3** and 5 mol% hydrobenzamide **2a** related to the β-keto compound **3** at 80 °C for 1 hour. Reported conversions are based on the ratio of peaks of the HPLC chromatogram measured with a UV detector operating at 300 nm.

4.2.5 Decarboxylation

The original Knoevenagel reaction involves a condensation step in which piperidine often is used as an organocatalyst. We demonstrated that piperidine could be replaced successfully with precursor ammonia released from ammonium salts. In our Green Knoevenagel reaction, the in situ produced double Schiff base plays a role as a catalytic intermediate in this condensation step providing cinnamic dicarboxylic acids.[25]

This condensation step is followed in the Doebner modification by a decarboxylation step to cinnamic acids, often using pyridine as a solvent and organocatalyst[13,29]. Since cinnamic acids are produced from the cinnamic dicarboxylic acids after raising the original reaction mixture to a temperature of 110 °C, there is an indication that hydrobenzamide **2a** or degradation products of hydrobenzamide **2a** also participate in this subsequent decarboxylation step.[30-32] Purified cinnamic dicarboxylic acids without the presence of the double Schiff base performed no decarboxylation at a temperature of 110 °C

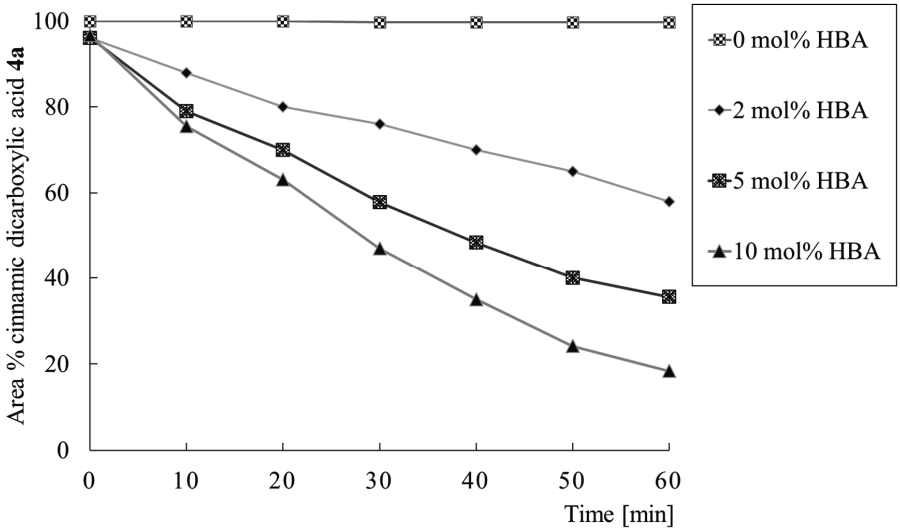

Figure 4.2: Decarboxylation of cinnamic dicarboxylic acid **4a** using various amounts of hydrobenzamide **2a** (HBA) at 110 °C. Cinnamic dicarboxylic acid **4a** and hydrobenzamide **2a** were mixed with a minimum amount (e.g., 0.5 mL) of ethyl acetate after which ethyl acetate was removed by distillation under reduced pressure at 40 °C. Reported conversions are based on the ratio of peaks of the HPLC chromatogram measured with a UV detector operating at 300 nm.

Figure 4.2 shows the decarboxylation of purified cinnamic dicarboxylic acid **4a** performed at a temperature of 110 °C. Hydrobenzamide **2a** accelerates the decarboxylation of cinnamic dicarboxylic acid **4a** towards cinnamic acid **5a**. Without the addition of a hydrobenzamide **2a**, no significant decarboxylation occurs. Using 10 mol% hydrobenzamide **2a**, almost full conversion towards cinnamic acid **5a** is reached within 2 hours. However, the consecutive decarboxylation towards styrene is visible for approximately 10%, which reduces the yield of cinnamic acid **5a**. With lower amounts or hydrobenzamide **2a**, virtually no styrene formation is visible. Our data reveal that the decarboxylation of cinnamic dicarboxylic acid **4a** obeys first-order kinetics, which follows from a linear relationship between $\frac{\ln(x_{\mathbf{4a}}(t))}{x_{\mathbf{4a}}(0)}$ and time.

A possible explanation of the organocatalysis of the decarboxylation by hydrobenzamide **2a** can be found in the suggestion that tertiary amines can serve as a Lewis base.[33,34] As shown in Scheme 4.3, hydrobenzamide **2a** deprotonates cinnamic dicarboxylic acid **4a** and creates a carboxylate anion. Increasing the temperature leads to decarboxylation, and finally, cinnamic acid **5a** is formed.

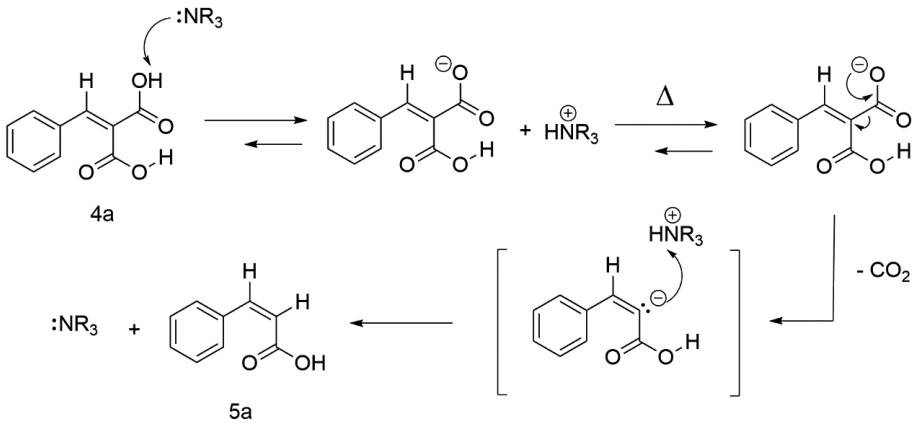

Scheme 4.3: Mechanism of the decarboxylation of cinnamic dicarboxylic acid **4a** towards cinnamic carboxylic acid **5a** catalyzed by a Lewis base NR_3 (e.g., hydrobenzamide **2a**).

4.2.6 Thermal stability hydrobenzamides

Because the decarboxylation is performed at an elevated temperature (i.e., 110 °C), the thermal stability of hydrobenzamide **2a** is essential. The thermal stability of hydrobenzamide **2a** was therefore investigated with thermogravimetric analysis (TGA). The feature of this analysis is to determine the initial decomposition temperature (onset), the temperature when 50 wt.% of hydrobenzamide is decomposed ($D_{½}$), and the final residue in a nitrogen atmosphere.[35] As demonstrated by the results given in Figure 4.3, the TGA curve of hydrobenzamide **2a** has an onset at a temperature of 254 °C, a $D_{½}$ at a temperature of 281 °C and above a temperature of 320 °C there is no residue left. Above a temperature of 320 °C, the in situ formed catalytic intermediate has entirely disappeared. In our opinion, at a decarboxylation temperature of 110 °C, hydrobenzamide **2a** is stable to act as a Lewis base in the decarboxylation of dicarboxylic cinnamic acid **4a**.

In summary, it can be concluded that in situ formed catalytic intermediates have a dual function in the Green Knoevenagel. First, they are a catalytic intermediate in the condensation reaction of coupling benzaldehyde derivatives with malonic acid and play another catalytic role in the consecutive decarboxylation step. More research is prepared on aspects of formation, stability, and catalytic activity of these intermediates in the Green Knoevenagel reaction.

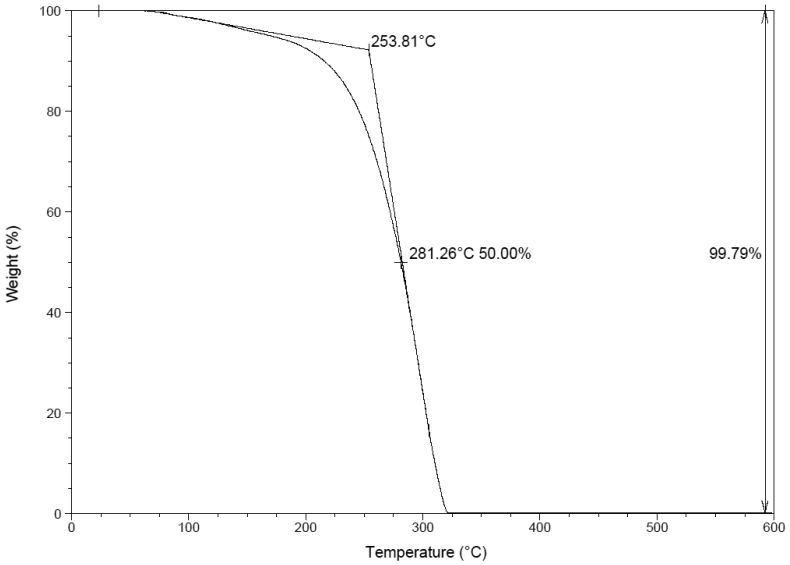

Figure 4.3: TGA thermograph of hydrobenzamide **2a**. TGA analysis was performed with a 20 °C/min heating rate in nitrogen.

4.3 Conclusions

It has been demonstrated that in the Green Knoevenagel reaction of benzaldehyde **1a** and malonic acid **3**, the carbon-carbon formation reaction is catalyzed by an in situ formed double Schiff base. A mechanism for this Green Knoevenagel reaction has been proposed. In the proposed mechanism, benzaldehyde reacts with the precursor ammonia released from ammonium salts to form a catalytically active double Schiff base. A closed catalytic cycle explains why various ammonium salts, including ammonium bicarbonate, have been correctly reported as catalysts in Knoevenagel-like reactions. Several catalytically active intermediates from derivatives of benzaldehyde were isolated and characterized. Unfortunately, it was not possible to isolate or characterize the benzaldehyde derivatives with a phenolic-group at the para position of benzaldehyde. However, the results of mass spectrometry points to the existence of these putative in situ formed catalytic intermediates.

In addition to malonic acid **3**, other keto compounds were tested as reaction partners for benzaldehyde. The acidity of the α-hydrogen in the keto compounds appears to play a major role in the interaction between the keto compound and the double Schiff base **2a**. Furthermore, these in situ formed double Schiff bases play another catalytic role in the consecutive decarboxylation reaction to various cinnamic acids.

4.4 Experimental section

4.4.1 General remarks

Reagents: Syringaldehyde (**1**), and all other chemicals (99% purity) were purchased from Sigma-Aldrich and were used as received. DMSO-*d6* was purchased from Cambridge Isotope, with 99 atom% deuterated.

Instrumentation: ^{1}H NMR spectroscopy measurements were performed on an Agilent 400-MHz NMR system with DMSO-*d6* as a solvent. Chemical shifts are reported in ppm, relative to tetramethylsilane (TMS).

HPLC analysis was carried out using a reversed-phase liquid chromatographic system (Agilent 1100 series) equipped with a diode array detector operating at 300 nm (Agilent 1100 series) and an autosampler injector with a 20 µL loop (Agilent 1100 series G1316A). The system was equipped with a Grace Alltima C18 5 µm column (250 mm × 4.6 mm). The determination of the concentration of the components in the reaction mixtures was carried out by the external standard method and was based on peak areas. HPLC measurements were made with the following settings: Flowrate 1.0 mL/min at a temperature of 25 °C, eluent A = methanol, eluent B = acetic acid buffer (99% milliQ, 1% acetic acid). The samples were eluted using the following gradient: 40% A and 60% B set for 6 min, gradient to 100% A and 0% B in subsequent 10 min, 100% A and 0% B set for 5 min, followed by 40% A and 60% B set for 8 min.

LC-MS analysis was performed using a liquid chromatographic system (Agilent 1100 series) equipped with a Luna 3 µm C18 column (200 × 2.0 mm).

Thermogravimetric analysis (TGA) was performed on a Q50 TA Instruments TGA, using nitrogen as a purge gas, at a heating rate of 20 °C/min in the range of 0-600 °C.

Melting points were determined with the Hanon Automatic Video Melting Point apparatus MP450.

4.4.2 Experimental procedures and characterization

*Optimized protocol for the synthesis of hydrobenzamide (**2a**):*

A mixture of benzaldehyde (**1a**, 1.44 g, 15 mmol) and ammonium bicarbonate (0.79 g, 10 mmol) was brought to a temperature of 50 °C, resulting in a solid white substance in 30 minutes. The solid was purified by suspending the obtained precipitate in 10 mL 30% (m/m) ammonia and subsequently removing the solvent by filtration.

*Protocol for the green Knoevenagel condensation towards cinnamic dicarboxylic acid **4a** with 10 mol% hydrobenzamide **2a**:*

Malonic acid **3** (1.0 g, 10 mmol) was dissolved in benzaldehyde (**1a**, 0.96 g, 10.0 mmol) and hydrobenzamide (**2a**, 0.26 g, 1.0 mmol) was subsequently added. The reaction mixture was stirred and kept at 60 °C for 1 hour to reach complete benzaldehyde conversion. Samples of 2 µl were taken for reversed-phase HPLC analysis and diluted in 7.5 mL methanol, filtered, and analyzed using the method described in section 2.2. The calculated percentage of the peak area of cinnamic dicarboxylic acid (**4a**) is in relation to the total peak area.

4-Acetoxybenzaldehyde (1m)

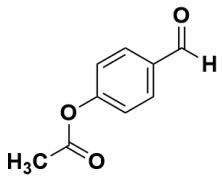

A mixture of 4-hydroxybenzaldehyde **1j** (1.22 g, 10 mmol), sodium acetate (41 mg, 0.5 mmol) dissolved in acetic anhydride (1.53 g, 15 mmol) was stirred and heated to 90 °C for 30 minutes. In the workup procedure, 10 mL of ethyl acetate was added to the reaction mixture and washed with water (3 × 5 mL). The organic layer was acidified with a 1.0 M HCl solution to a pH of 3, the layers were separated, and the organic layer was washed a final time with 5 mL of brine solution. After drying the organic layer over $MgSO_4$, ethyl acetate was removed under reduced pressure, and the liquid was stored under a nitrogen atmosphere (1.54 g, 94% yield).

^{1}H NMR (400 MHz, DMSO) δ (ppm) = 10.01 (s, 1H), 8.01 – 7.97 (m, 2H), 7.42 – 7.36 (m, 2H), 2.32 (s, 3H).

4-Acetoxyvanillin (1n)

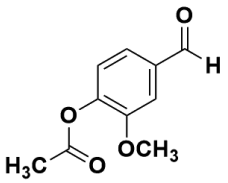

A mixture of vanillin **1k** (1.52 g, 10 mmol), sodium acetate (41 mg, 0.5 mmol) dissolved in acetic anhydride (1.53 g, 15 mmol) was stirred and heated to 90 °C for 30 minutes. In the workup procedure, 10 mL of ethyl acetate was added to the reaction mixture and washed with water (3 × 5 mL). The organic layer was acidified with a 1.0 M HCl solution to a pH of 3, the layers were separated, and the organic layer was washed a final time with 5 mL of brine solution. After drying the organic layer over $MgSO_4$, ethyl acetate was removed under reduced pressure, and the product was dried at 50 °C in a vacuum oven overnight. The melting point range of the collected white solid (1.82 g, 93% yield) was 76.2 - 77.8 °C (uncorrected).
^{1}H NMR (400 MHz, DMSO) δ (ppm) = 9.97 (s, 1H), 7.63 – 7.55 (m, 2H), 7.36 (d, J = 8.0 Hz, 1H), 3.87 (s, 3H), 2.30 (s, 3H).

4-Acetoxysyringaldehyde (1o)

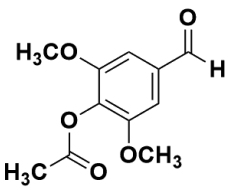

A mixture of syringaldehyde **1l** (1.82 g, 10 mmol), sodium acetate (41 mg, 0.5 mmol) dissolved in acetic anhydride (1.53 g, 15 mmol) was stirred and heated to 90 °C for 30 minutes. In the workup procedure, 10 mL of ethyl acetate was added to the reaction mixture and washed with water (3 × 5 mL). The organic layer was acidified with a 1.0 M HCl solution to a pH of 3, the layers were separated, and the organic layer was washed a final time with 5 mL of brine solution. After drying the organic layer over $MgSO_4$, ethyl acetate was removed under reduced pressure, and the product was dried at 50 °C in a vacuum oven overnight. The melting point range of the collected white solid (2.00 g, 89% yield) was 114.9 - 116.9 °C (uncorrected).
^{1}H NMR (400 MHz, DMSO) δ (ppm) = 9.95 (s, 1H), 7.33 (s, 2H), 3.86 (s, 6H), 2.30 (s, 3H).

Hydrobenzamide (2a)

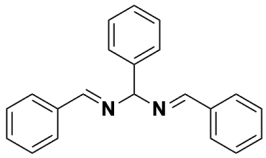

A mixture of benzaldehyde (**1a**, 1.59 gram, 15 mmol) and ammonium bicarbonate (0.79 gram, 10 mmol) was brought to a temperature of 50 °C, resulting in a solid white substance in 30 minutes. The solid was purified by suspending the obtained precipitate in 10 mL 30% (m/m) ammonia and subsequently removing the solvent by filtration. The melting point range of the collected light yellow solid (1.40 g, 94% yield) was 102.6 - 104.3 °C (uncorrected).

^{1}H NMR (400 MHz, DMSO) δ (ppm) = 8.67 (s, 2H), 7.86 (dd, J = 7.2, 2.2 Hz, 4H), 7.55 – 7.44 (m, 8H), 7.38 (t, J = 7.5 Hz, 2H), 7.30 (t, J = 7.3 Hz, 1H), 6.04 (s, 1H).

^{13}C NMR (101 MHz, DMSO) δ (ppm) = 161.08, 142.72, 136.28, 131.61, 129.21, 128.89, 128.82, 128.10, 127.58, 92.10. M calculated: 298.15 g/mol;

MS (ESI) *m/z* observed $[M+H]^+$: 299 $[M-H]^-$: 297

Hydro-4-methyl-benzamide (2b)

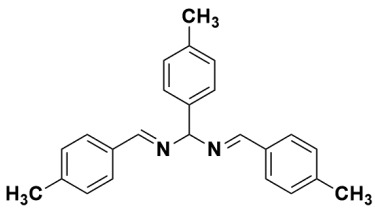

A mixture of 4-methylbenzaldehyde (**1b**, 1.80 gram, 15 mmol) and ammonium bicarbonate (0.79 gram, 10 mmol) was brought to a temperature of 50 °C, resulting in a solid yellow-white substance in 30 minutes. The solid was purified by suspending the obtained precipitate in 10 mL 30% (m/m) ammonia and subsequently removing the solvent by filtration. The melting point range of the collected white solid (1.61 g, 95% yield) was 92.2 - 93.6 °C (uncorrected). **^{1}H NMR** (400 MHz, DMSO) δ (ppm) = 8.58 (s, 2H), 7.73 (d, J = 8.1 Hz, 4H), 7.37 (d, J = 8.0 Hz, 2H), 7.27 (d, J = 8.0 Hz, 4H), 7.17 (d, J = 7.9 Hz, 2H), 5.92 (s, 1H), 2.34 (s, 6H), 2.27 (s, 3H).

^{13}C NMR (101 MHz, DMSO) δ (ppm) = 160.51, 141.41, 140.06, 137.13, 133.79, 129.78, 129.37, 128.77, 127.45, 92.22, 21.54, 21.19. M calculated: 340.19 g/mol;

MS (ESI) *m/z* observed $[M+H]^+$: 341 $[M-H]^-$: 339

Hydroanisamide (2c):

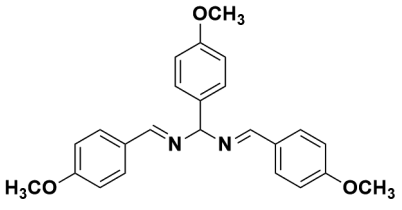

A mixture of 4-methoxybenzaldehyde (**1c**, 2.04 gram, 15 mmol) and ammonium bicarbonate (0.79 gram, 10 mmol) was brought to a temperature of 50 °C, resulting in a solid white substance in 30 minutes. The solid was purified by suspending the obtained precipitate in 10 mL 30% (m/m) ammonia and placed in an ultrasonic bath at room temperature for 1 hour. The resulting solution was freeze-dried to obtain white flakes. The melting point range of the collected white solid (1.89 g, 97% yield) was 125.4-127.4 °C (uncorrected).

^{1}H NMR (400 MHz, DMSO) δ (ppm) = 8.54 (s, 2H), 7.79 (d, J = 8.8 Hz, 4H), 7.41 (d, J = 8.7 Hz, 2H), 7.02 (d, J = 8.8 Hz, 4H), 6.93 (d, J = 8.7 Hz, 2H), 5.86 (s, 1H), 3.80 (s, 6H), 3.73 (s, 3H).

^{13}C NMR (101 MHz, DMSO) δ (ppm) = 161.99, 159.69, 159.10, 135.46, 130.42, 129.21, 128.63, 114.57, 114.16, 92.21, 55.76, 55.52. M calculated: 388.18 g/mol;

MS (ESI) *m/z* observed $[M+H]^+$: 389 $[M-H]^-$: 387

Hydro-4-methylthio-benzamide (2d):

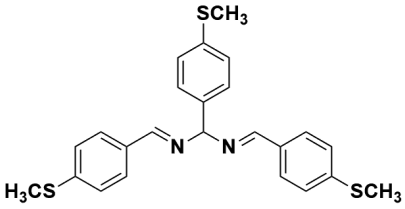

A mixture of 4-methylthiobenzaldehyde (**1d**, 2.28 gram, 15 mmol) and ammonium bicarbonate (0.79 gram, 10 mmol) was brought to a temperature of 50 °C, resulting in a solid yellow-white substance in 30 minutes. The suspension was separated using a centrifuge and dried at room temperature. The solid was purified by suspending the obtained precipitate in cold ethanol and centrifuging to reobtain the pellet. The melting point range of the collected white solid (2.07 g, 95% yield) was 99.2-101.9 °C (uncorrected).

^{1}H NMR (400 MHz, DMSO) δ (ppm) = 8.57 (s, 2H), 7.77 (d, J = 8.5 Hz, 4H), 7.42 (d, J = 8.3 Hz, 2H), 7.32 (d, J = 8.4 Hz, 4H), 7.27 (d, J = 8.4 Hz, 2H), 5.93 (s, 1H), 2.51 (s, 6H), 2.45 (s, 3H).

^{13}C NMR (101 MHz, DMSO) δ (ppm) = 160.39, 142.82, 139.63, 137.84, 132.74, 129.21, 128.14, 126.51, 125.83, 91.77, 15.30, 14.65.

M calculated: 436.11 g/mol;

MS (ESI) *m/z* observed $[M+H]^+$: 437 $[M-H]^-$: 435

Hydro-4-fluoro-benzamide (2e):

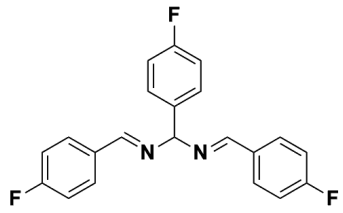

A mixture of 4-fluorobenzaldehyde (**1e**, 1.86 gram, 15 mmol) and ammonium bicarbonate (0.79 gram, 10 mmol) was brought to a temperature of 50 °C, resulting in a solid white substance in 30 minutes. The solid was purified by suspending the obtained precipitate in 10 mL 30% (m/m) ammonia and placed in an ultrasonic bath at room temperature for 1 hour. The resulting solution was freeze-dried to obtain white flakes. The melting point range of the collected white solid (1.69 g, 96% yield) was 72.6 - 74.3 °C (uncorrected).

^{1}H NMR (400 MHz, DMSO) δ (ppm) = 8.66 (s, 2H), 8.00 – 7.89 (m, 4H), 7.60 – 7.51 (m, 2H), 7.36 – 7.28 (m, 4H), 7.25 – 7.19 (m, 2H), 6.04 (s, 1H).

^{13}C NMR (101 MHz, DMSO) δ (ppm) = 160.08, 138.90, 132.84, 131.14, 129.50, 116.34, 116.12, 115.74, 115.53, 90.92. M calculated: 352.12 g/mol;

MS (ESI) *m/z* observed $[M+H]^+$: 353 $[M-H]^-$: 351

Hydro-4-chloro-benzamide (2f):

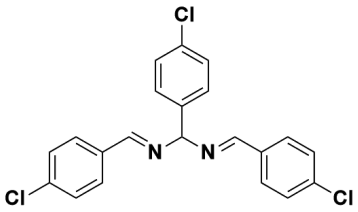

A mixture of 4-chlorobenzaldehyde (**1f**, 2.11 gram, 15 mmol) and ammonium bicarbonate (0.79 gram, 10 mmol) was brought to a temperature of 50 °C, resulting in a solid yellow-white substance in 30 minutes. The suspension was separated using a centrifuge and dried at room temperature. The solid was purified by suspending the obtained precipitate in cold ethanol and centrifuging to reobtain the pellet. The melting point range of the collected light yellow solid (1.92 g, 96% yield) was 88.3 - 89.8 °C (uncorrected).

^{1}H NMR (400 MHz, DMSO) δ (ppm) = 8.65 (s, 2H), 7.88 (d, J = 8.4 Hz, 4H), 7.59 – 7.49 (m, 6H), 7.45 (d, J = 8.4 Hz, 2H), 6.06 (s, 1H).

^{13}C NMR (101 MHz, DMSO) δ (ppm) = 160.56, 141.34, 136.36, 134.97, 132.82, 130.52, 129.42, 129.33, 128.92, 90.64. M calculated: 400.03 g/mol on basis of 3 isotopes ^{35}Cl;

MS (ESI) *m/z* observed $[M+H]^+$: 401 (3 isotopes ^{35}Cl) and 403 (2 isotopes ^{35}Cl), *m/z* observed $[M-H]^-$: 399 (3 isotopes ^{35}Cl) and 401 (2 isotopes ^{35}Cl)

Hydro-4-bromo-benzamide (2g):

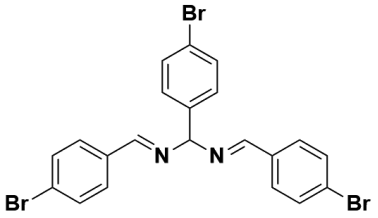

A mixture of 4-bromobenzaldehyde (**1h**, 2.78 gram, 15 mmol) and ammonium bicarbonate (0.79 gram, 10 mmol) was brought to a temperature of 50 °C, resulting in a solid yellow-white substance in 30 minutes. The suspension was separated using a centrifuge and dried at room temperature. The solid was purified by suspending the obtained precipitate in cold ethanol and centrifuging to reobtain the pellet. The melting point range of the collected light yellow solid (2.46 g, 93% yield) was 117.4 – 118.9 °C (uncorrected).

^{1}H NMR (400 MHz, DMSO) δ (ppm) = 8.63 (s, 2H), 7.80 (d, J = 8.5 Hz, 4H), 7.68 (d, J = 8.4 Hz, 4H), 7.58 (dd, J = 8.9, 2.0 Hz, 2H), 7.45 (d, J = 8.5 Hz, 2H), 6.03 (s, 1H).

^{13}C NMR (101 MHz, DMSO) δ (ppm) = 160.76, 141.71, 135.29, 132.27, 131.86, 130.74, 129.79, 125.29, 121.40, 90.67. M calculated: 531.88 g/mol on basis of 3 isotopes ^{79}Br;

MS (ESI) *m/z* observed $[M+H]^+$: 537 (1 isotopes ^{79}Br) and 539 (3 isotopes ^{81}Br), *m/z* observed $[M-H^-$: 533 (2 isotopes ^{79}Br) and 535 (2 isotopes ^{81}Br)

Hydro-4-dimethylamino-benzamide (2h):

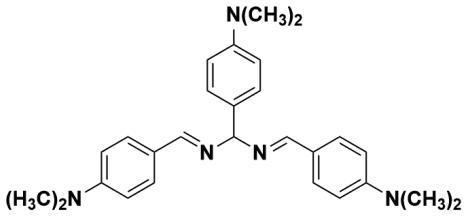

A mixture of 4-dimethylamino-benzaldehyde (**1h**, 2.24 gram, 15 mmol) and ammonium bicarbonate (0.79 gram, 10 mmol) was brought to a temperature of 50 °C, resulting in a solid yellow-white substance in 30 minutes. The solid was purified by suspending the obtained precipitate in 10 mL 30% (m/m) ammonia and subsequently removing the solvent by filtration. The melting point range of the collected light yellow solid (2.03 g, 95% yield) was 171 - 173 °C (uncorrected).

^{1}H NMR (400 MHz, DMSO) δ (ppm) = 8.37 (s, 2H), 7.61 (d, J = 8.3 Hz, 4H), 7.24 (d, J = 8.2 Hz, 2H), 6.71 (dd, J = 15.9, 8.4 Hz, 6H), 5.66 (s, 1H), 2.97 (s, 12H), 2.85 (s, 6H).

^{13}C NMR (101 MHz, $CDCl_3$) δ (ppm) = 159.67, 152.13, 150.16, 131.52, 130.16, 128.03, 124.72, 112.72, 111.51, 93.61, 40.83, 40.26.

Hydro-4-phenyl-benzamide (2i):

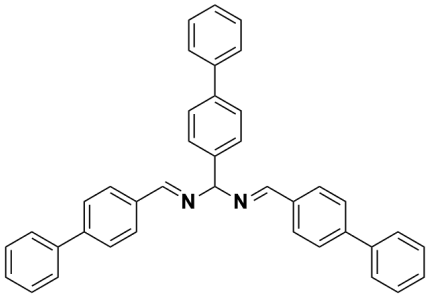

Ammonium acetate (1.54 gram, 20 mmol) was added to a mixture of 4-phenylbenzaldehyde (**1i**, 2.78 gram, 15 mmol), 5.0 ml triethylamine, and 5.0 ml methanol and stirred at room temperature for 30 minutes. The white solid was purified by suspending the obtained precipitate in 20 ml methyl-tert-butyl ether and centrifuging to reobtain the pellet. The melting point range of the collected white solid (3.16 g, 97% yield) was 151.4 - 153.9 °C (uncorrected).

^{1}H NMR (400 MHz, $CDCl_3$) δ (ppm) = 8.66 (s, 6H), 7.95 (d, J = 8.3 Hz, 12H), 7.66 (d, J = 8.3 Hz, 12H), 7.63 – 7.56 (m, 30H), 7.47 – 7.41 (m, 17H), 7.40 – 7.32 (m, 10H), 6.06 (s, 3H).

Hydro-4-acetoxy-benzamide (2m):

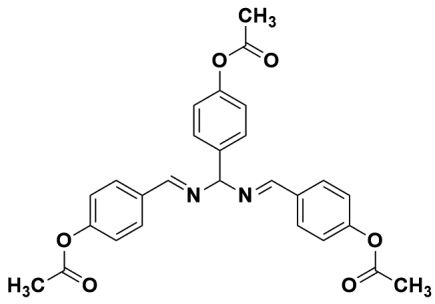

A mixture of 4-acetoxy benzaldehyde **1m** (0.82 gram, 5 mmol) and ammonium bicarbonate (0.79 gram, 10 mmol) was brought to a temperature of 85 °C, resulting in a solid yellow substance in 30 minutes. The solid was washed with 2.5 mL water and recrystallized (methyl-tert-butylether). The melting point range of the collected light yellow solid (0.19 g, 8% yield) was 76.2 - 77.3 °C (uncorrected).

Hydro-4-acetoxyvanillin-amide (2n):

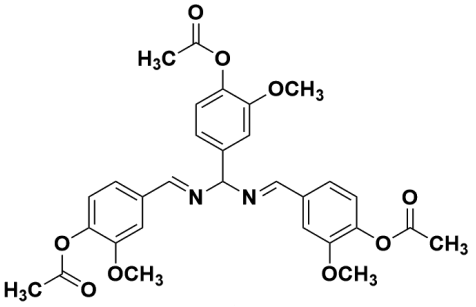

A mixture of 4-acetoxy vanillin **1n** (0.97 gram, 5 mmol) and ammonium bicarbonate (0.79 gram, 10 mmol) was brought to a temperature of 85 °C, resulting in a solid pale yellow substance in 30 minutes. The solid was washed with 2.5 mL water and recrystallized (methyl-tert-butylether). The melting point range of the collected light yellow solid (0.28 g, 10% yield) was 57.0 - 58.9 °C (uncorrected).

Hydro-4-acetoxysyring-amide (2o):

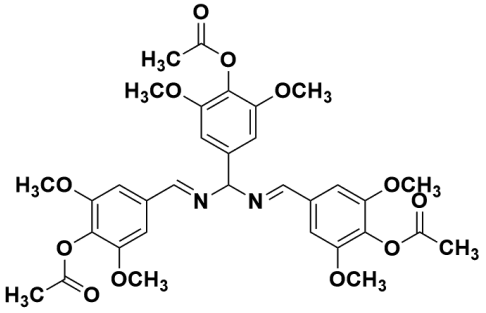

A mixture of 4-acetoxy syringaldehyde **1o** (1.12 gram, 5 mmol) and ammonium bicarbonate (0.79 gram, 10 mmol) was brought to a temperature of 130 °C, resulting in a solid pale yellow substance in 30 minutes. The solid was washed with 2.5 mL water and recrystallized (methyl-tert-butylether). The melting point range of the collected light yellow solid (0.42 g, 13% yield) was 151.3 - 154.3 °C (uncorrected).

^{1}H NMR (400 MHz, DMSO) δ (ppm) = 8.61 (s, 4H), 7.27 (s, 8H), 6.91 (s, 4H), 6.00 (s, 2H), 3.83 (s, 24H), 3.78 (s, 13H), 2.26 (d, J = 5.4 Hz, 12H), 2.25 (s, 6H).

4.5 References

1. Jacobsen, E. N.; Finney, N. S. Synthetic and biological catalysts in chemical synthesis: how to assess practical utility. *Chemistry & Biology* **1994**, *1*, 85-90.
2. Heveling, J. Heterogeneous Catalytic Chemistry by Example of Industrial Applications. *Journal of Chemical Education* **2012**, *89*, 1530-1536.
3. Wang, Q.; Guo, J.; Chen, P. Recent progress towards mild-condition ammonia synthesis. *Journal of Energy Chemistry* **2019**, *36*, 25-36.
4. Vu, M.; Sakar, M.; Do, T. Insights into the Recent Progress and Advanced Materials for Photocatalytic Nitrogen Fixation for Ammonia (NH_3) Production. *Catalysts* **2018**, *8*.
5. Mandal, S.; Mandal, S.; Ghosh, S. K.; Ghosh, A.; Saha, R.; Banerjee, S.; Saha, B. Review of the aldol reaction. *Synthetic Communications* **2016**, *46*, 1327-1342.
6. Knoevenagel, E. Condensation von Malonsäure mit aromatischen Aldehyden durch Ammoniak und Amine. *Berichte der deutschen chemischen Gesellschaft* **1898**, *31*, 2596-2619.
7. Knoevenagel, E. Condensation zwischen Malonester und Aldehyden unter dem Einfluss von Ammoniak und organischen Aminen. *Berichte der deutschen chemischen Gesellschaft* **1898**, *31*, 2585-2595.
8. Davey, R. M.; Stamford, N. P. J. Catalytic enamines from dialkylamide-dialkylacetals. *Tetrahedron Letters* **2012**, *53*, 2537-2539.
9. List, B. Emil Knoevenagel and the roots of aminocatalysis. *Angewandte Chemie (International ed. in English)* **2010**, *49*, 1730-1734.
10. Wan, J.; Jing, Y.; Liu, Y.; Sheng, S. Metal-free synthesis of cyano acrylates via cyanuric chloride-mediated three-component reactions involving a cascade consists of Knoevenagel condensation/cyano hydration/esterification. *RSC Adv* **2014**, *4*, 63997-64000.
11. Joharian, M.; Morsali, A.; Azhdari Tehrani, A.; Proserpio, D. M. Water-stable fluorinated metal–organic frameworks (F-MOFs) with hydrophobic properties as efficient and highly active heterogeneous catalysts in aqueous solution. *Green Chemistry* **2018**, *20*, 5336-5345.
12. Raj, M.; Singh, V. K. Organocatalytic reactions in water. *Chem. Commun.* **2009**, 6687-6703.
13. van Schijndel, J.; Canalle, L. A.; Smid, J.; Meuldijk, J. Conversion of Syringaldehyde to Sinapinic Acid through Knoevenagel-Doebner Condensation. *Open Journal of Physical Chemistry* **2016**, *6*, 101-108.
14. Crowell, T. I.; McLeod, R. K. Kinetics of hydrobenzamide formation from p-dimethylaminobenzaldehyde and ammonia. Role of the imine. *The Journal of Organic Chemistry* **1967**, *32*, 4030-4033.
15. Crowell, T. I.; Peck, D. W. Kinetic Evidence for a Schiff Base Intermediate in the Knoevenagel Condensation1. *Journal of the American Chemical Society* **1953**, *75*, 1075-1077.
16. Kamal, A.; Ahmad, A.; Qureshi, A. A. Syntheses of some substituted hexamines in aqueous medium. *Tetrahedron* **1963**, *19*, 869-872.
17. Nishiyama, K.; Saito, M.; Oba, M. Formation of N,N′-Disubstituted Methanediamine Derivatives from Hexamethyldisilazane and Aldehydes via Stepwise Reactions. *Bulletin of the Chemical Society of Japan* **1988**, *61*, 609-611.
18. Sim, S. K.; Hunter, D. H. 2,4-Diazapentadienes. I. Prototropy, Cyclization, and Addition-Elimination. *Canadian Journal of Chemistry* **1972**, *50*, 669-677.
19. Laurent, M. A. Ueber das Hydrobenzamid. *Annalen der Pharmacie* **1837**, *21*, 130-134.
20. Rao, V. K.; Reddy, S. S.; Krishna, B. S.; Naidu, K. R. M.; Raju, C. N.; Ghosh, S. K. Synthesis of Schiff's bases in aqueous medium: a green alternative approach with effective mass yield and high reaction rates. *Green Chemistry Letters and Reviews* **2010**, *3*, 217-223.
21. Djemili, A.; Lakrout, S.; Cheraiet, Z.; Berredjem, M.; Aouf, N. A simple and highly efficient solvent- and catalyst-free synthesis of novel N-sulfamoyl imines. *Green Chemistry Letters and Reviews* **2015**, *8*, 48-53.

22. Lokhande, R.; Sonawane, J.; Roy, A.; Ravishankar, L. Solvent-free reductive amination of aromatic aldehydes catalyzed by $CeCl_3 \cdot 7H_2O$. *Green Chemistry Letters and Reviews* **2011**, *4*, 69-72.
23. Zhong, G.; Zhong, Q. Solid–solid synthesis, characterization, thermal decomposition and antibacterial activities of zinc(II) and nickel(II) complexes of glycine–vanillin Schiff base ligand. *Green Chemistry Letters and Reviews* **2014**, *7*, 236-242.
24. Gupta, K. C.; Sutar, A. K. Catalytic activities of Schiff base transition metal complexes. *Coordination Chemistry Reviews* **2008**, *252*, 1420-1450.
25. van Schijndel, J.; Canalle, L. A.; Molendijk, D.; Meuldijk, J. The green Knoevenagel condensation: solvent-free condensation of benzaldehydes. *Green Chemistry Letters and Reviews* **2017**, *10*, 404-411.
26. Corey, E. J.; Kühnle, F. A simplified synthesis of (±)-1,2-diphenyl-1,2-diaminoethane (1) from benzaldehyde and ammonia. Revision of the structures of the long-known intermediates “hydrobenzamide” and “amarine”. *Tetrahedron Letters* **1997**, *38*, 8631-8634.
27. Francis, F. Notiz über die Einwirkung von Ammoniak auf Benzaldehyd und die Darstellung von Benzaldehyd-Ammoniak. *Berichte der deutschen chemischen Gesellschaft* **1909**, *42*, 2216-2218.
28. Bordwell, F. G. Equilibrium acidities in dimethyl sulfoxide solution. *Accounts of Chemical Research* **1988**, *21*, 456-463.
29. Doebner, O. Synthese der Sorbinsäure. *Ber. Dtsch. Chem. Ges.* **1900**, *33*, 2140-2142.
30. van Schijndel, J.; Molendijk, D.; Canalle, L. A.; Rump, E. T.; Meuldijk, J. Temperature Dependent Green Synthesis of 3-Carboxycoumarins and 3,4-unsubstituted Coumarins. *Current Organic Synthesis* **2019**, *16*, 130-135.
31. Borah, A. J.; Yan, G. Decarboxylative functionalization of cinnamic acids. *Org. Biomol. Chem.* **2015**, *13*, 8094-8115.
32. Patra, T.; Maiti, D. Decarboxylation as the Key Step in C−C Bond-Forming Reactions. *Chem. Eur. J.* **2017**, *23*, 7382-7401.
33. Oliveri, I. P.; Maccarrone, G.; Di Bella, S. A Lewis Basicity Scale in Dichloromethane for Amines and Common Nonprotogenic Solvents Using a Zinc(II) Schiff-Base Complex as Reference Lewis Acid. *J. Org. Chem.* **2011**, *76*, 8879-8884.
34. Laurence, C.; Gal, J. F. *Lewis Basicity and Affinity Scales: Data and Measurement.* John Wiley & Sons Ltd: Chichester, U.K., **2010**
35. Tiwari, A.; Hihara, L. H. Thermal stability and thermokinetics studies on silicone ceramer coatings: Part 1-inert atmosphere parameters. *Polymer Degradation and Stability* **2009**, *94*, 1754-1771.

5 Repeatable molecularly recyclable semi-aromatic polyesters derived from lignin

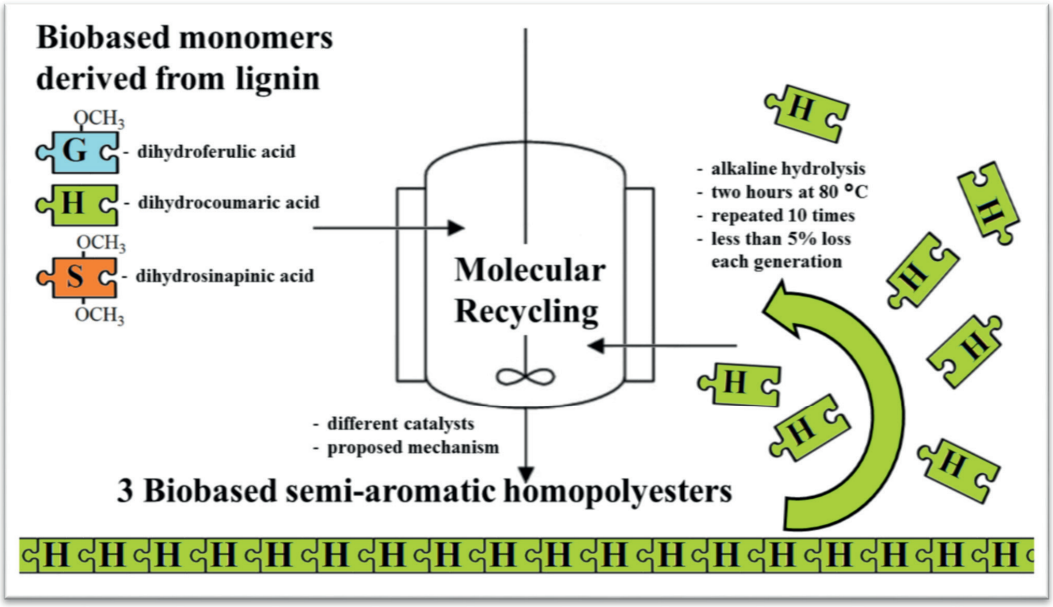

This chapter has been submitted for publication.

Abstract

The design of molecularly recyclable polymers contributes to a possible solution to the end-of-use issue of polymeric materials and gives a closed-loop approach towards a circular materials economy. The biobased semi-aromatic polyesters (e.g., poly(phloretic acid), poly(dihydroferulic acid), and poly(dihydro-sinapinic acid)), described in this paper, can be derived entirely from biomass (mainly lignin) and exhibit thermal properties similar to those of certain commodity polymeric materials. These polyesters with ligno-phytochemicals as monomer have so far demonstrated complete and almost infinite molecular recyclability with a loss of total mass less than 5% per cycle. Moreover, molecular weight and thermal properties (T_g, T_m and T_{cryst}) of the tenth generation polymeric material are identical to those of the first generation.

5.1 Introduction

Since polymeric materials are produced chemically, it may be evident that the way these materials are treated at the end of their technical lifetime is also chemical.[1] With chemical recycling, the monomers are recovered from the polymeric material, resulting in the retainment of valuable chemical information. This retainment of pricey chemical substances is in contrast to the conversion of materials into CO_2 and H_2O by incineration or microbial conversion. Chemical recycling can be classified into two groups.[2] In the first group, polymeric waste is converted directly with gasification or pyrolysis into products with a higher added value compared to original polymeric material.[3,4] In the second group, also referred to as molecular recycling, polymeric waste is depolymerized back to the starting material and then polymerized again to yield virgin-like materials.[5] However, polymeric material that depolymerizes easily often lacks suitable mechanical and thermal properties to be widely applicable in various products.[6] The central paradox of the "plastic" problem is that we request our plastics to be readily recyclable and not to persist in the environment. However, they must also be sufficiently robust to perform satisfactorily in their desired application.

Biobased polymers are polymers produced partially or entirely from renewable natural resources such as microorganisms, plants, or trees.[7] It may also refer to polymers produced by synthetic chemistry and composed of monomers originating from biological sources such as vegetable oils, sugars, fats, or lignin.[8] Lignin is found in all vascular plants and is the second most abundant organic biopolymer (after cellulose). It accounts for approximately 30% of the organic carbon in the biosphere. Among the biomass, lignin is the only sustainable alternative to substitute fossil-based aromatic compounds. Lignin is mainly composed of phenyl propane units containing methoxy and hydroxyl groups.[9] Hence, novel technological developments are required for the decomposition of the chemical structure of lignin into the ligno-phytochemicals.[10,11]

Molecularly recyclable polyesters typically contain a high fraction of aliphatic ester groups because derivatives of aliphatic carboxylic acids are several orders of magnitude more electrophilic than the analogous derivatives of aromatic carboxylic acids.[12] Polyesters derived from aromatic dicarboxylic acids are therefore much less electrophilic and, thus, far less sensitive to hydrolysis than aliphatic polyesters, as evidenced by the stability of poly(ethylene terephthalate) (PET)-based textile fibers to washing or rainy weather.[13]

For the abovementioned reasons, we are interested in producing polyesters of 4-hydroxy-dihydrocinnamic acids, including an aliphatic ester into the

thermoplastic polymer backbone. An aromatic component is incorporated to improve the materials performance intrinsically.[14] Previous research by e.g., Kricheldorf[15], Meier[16], and Miller[17,18] showed that it is challenging to polymerize these 4-hydroxy-dihydrocinnamic acids, as shown in Scheme 5.1. These polymerizations were often not successful due to side effects like crosslinking and decarboxylation, and particularly the polymerization mechanism remains unclear. This chapter attempts to provide more insight into the polymerization mechanism. The chapter will also show the conditions allowing a high yield synthesis of molecularly recyclable semi-aromatic polyesters (e.g., poly(phloretic acid), poly(dihydroferulic acid), and poly(dihydrosinapinic acid)), that can be repeatedly recycled to its starting material.

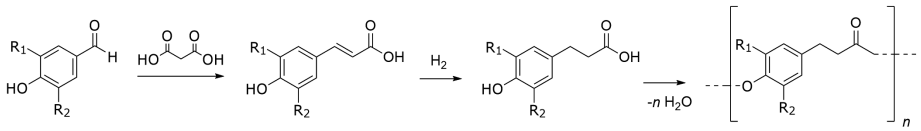

1 **2** **3** **5** polyester

a R_1 = H, R_2 = H
b R_1 = H, R_2 = OCH_3
c R_1 = OCH_3, R_2 = OCH_3

5a poly-H
5b poly-G
5c poly-S

Scheme 5.1: Synthetic scheme for the preparation of molecularly recyclable semi-aromatic polyesters, from bio-renewable feedstocks as ligno-phytochemicals **1** and **2**.

5.2 Results and discussion

Previously, a green, efficient, and scalable method has been developed, producing cinnamic acid analogs from 4-hydroxybenzaldehydes **1** by condensation with malonic acid.[19,20] By applying this Green Knoevenagel reaction and subsequent hydrogenation, polymerizable 4-hydroxy-dihydrocinnamic acids as monomers became available. These monomers are, in our opinion, suitable for conversion into the designed molecularly recyclable polymers e.g., poly(phloretic acid), poly(dihydroferulic acid), and poly(dihydrosinapinic acid). Although all three homopolyesters are independently synthesized, the route to the polymers is described for poly(phloretic acid).

First, *p*-coumaric acid **2a** was synthesized in high yield (>95% based on 4-hydroxy benzaldehyde) with the Green Knoevenagel reaction. Hereafter, *p*-coumaric acid **2a** was hydrogenated to obtain *p*-dihydrocoumaric acid (phloretic acid) **3a** with a yield of more than 95% based on *p*-coumaric acid **2a**. Direct polymer synthesis with melt polymerization of **3a**, however, gave in all cases a low yield due to sublimation and low reactivity of the monomer. These attempts demonstrated that it was possible to follow the oligomerization with LC-MS. Additionally, it is essential to emphasize that from the oligomers the monomers could always be quickly recovered by hydrolysis in a 1 M NaOH solution.

To prevent sublimation of phloretic acid, **3a** was acetylated with acetic anhydride in combination with sodium acetate in order to obtain the corresponding acetylated phloretic acid **4a**. In addition to acetylation, also dimerization and oligomerization were observed as reported earlier by Kricheldorf et al.[12,21] Ultimately, this inspired us to optimize the molar ratio of acetic anhydride as well as that of sodium acetate and phloretic acid to increase the selectivity towards the envisioned acetylated oligomers. The optimal ratio appeared to be 2.0 equivalents of acetic anhydride, 0.2 equivalents of sodium acetate based on 1.0 equivalent of the phloretic acid **3a**. Note that according to HPLC results, under these conditions more dimers and trimers were produced than acetylated monomers **4a**. Amongst others, by their molecular weight, these dimers and oligomers exhibit less sublimation in a melt polymerization and these "pre-polymers" would be qualified to serve as starting material for further polymer synthesis in the melt.[22] The formation of dimers and trimers also proves the requirement of 4-acetoxy-dihydro-cinnamic acid **4** as a monomer in which an activated acid group can attack the 4-acetoxy group[23] as figured in Scheme 5.2.

Scheme 5.2 shows a possible mechanism of the step-growth polycondensation in which the presence of the acetoxy group is a prerequisite, and the amount of base is decisive.[24] As shown in step i in Scheme 5.2, the base will first deprotonate the carboxylic group and thereby enhances its nucleophilicity. Subsequently, the deprotonated acid group attacks the acetoxy group of the other monomer. After step ii a tetrahedral state is created whereby the phenoxide group is transferred (phenoxide-shift) to the other carbonyl group in step iii. After this phenoxide-shift in step iv, acetic acid splits off after taken a proton from the former

protonated base. With applied vacuum, the acetic acid molecule is removed from the reaction mixture as the by-product of this step-growth polycondensation.[25] In this closed cycle, the chain length has increased with one monomeric unit and is ready for the next cycle.

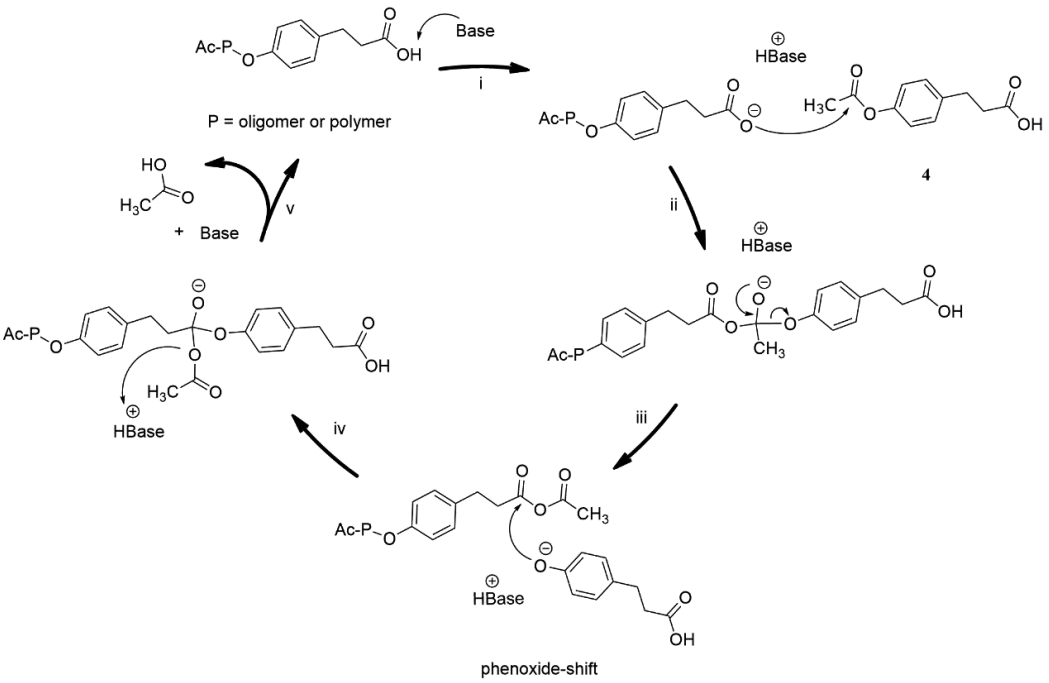

Scheme 5.2: Proposed mechanism of the step-growth polycondensation of phloretic acid monomers and oligomers.

The number average degree of polymerization (DP_n) of the acetylated oligomers was obtained with ^{1}H NMR end group analyses and GPC measurements. Figure 5.1 shows the ^{1}H NMR spectrum of acetylated phloretic acid **4a** (bottom) as well as the ^{1}H NMR spectra of samples taken during the polymerization. Referring to the basic units of lignin (*p*-hydroxycinnamyl (**H**), guaiacyl (**G**), and syringyl (**S**) lignin), this homopolyester poly(phloretic acid), is named "poly-H" as the others poly(dihydroferulic acid), and poly(dihydrosinapinic acid) are named respectively "poly-G" and "poly-S". As shown in Figure 5.1, the area of the acetyl group as an end group decreases, and the number average degree of polymerization (DP_n) can be determined.

All products of poly-H, dissolve well in a mixture of $CF_3COOD/CDCl_3$ for ^1H NMR measurements but not in the solvent hexafluoro-2-propanol (HFIP) for GPC measurements. Several GPC systems with various mobile phases were tested. Since the homopolyesters poly-H, poly-G, and poly-S were not soluble in standard organic solvents such as dimethylformamide (DMF), hexafluoro-2-propanol (HFIP), chloroform ($CHCl_3$) and tetrahydrofuran (THF), another method was developed in order to determine their number average molecular weight (M_n). DSC thermograms of poly-H show a high crystallinity, which possibly decreasing solubility. Several attempts were tried to induce amorphicity of poly-H by heating the sample to above its melting point and quenching the sample by using liquid nitrogen. This way, it was expected that the polymer chains would not be able to crystallize almost completely and consequently become (more) amorphous. Samples were dissolved in DMF and measured with the GPC. However, GPC analysis with DMF as an eluent still resulted in low M_n values ranging from 1,900 to 2,100 kDa.

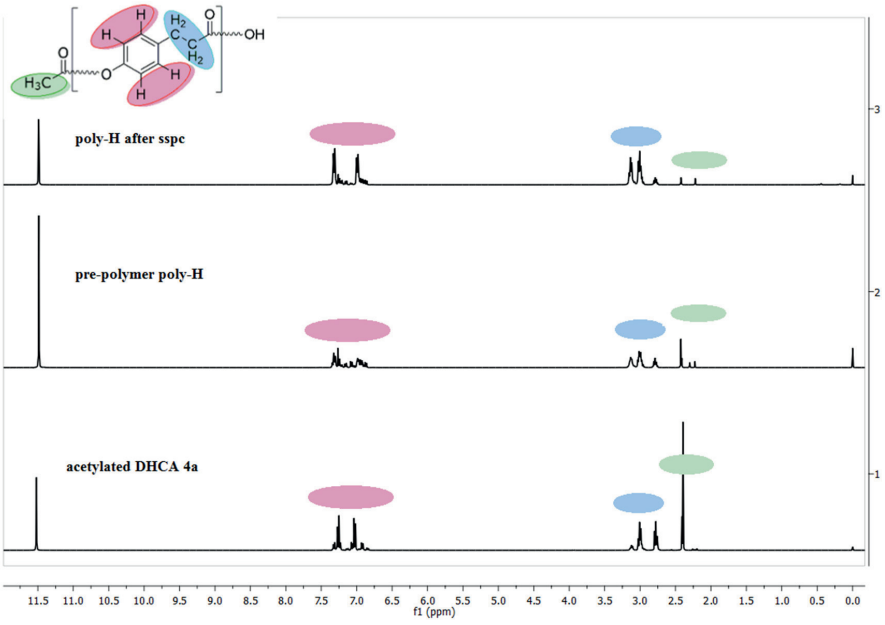

Figure 5.1: Overlays of ^1H NMR spectra (25 °C, $CF_3COOD/CDCl_3$, with residual solvent peaks at 11.49, 7.27 ppm for CF_3COOH and $CHCl_3$, respectively) of (a) product of acetylation of *p*-dihydrocoumaric acid **3a** (bottom); (b) pre-polymer poly-H after the stage of pre-polymerization (middle) (144 °C, 3 hours); (c) poly-H after melt phase polycondensation (240 °C, 3 hours, vacuum, top).

Further research[26] indicated that by blending atactic polystyrene into the polyester, higher amorphicity could be achieved. Therefore, polystyrene and poly-H were added together in the alumina DSC pan, heated and quenched in liquid nitrogen. After the removal of polystyrene, the samples dissolved in DMF and showed the presence of high molecular weight material, as demonstrated in Table 5.1. It must be emphasized that the molecular weight values are only indicative since the GPC system was calibrated with a polystyrene standard. With HFIP as eluent using a PMMA calibration standard, a number average molecular weight M_n of 69 kDa was measured of commercially obtained PET (Arnite® A04 900). Note that with the same PET, an M_n of 73 kDa was measured in this set-up with DMF as eluent using a polystyrene calibration standard. It was tried to dissolve the amorphous poly-H in HFIP in order to confirm molecular weights with another GPC system. However, no complete solubility of the polyesters in the HFIP solvent was realized, and the analysis resulted only in low molecular weight elution peaks. The lack of solubility of the polyesters in organic solvents agrees with the research of Miller[17] and Kaneko[27]. However, their researches on solubility in eluents for GPC analysis were not continued, and alternative methods, such as viscosity measurements and ^{1}H NMR end group analysis, were used for molecular weight indication.

The efficient polymerization of the "pre-polymers" in the melt gave a solid white polymeric substance. A recurring problem with this manner of melt polymerization was the increasing degradation of the polymeric material with a stepwise increase of the temperature. It turned out to be challenging to find an optimal combination of higher molecular weight build-up with minimal degradation. Therefore, it was examined whether the condensation polymerization could be carried out in an amount of solvent as small as possible, so hampering an increase of viscosity upon polymerization ("solvent assisted poly-condensation").[28] With 1,2-xylene, which appeared to be a proper choice, several catalysts have been tested to improve the phenoxide-shift in step iii in the proposed mechanism, as presented in Scheme 5.2. Zinc(II)acetate gave the best results in both molecular weight and polymerization time, as shown in Table 5.1. Before the final melt phase polycondensation, the solvent 1,2-xylene was removed. During the final stage of the polymerization the temperature was raised to 240 °C and high vacuum was applied. Both ^{1}H NMR end group analysis and GPC provide molecular weight information. The GPC information was always after forced

amorphicity in liquid nitrogen accompanied with atactic polystyrene. From the obtained results presented in Table 5.1, it is visible that the GPC M_n values of the polymer samples are almost a factor two higher than the corresponding values obtained with ^{1}H NMR. This variation is related to the differences of hydrodynamic volumes of the synthesized polymers and the polystyrene standards used during the GPC measurements.[29] The products have been thermally characterized with DSC and TGA.

It should be noted that the molecularly recyclable semi-aromatic polyesters seem to have comparable thermal properties to PET. The T_m of poly-H, for example, is around 230 °C, and this is 35 degrees lower than PET with a T_m of 265 °C. The glass transition temperatures are also comparable and in proportion to PET with a T_g of 67 °C. Poly-H has a higher cooling-cycle crystallization temperature T_{cryst} (218 °C) compared to PET (T_{cryst} = 190 °C).[30] Additionally, PET typically exhibits a peak decomposition temperature near 470 °C (50% mass loss under nitrogen, as measured by thermal gravimetric analysis).[31]

Table 5.1: Polymerization and characterization of poly-H **5a**, poly-G **5b**, and poly-S **5c** in the melt and solvent assisted with different catalysts.

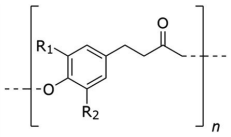

5a poly-H : R_1 = H, R_2 = H
5b poly-G : R_1 = H, R_2 = OCH_3
5c poly-S : R_1 = OCH_3, R_2 = OCH_3

Entry		Catalyst (1 mol%)	DP[a]	M_n[a] (kDa)	M_n[b] (kDa)	M_w[b] (kDa)	DP[b]	PDI[b]	T_g[c] (°C)	T_{cryst}[c] (°C)	T_m[c] (°C)	$T_{50\%}$[d] (°C)
1	poly-H, 1,2-xylene	none	186	27.5	43.6	57.2	295	1.3	35	223	235	416
2	poly-H, diphenyl ether	none	188	27.8	40	51.7	269	1.3	36	225	241	419
3	poly-H, anisole	none	176	26	41.6	56	281	1.3	32	219	238	411
4	poly-H, 1,2-xylene	$Zn(OAc)_2$	260	38.4	65.2	83.7	440	1.3	42	218	229	428
5	poly-H, 1,2-xylene	$Zn(Cl)_2$	246	36.4	62.3	74.9	421	1.2	42	219	231	402
6	poly-H, 1,2-xylene	$Sn(Cl)_2$	245	36.2	59	69.1	398	1.2	n.o.	223	228	399
7	poly-H, 1,2-xylene	$Sn(Oct)_2$	231	34.1	54.8	64.1	370	1.2	41	221	234	406
8	poly-H, 1,2-xylene	Sb_2O_3	184	27.1	35.5	41.6	240	1.2	n.o.	217	231	409
9	poly-G, 1,2-xylene	$Zn(OAc)_2$	200	35.6	48.2	57	270	1.2	76	193	243	373
10	poly-S, 1,2-xylene	$Zn(OAc)_2$	180	37.4	62.9	83.3	297	1.3	105	176	197	321
	PET, commercial grade				73	119	380	1.6	67	190	265	470

[a] Degree of Polymerization and M_n by ^{1}H NMR end group analysis.
[b] Obtained by GPC in DMF at 70 °C versus polystyrene standards.
[c] Determined by DSC after forced amorphicity, n.o. = not observed
[d] Determined by TGA.

The depolymerization was investigated in aqueous media to get a clear picture of the total cycle and allowing the recovery of monomers for reuse.[32,33] Samples were placed in phosphate buffered saline (PBS) buffer with a pH of 7.4, and in a diluted acid-solution and alkaline-solution below 0.001 M. The polymers proved to be resilient to degradation in these solutions at room temperature for over five weeks. The poor hydrolytic degradability is probably due to the hydrophobic nature of the materials.

Molecular recycling of poly-H was further investigated by alkaline hydrolysis, using a 1 M NaOH solution at a temperature of 80 °C. The alkaline hydrolysis of poly-H, using a 1 M NaOH solution and a temperature of 80 °C, was studied over time. A calibration curve of phloretic acid **3a** (*p*-dihydrocoumaric acid DHCA) was set up with HPLC analysis in order to calculate the yield percentages of hydrolyzed poly-H samples. The hydrolysis of poly-H resulted in the monomer phloretic acid **3a** after 1 hour, which was confirmed with HPLC, ^{1}H NMR, and melting point analysis. As demonstrated in Figure 5.2, more prolonged reaction times did not lead to higher phloretic acid **3a** yields.

A reliable way to correctly determine the molecular recycling mass balance is to compare the amount of monomer before polymerization and after depolymerization. The mass balance of the molecular recycling cycle of poly-H has been determined by polymerization of 5.00 grams of phloretic acid **3a** to poly-H. This polyester was depolymerized to phloretic acid **3a**. The regenerated mass of phloretic acid **3a** after the first depolymerization was 4.56 gram. This procedure indicates that by weight, 91% of the monomer is recovered during one cycle. The most substantial loss occurred in the liquid-liquid extraction step with ethyl acetate using equal volumes of ethyl acetate and the aqueous phloretic acid **3a** solution. Isolation of phloretic acid **3a** from the organic layer was performed by evaporation of ethyl acetate under reduced pressure (400 mbar) at a temperature of 40 °C.

The partition coefficient of phloretic acid **3a** was determined between equal volumes of acidified water (pH of 1) and ethyl acetate. It must be indicated that ethyl acetate is slightly soluble in water, and a ternary phase diagram is necessary for a detailed design of the extraction process. However, for a preliminary study to verify if the molecular recycling of phloretic acid **3a** is realistic, the determination of a ternary phase diagram has not been taken into account. A proper indication of the partition coefficient of phloretic acid **3a** between equal volumes of acidified water (pH of 1) and ethyl acetate at room temperature was determined to be approximately 40 $\left[\frac{dm^3_{water}}{dm^3_{ethyl\ acetate}}\right]$. The liquid-liquid extraction step with every generation could be optimized to less than 5% monomer loss due to experimental conditions and operation scale.

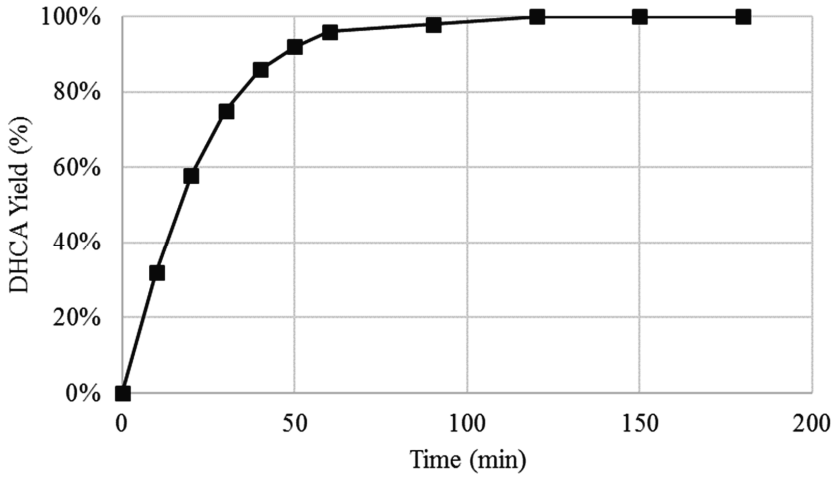

Figure 5.2: Alkaline hydrolysis (1 M NaOH solution, 80 °C) of poly-H over time, determined by DHCA yield based on HPLC peak areas at 254 nm.

Molecular recycling, being a naturally occurring process, has inspired us to design polymers together with their recycling route in the same way. Hence, towards reaching completely sustainable cycles, polymer material requires consecutive polymerization, depolymerization, and re-polymerization with changes in their quantity or final properties to be as small as possible. With this in mind and as a proof of principle, we have produced ten generations of poly-H and brought it back to its monomeric unit every time, as shown in Figure 5.3. The losses of the monomer phloretic acid **3a** were reasonably limited so that after ten generations, approximately 50% of the initial amount of monomer phloretic acid **3a** remained. We have demonstrated that this not only applies to poly-H but the same almost complete sustainable cycle is possible with poly-G and poly-S.

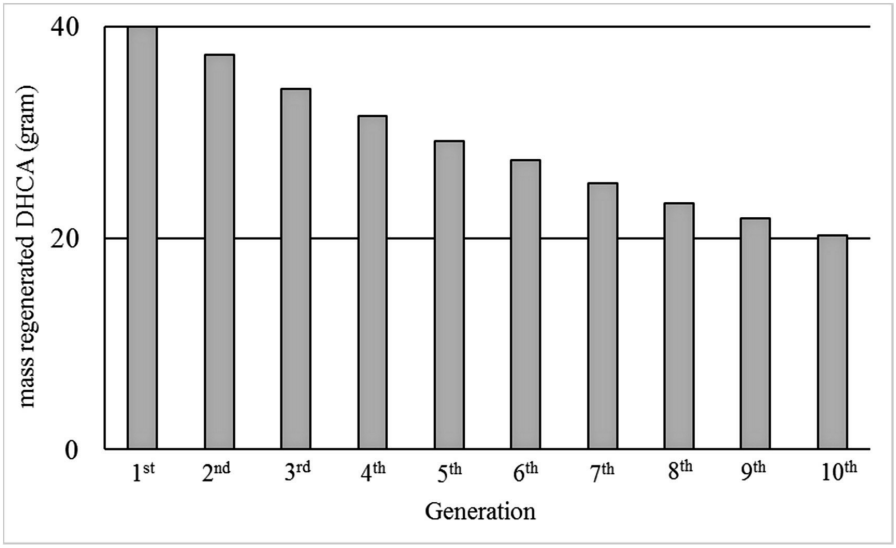

Figure 5.3: Observed regenerated mass of the monomer phloretic acid **3a** as a function of the number of recycling steps.

Since this study focusses on both the molecular recycling process, as well as the retainment of polymer properties during various cycles, thermal analysis was performed on all ten successive generations. The thermograms of poly-H and their successive generations (poly-H generation 2.0 up to poly-H generation 10.0) polymeric material are shown in Figure 5.4. DSC analysis of poly-H shows an endothermic melting signal (T_m) at 229 °C and an exothermic signal at 218 °C,

indicating crystallization. The polymers from re-polymerized phloretic acid **3a** poly-H 2.0 up to poly-H 10.0, exhibit similar thermal properties. Glass transition temperatures (T_g) or cold crystallization signals are not visible in the thermograms of poly-H and their successive generations, which points to the absence of amorphous polymeric material.

This is one of the first times a complete sustainable cycle is presented where a polymeric material is formed by polymerization, depolymerized, and then re-polymerized with only minor changes in their quantity or final properties.[6,34,35] Note that efforts have to be made to reduce the amount of salt produced by acidifying the NaOH solution with sulfuric acid. Given the principles of Green Chemistry, the conditions of depolymerization and reprocessing can also be improved. Further studies could focus on the investigation of the hydrolysis mechanism in aqueous solutions of the obtained semi-aromatic polyesters poly-H, poly-G, and poly-S. Currently, the detailed mechanism of the depolymerization, as well as rate coefficients of the fundamental reaction steps occurring, are not published. An autocatalytic mechanism might play a role in this process, which is assumed to play a role in the hydrolysis of aliphatic polyester PLA.[36-38]

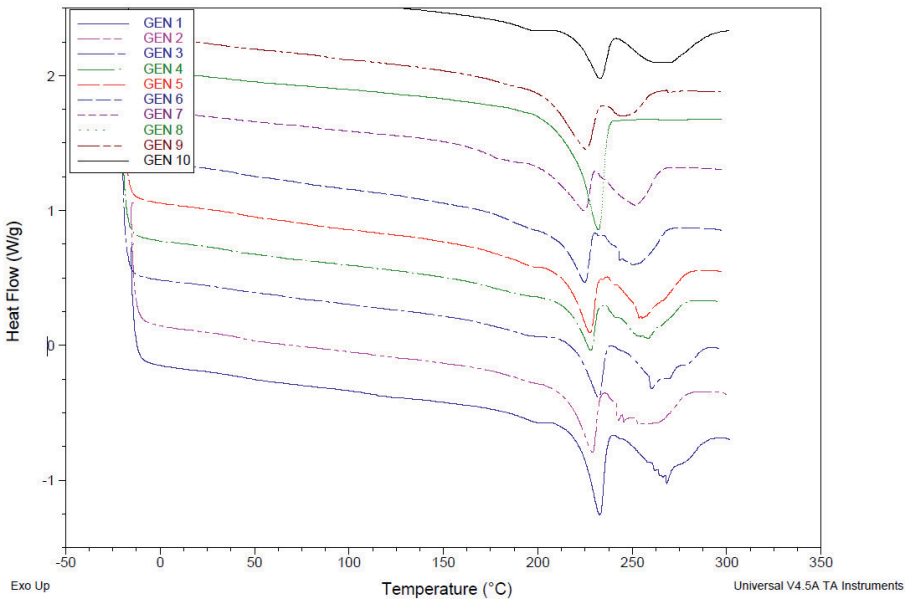

Figure 5.4: Thermal analysis of the ten generations of poly-H.

5.3 Conclusions

Three ligno-phytochemicals were successfully synthesized as a monomer by application of the Green Knoevenagel condensation reaction, hydrogenation, and acetylation of 4-hydroxy benzaldehyde (**1a**), vanillin (**1b**), and syringaldehyde (**1c**). All three monomers were polymerized into semi-aromatic molecularly recyclable polyesters and were depolymerized to their monomers, as confirmed with HPLC, melting point, and ^{1}H NMR analysis. After depolymerization, the monomers were easily extracted and subsequently re-polymerized. The higher-generation polymeric material exhibited similar thermal properties as the first generation polymeric material, indicating that the selected monomers are suitable for repolymerization. The highly crystalline nature of the polymeric materials caused their lack of solubility in organic solvents. This lack of solubility is the reason why a method has been developed to achieve a higher degree of amorphicity. Estimation of the molecular weight of the polyesters was made, indicating the presence of high molecular weight material with M_n values in the range of approximately 50 to 70 kDa. Depolymerization reactions of all three semi-aromatic polyesters indicate that monomer yields can be obtained with a loss of total mass less than 5% per cycle.

5.4 Experimental section

5.4.1 General remarks

Reagents: Syringaldehyde (**1**), and all other chemicals (99% purity) were purchased from Sigma-Aldrich and were used as received. DMSO-*d6* was purchased from Cambridge Isotope, with 99 atom% deuterated. Virgin PET granules (Arnite® A04 900) were purchased from DSM.

Instrumentation: ^{1}H NMR spectroscopy measurements were performed on an Agilent 400-MHz NMR system with DMSO-d_6 as solvent. Data was acquired using VnmrJ3 software. Chemical shifts are reported in ppm, relative to tetramethylsilane (TMS).

HPLC analysis was carried out using a Liquid Chromatographic system (Agilent 1100 series) equipped with a diode array detector (Agilent 1100 series) and an autosampler injector with a 20 µL loop (Agilent 1100 series G1316A). The system was equipped with a Luna 5 µm C18 column (250 mm × 4.6 mm). HPLC measurements were made with the following settings: Flow 1.0 mL/min at a temperature of 20 °C, Eluent A = methanol, Eluent B = acetic acid buffer (99%

milliQ, 1% acetic acid). DAD wavelength of 300 nm. The samples were eluted by the following gradient: 40% A and 60% B as initial conditions and set for 6 min, gradient to 100% A and 0% B in 10 min, 100% A and 0% B set for 5 min, end conditions 40% A and 60% B are set for 8 min.

LC-MS analysis was performed using a Liquid Chromatographic system (Agilent 1200 series) equipped with a Luna 3 µm C18 column (250 × 2.0 mm) and an ion trap (Agilent 6300 series).

The hydrogenation was conducted in 2 M aqueous NaOH-solution using Raney Nickel catalyst and was carried out at a temperature of 60 °C. A 450 ml Parr Series 3910 shaker type hydrogenation apparatus was employed.

Size exclusion chromatography (SEC-HFIP) was measured on a system equipped with a Waters 1515 Isocratic HPLC pump, a Waters 2414 refractive index detector (40 °C), a Waters 2707 autosampler, a PSS PFG guard column followed by 2 PFG-linear-Xl (7µm, 8 × 300 mm) column in series at 40 ºC. 1,1,1,3,3,3-Hexafluoroisopropanol (HFIP, Biosolve) with potassium trifluoroacetate (20 mmol L^{-1}) was used as eluent at a flow rate of 0.8 mL min^{-1}. The molecular weights were calculated against poly(methyl methacrylate) standards (Polymer Laboratories, M_p = 580 g mol^{-1} up to $M_p = 7.1 \times 10^6$ g mol^{-1}). Samples were prepared in the eluent at a concentration of 2-3 mg mL^{-1}. Before GPC analysis was performed, the samples were filtered through a 0.2 µm PTFE filter (13 mm, PP housing, Alltech).

Size exclusion chromatography (SEC-DMF) was performed using a liquid chromatographic system (Agilent 1100 series G1362A) equipped with a Varian PLgel column (300 × 7.5 mm) at 70 °C, a refractive index detector (70 ºC) and an UV-vis absorbance detector. Dimethylformamide (DMF) was used as eluent at a flow rate of 1.0 mL/min. The molecular weights were calculated with respect to polystyrene standards (Polymer Laboratories, M_n = 500 g mol^{-1} up to $M_n = 2 \times 10^6$ g mol^{-1}). Before the GPC analysis, the samples were filtered through a 0.45 µm PTFE filter.

Differential scanning thermograms were obtained with a DSC Q20 from TA Instruments. About 5-10 mg of each sample were massed and added to a sealed pan that went through a heat/cool/heat cycle at 10 °C/min. Reported data are from the second full cycle. The temperature range depends on the experiment but was limited to 300 °C by the instrument.
Thermogravimetric analyses (TGA) were measured under nitrogen with a TGA Q500 from TA Instruments. About 5–10 mg of each sample was heated at 10 °C/min from 25 to 990 °C.
Melting points were determined with the Hanon Automatic Video Melting Point apparatus MP450.
The depolymerization of polymers was performed in test tubes in an Eppendorf ThermoMixer C with a thermoblock.

5.4.2 Experimental procedures and characterization

*Protocol for the Green Knoevenagel condensation towards **2a** with 5 mol% ammonium bicarbonate:*

Malonic acid (20.81 g, 200.0 mmol) together with 4-hydroxy benzaldehyde, (**1a**, 24.42 g, 200.0 mmol) was dissolved in 20.0 mL ethyl acetate, and ammonium bicarbonate NH_4HCO_3 (790.6 mg, 10.0 mmol) was subsequently added. The reaction mixture was kept for 2 hours at 110 °C for complete conversion to *p*-coumaric acid **2a**. Samples of 2.0 µL were taken for reversed-phase HPLC analysis and diluted in 7.5 mL methanol, filtered, and analyzed using the method described in section 5.4.1. The calculated percentage of the peak area of the component of interest is in relation to the total area of peaks.

*Representative procedure for the hydrogenation of **2a** towards **3a** with Raney nickel:*

A 450 ml Parr® shaker type hydrogenation apparatus was charged with *p*-coumaric acid **2a** (24.62 gram, 150 mmol) dissolved in 300 mL 2 M NaOH solution and 1.5 gram of Raney Nickel™ slurry was added. The reactor was pressurized with hydrogen (3 bar), and the reaction was shaken at 80 °C for 3 hours. After this time, the reactor was cooled to room temperature and slowly depressurized. Most of the catalyst was retrieved with a magnet, but the solution was also passed through a 0.2 μm Whatman filter. Subsequently, it was acidified with 4 M HCl solution towards a pH of 2 and extracted with ethyl acetate (4 x 50 mL). After drying over $MgSO_4$, the solvent was removed under reduced pressure, and the solid product *p*-dihydrocoumaric acid **3a** was subsequently dried at 60 °C in a vacuum oven.

*Protocol for the acetylation of **3a** with sodium acetate as a base towards acetylated monomers **4a** and oligomers (pre-polymer):*

p-Dihydrocoumaric acid **3a** (16.62 g, 100 mmol) was dissolved in acetic anhydride (14.2 mL, 150 mmol) and the base sodium acetate (0.82 g, 10 mmol) was added, the solution was stirred and kept for 1 hour at 90 °C for complete conversion of **3a** towards 4-acetoxy dihydrocoumaric acid **4a** and acetylated oligomers. The solid was dissolved in 25 mL acetone, precipitated (solvent-non solvent) into 250 mL 0.1 M HCl and filtered under vacuum.

Representative procedure for the polymerization of acetylated monomers and oligomers:

To the monomers, **4a** and pre-polymer (20.8 g, 100 mmol) in a flask equipped with an overhead stirrer 10 mol% finely powdered NaOH (400 mg, 10.0 mmol) was added and heated for 3 hours at 140 °C. The reaction was stirred at ~100 rpm by the overhead stirrer. A solvent assisted polymerization was created by adding 25.0 mL of o-xylene and zinc(II)acetate (180 mg, 1 mmol). The mixture was refluxed at 144 °C for 3 hours with H_2O removal using a Dean–Stark head. The reaction mixture was cooled down, and the o-xylene was removed by applying a vacuum (<10 mbar). During the final stage of the polymerization, the temperature was raised to 240 °C and a high vacuum (<1 mmHg) was applied for 3 hours. The polymer poly-H **5a** was cooled to room temperature and washed with methanol to eliminate **4a** and oligomers.

Representative procedure for the depolymerization of poly-H in 1 M NaOH:
The release of phloretic acid **3a** from polymer poly-H **5a** was evaluated by chemical recycling in 1 M NaOH. To measure hydrolytic degradation, poly-H **5a** was finely divided (particles smaller than 180 μm). It was distributed in 8 test tubes with equal amounts of 20 mg poly-H to which 1.0 mL of 1 M NaOH had been added and incubated at three different temperatures (RT, 50, and 80 °C) with agitation at 500 rpm using a controlled environment incubator shaker. At various times a test tube was neutralized with 1.0 mL of 0.5 M H_2SO_4, 2.0 mL of methanol was added, and the test tube was analyzed by high-performance liquid chromatography (HPLC) according to the above method. All samples were filtered using 0.45 μm PTFE syringe filters and subsequently injected (20 μL) using an autosampler. Absorbance was monitored at $\lambda = 275$ nm, and the concentration was calculated from a calibration curve of known phloretic acid **3a** standard solutions.

5.5 References

1. Rahimi, A.; García, J. M. Chemical recycling of waste plastics for new materials production. *Nature Reviews Chemistry* **2017***, 1*, 41570.
2. Sardon, H.; Dove, A. P. Plastics recycling with a difference. *Science* **2018***, 360*, 380-381.
3. Jones, G. O.; Yuen, A.; Wojtecki. R. J.; Hedrick, J. L.; García, J. M. Computational and experimental investigations of one-step conversion of poly(carbonate)s into value-added poly(aryl ether sulfone)s. *Proceedings of the National Academy of Sciences of the United States of America* **2016***, 113*, 7722-7726.
4. García, J. M.; Jones, G. O.; Virwani, K.; McCloskey, B. D.; Boday, D. J.; ter Huurne, G. M.; Horn, H. W.; Hedrick, J. L. Recyclable, Strong Thermosets and Organogels via Paraformaldehyde Condensation with Diamines. *Science* **2014***, 344*, 732-735.
5. Brutman, J. P.; De Hoe, G. X.; Schneiderman, D. K.; Le, T. N.; Hillmyer, M. A. Renewable, Degradable, and Chemically Recyclable Cross-Linked Elastomers. *Industrial & Engineering Chemistry Research* **2016***, 55*, 11097-11106.
6. Hong, M.; Chen, E. Y. Completely recyclable biopolymers with linear and cyclic topologies via ROP of γ-butyrolactone. *Nature chemistry* **2016***, 8*, 42-49.
7. Llevot, A.; Grau, E.; Grelier, S.; Cramail, H. From Lignin-derived Aromatic Compounds to Novel Biobased Polymers. *Macromolecular Rapid Communications* **2016***, 37*, 9-28.
8. Hernández, N.; Williams, R. C.; Cochran, E. W. The battle for the "green" polymer. Different approaches for biopolymer synthesis: bioadvantaged vs. bioreplacement. *Organic & biomolecular chemistry* **2014***, 12*, 2834-2849.
9. Lochab, B.; Shukla, S.; Varma, I. K. Naturally occurring phenolic sources: monomers and polymers. *RSC Advances* **2014***, 4*, 21712-21752.
10. Fache, M.; Boutevin, B.; Caillol, S. Vanillin, a key-intermediate of biobased polymers. *European Polymer Journal* **2015***, 68*, 488-502.
11. Pinto, P. C. R.; Costa, C. E.; Rodrigues, A. E. Oxidation of Lignin from Eucalyptus globulus Pulping Liquors to Produce Syringaldehyde and Vanillin. *Ind. Eng. Chem. Res.* **2013***, 52*, 4421-4428.
12. Kricheldorf, H. R.; Stukenbrock, T. Telechelic, star-shaped and hyperbranched polyesters of β-(4-hydroxyphenyl) propionic acid. *Polymer* **1997***, 38*, 3373-3383.
13. Gilding, D. K.; Reed, A. M. Biodegradable polymers for use in surgery: poly(ethylene oxide) poly(ethylene terephthalate) copolymers: 1. *Polymer* **1979***, 20*, 1454-1458.
14. Jiang, Y.; Loos, K. Enzymatic Synthesis of Biobased Polyesters and Polyamides. *Polymers* **2016***, 8*, 243.
15. Kricheldorf, H. R.; Stukenbrock, T. New polymer syntheses, 92. Biodegradable, thermotropic copolyesters derived from β-(4-hydroxyphenyl)propionic acid. *Macromolecular Chemistry and Physics* **1997***, 198*, 3753-3767.
16. Kreye, O.; Oelmann, S.; Meier, M. A. Renewable Aromatic-Aliphatic Copolyesters Derived from Rapeseed. *Macromolecular Chemistry and Physics* **2013***, 214*, 1452-1464.
17. Mialon, L.; Pemba, A. G.; Miller, S. A. Biorenewable polyethylene terephthalate mimics derived from lignin and acetic acid. *Green Chemistry* **2010***, 12*, 1704-1706.
18. Nguyen, H. T. H.; Reis, M. H.; Qi, P.; Miller, S. A. Polyethylene ferulate (PEF) and congeners: polystyrene mimics derived from biorenewable aromatics. *Green Chemistry* **2015***, 17*, 4512-4517.
19. van Schijndel, J.; Canalle, L. A.; Molendijk, D.; Meuldijk, J. The green Knoevenagel condensation: solvent-free condensation of benzaldehydes. *Green Chemistry Letters and Reviews* **2017***, 10*, 404-411.
20. van Schijndel, J.; Molendijk, D.; Spakman, H.; Knaven, E.; Canalle, L. A.; Meuldijk, J. Mechanistic considerations and characterization of ammonia-based catalytic active intermediates of the green Knoevenagel reaction of various benzaldehydes. *Green Chemistry Letters and Reviews* **2019***, 12*, 323-331.

21. Kricheldorf, H. R.; Conradi, A. New polymer syntheses 16. LC-copolyesters of 3-(4-hydroxyphenyl) propionic acid and 4-hydroxy benzoic acids. *Journal of Polymer Science Part A: Polymer Chemistry* **1987***, 25*, 489-504.
22. Chen, Y.; Tan, L.; Yang, Y.; Wang, X. Study on biodegradable aromatic/aliphatic copolyesters. *Brazilian Journal of Chemical Engineering* **2008***, 25*, 321-335.
23. Han, X.; Williams, P. A.; Hall, H. K.; Linstid, H. C.; Lee, C. A Change in Mechanism from Acidolysis to Phenolysis in the Bulk Copolymerization of 4-Acetoxybenzoic Acid and 6-Acetoxy-2-naphthoic Acid. *Macromolecules* **1996***, 29*, 8313-8320.
24. Bloom, M. E.; Vicentin, J.; Honeycutt, D. S.; Marsico, J. M.; Geraci, T. S.; Miri, M. J. Highly renewable, thermoplastic tetrapolyesters based on hydroquinone, p-hydroxybenzoic acid or its derivatives, phloretic acid, and dodecanedioic acid. *Journal of Polymer Science Part A: Polymer Chemistry* **2018***, 56*, 1498-1507.
25. Padias, A. B.; Hall, H. K. Mechanism Studies of LCP Synthesis. *Polymers* **2011***, 3*, 833-845.
26. Wellen, R. M. R. Effect of polystyrene on poly(ethylene terephthalate) crystallization. *Materials Research* **2014***, 17*, 1620-1627.
27. Kaneko, T.; Kaneko, D.; Wang, S. High-performance lignin-mimetic polyesters. *Plant Biotechnology* **2010***, 27*, 243-250.
28. Moon, S.; Lee, C.; Taniguchi, I.; Miyamoto, M.; Kimura, Y. Melt/solid polycondensation of l-lactic acid: an alternative route to poly(l-lactic acid) with high molecular weight. *Polymer* **2001***, 42*, 5059-5062.
29. Cakir, S.; Kierkels, R.; Koning, C. E. Polyamide 6-polycaprolactone multiblock copolymers: synthesis, characterization, and degradation. *Journal of Polymer Science, Part A: Polymer Chemistry* **2011***, 49*, 2823-2833.
30. Lu, X. F.; Hay, J. N. Isothermal crystallization kinetics and melting behaviour of poly(ethylene terephthalate). *Polymer* **2001***, 42*, 9423-9431.
31. Sánchez, M. E.; Morán, A.; Escapa, A.; Calvo, L. F.; Martínez, O. Simultaneous thermogravimetric and mass spectrometric analysis of the pyrolysis of municipal solid wastes and polyethylene terephthalate. *Journal of Thermal Analysis and Calorimetry* **2007***, 90*, 209-215.
32. Ouimet, M. A.; Stebbins, N. D.; Uhrich, K. E. Biodegradable Coumaric Acid-Based Poly(anhydride-ester) Synthesis and Subsequent Controlled Release. *Macromolecular Rapid Communications* **2013***, 34*, 1231-1236.
33. Ouimet, M. A.; Griffin, J.; Carbone-Howell, A. L.; Wu, W.; Stebbins, N. D.; Di, R.; Uhrich, K. E. Biodegradable ferulic acid-containing poly(anhydride-ester): degradation products with controlled release and sustained antioxidant activity. *Biomacromolecules* **2013***, 14*, 854-861.
34. Zhu, J.; Watson, E. M.; Tang, J.; Chen, E. Y. A synthetic polymer system with repeatable chemical recyclability. *Science (New York, N.Y.)* **2018***, 360*, 398-403.
35. Gardea, F.; Garcia, J. M.; Boday, D. J.; Bajjuri, K. M.; Naraghi, M.; Hedrick, J. L. Hybrid Poly(aryl ether sulfone amide)s for Advanced Thermoplastic Composites. *Macromolecular Chemistry and Physics* **2014***, 215*, 2260-2267.
36. Antheunis, H.; Meer, van der, J.C.; Geus, de, M; Kingma, W.; Koning, C. E. Improved mathematical model for the hydrolytic degradation of aliphatic polyesters. *Macromolecules* **2009***, 42*, 2462-2471.
37. Antheunis, H.; Meer, van der, J.C.; Geus, de, M.; Heise, A.; Koning, C. E. Autocatalytic equation describing the change in molecular weight during hydrolytic degradation of aliphatic polyesters. *Biomacromolecules* **2010***, 11*, 1118-1124.
38. Casalini, T.; Rossi, F.; Lazzari, S.; Perale, G.; Masi, M. Mathematical Modeling of PLGA Microparticles: From Polymer Degradation to Drug Release. *Molecular pharmaceutics* **2014***, 11*, 4036-4048.

6 Molecularly recyclable poly(ethylene terephthalate) versus semi-aromatic polyesters

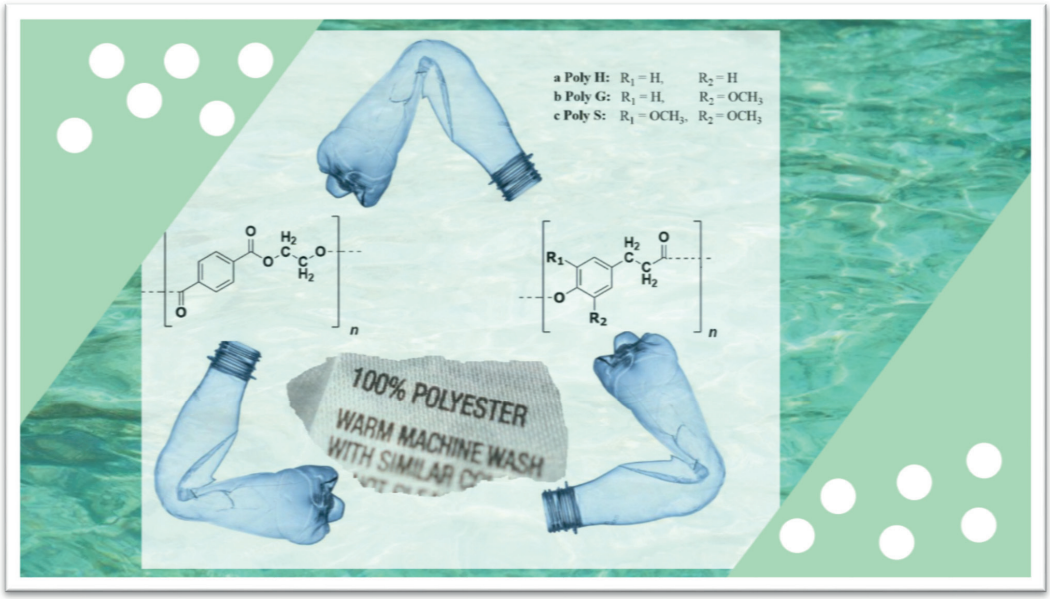

This chapter is being prepared for publication.

Abstract

The molecular recycling of poly(ethylene terephthalate) (PET) and the three semi-aromatic polyesters poly(phloretic acid) (poly-H), poly(dihydroferulic acid) (poly-G), and poly(dihydrosinapinic acid) (poly-S) has been studied in this chapter. Depolymerization of these polyesters has been carried out at neutral pH as well as by acid and base-catalyzed hydrolysis at three temperatures, i.e., 25 °C, 50 °C and 80 °C. A shrinking particle model was used to determine the global kinetics of the base-catalyzed depolymerization. The depolymerization rate rises with increasing temperature.

Base catalyzed depolymerization of virgin PET leads to an isolated yield of 38% after 48 hours reaction at 80 °C. Contrary to these results for PET, the monomers of the semi-aromatic polyesters poly-H, poly-G, and poly-S are recovered after 15 minutes in a facile manner. A shrinking particle model has valued the intrinsic reaction rate constants. It has been demonstrated that the rate coefficients of the depolymerization of the semi-aromatic polyesters poly-H, poly-G and poly-S are between 2 and 3 orders of magnitude higher than those for PET. Hydrolysis of PET in aqueous sulfuric acid is very slow, and no significant depolymerization was observed after 48 hours. The semi-aromatic polyesters poly-H, poly-G, and poly-S have also been hydrolyzed in an aqueous 4 M sulfuric acid solution. These polyesters were completely depolymerized after 8 hours at 80 °C. The advantage of acid-catalyzed depolymerization over depolymerization in an alkaline medium is the absence of salt formation.

6.1 Introduction

The polyester poly(ethylene terephthalate) (PET) has a well-known application in the packaging industry, e.g., in soft drink bottles. However, PET is largely used in the textile industry.[1,2] PET is manufactured from its monomers ethylene glycol (EG) and terephthalic acid (TPA) or dimethyl terephthalate (DMT) by respectively an esterification or a transesterification reaction.[3,4] Nearly all worldwide consumption of TPA and DMT is intended for the production of PET.[5] There are numerous chemical procedures suitable to recover the monomers. From a sustainability point of view, molecular recycling is most promising.[6]

The monomers TPA and EG are derived from petrochemical feedstocks.[7] Because the dependence of oil worldwide increased tremendously in the last century, the drive to reduce the use of petrochemical feedstocks grows. Therefore, investigations of recycling PET towards its building blocks (i.e., the monomers) remain important.[8] Recycling PET and other polymers can be carried out by thermal and mechanical methods.[9]

On the other hand, to reduce the amount of required petrochemical feedstock, it is possible to use other sources to produce polyesters. Biomass is a promising alternative source for the production of polymers because it consists of carbohydrates, fatty acids, fats, proteins, and lignin. Lignin is, after cellulose, the most common organic polymer in the world. In the previous chapter, it has already been demonstrated that it is possible to synthesize the semi-aromatic polyesters poly(phloretic acid) (poly-H), poly(dihydroferulic acid) (poly-G), and poly(dihydrosinapinic acid) (poly-S) from benzaldehydes derived from lignin. These polyesters may be an attractive alternative for PET because the building blocks of these polyesters also contain aromatic rings.[10]

Much research has already been performed on the depolymerization of PET. The most applied methods are glycolysis and to a lesser extent, methanolysis, aminolysis, and ammonolysis.[11] Hydrolysis is another method for PET recycling. The main disadvantage of hydrolysis of PET is the use of high temperatures (200-250 °C) and pressures (1.5 – 2.0 MPa) as well as the long-time needed for complete depolymerization. Hydrolysis of PET can be carried out as hydrolysis at a neutral pH[12], base-catalyzed hydrolysis, and acid-catalyzed hydrolysis.[13,14]

This chapter reports the results of the determination of the global kinetics of the hy1drolysis reactions of PET, poly-H; poly-G, and poly-S in a 1 M aqueous NaOH solution.[15-17] The hydrolysis of PET in demineralized water and in a 1 M sulfuric acid solution did not result in any significant breakdown of PET. After depolymerization, the monomers of all polyesters need to be isolated with high purity (>98%). Only for these levels of purity repolymerization with a desired molecular weight build-up is possible, and a closed cycle is realized, as shown in the previous chapter and Scheme 6.1. This chapter matches the chemical recycling processes of virgin PET granules (Arnite®), and PET-flakes of waste bottles and the three designed homopolyesters: poly-H, poly-G, and poly-S.

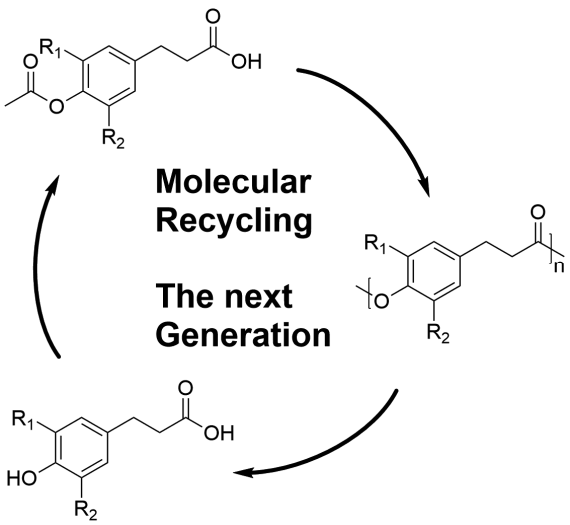

Scheme 6.1: Molecular recycling process for poly(phloretic acid) (poly-H, $R_1 = R_2 = H$), poly(dihydroferulic acid) (poly-G, $R_1 = OCH_3$ and $R_2 = H$), and poly(dihydrosinapinic acid) (poly-S, $R_1 = R_2 = OCH_3$).

6.2 Results and discussion

Previously, a green, efficient, and scalable method has been developed, producing cinnamic acid analogs from 4-hydroxybenzaldehyde by condensation with malonic acid.[18,19] By applying this Green Knoevenagel reaction and subsequent hydrogenation, polymerizable 4-hydroxy-dihydrocinnamic acid monomers became available. These monomers are, in our opinion, suitable for conversion into the designed molecularly recyclable polymers. Chapter 5 describes how these monomers are polymerized into semi-aromatic molecularly recyclable polyesters poly-H, poly-G, and poly-S. In this chapter, the results of the depolymerization of the semi-aromatic molecularly recyclable polyesters poly-H, poly-G, and poly-S are compared with the results of the depolymerization of virgin PET granules (Arnite®) and PET waste bottle crap.

First, a simple mathematical model was developed to describe the kinetics of depolymerization. It should be pointed out that the derivation of a comprehensive mathematical model is rather complicated since mass-transfer phenomena (between the solid and the liquid phase) occur in series with the hydrolysis reaction.[20]

One of the first assumptions is that all depolymerization reactions take place at the surface of a non-porous (highly crystalline) solid particle. The solid particle will shrink with time because the polymer is depolymerized into its monomer(s), which move to the bulk liquid phase by mass transfer. The shrinking particle model (also known as the shrinking core model[21]) has been developed to get insight into the global kinetics of depolymerization. The polymer particles are spherical with the same diameter, which is equal to the weighted average diameter of the particle size class. The depolymerization of the polymer is relatively slow (i.e., the time constant for reaction >> time constant for mass transfer), so the overall hydrolysis process is reaction controlled. Furthermore, the solid particles are ideally mixed with the liquid phase, and the catalyst (acid or base) concentration (C_C $[mol/m_L^3]$) at the locus of reaction remains constant during the reaction and is equal to the bulk concentration. The depolymerization reaction is assumed to be first-order in the polymer concentration (which is represented by the surface area ($S_P[m_S^2]$) of the polymer particle) and first-order in the acid or base concentration (sodium hydroxide or sulfuric acid). The reaction volume remains constant during the hydrolysis process, and no reversible reaction (i.e., ester formation) takes place.

The molar balance (eq. (1)) describes the depolymerization for one particle:

$$\frac{dN_P}{dt} = -k_r \times S_P \times C_C \quad (1),$$

where $N_P\ [mol]$ is the number of moles of the polymer repeating units in one particle and $k_r\ [m_L^3/(m_S^2 \cdot s)]$ is the reaction rate constant of depolymerization at the surface of the particle.

As $N_P = C_P \times V_P$, eq. (1) becomes

$$\frac{d(C_P \times V_p)}{dt} = -k_r \times S_P \times C_C \quad (2),$$

where C_P is the number of moles repeat units present per unit volume of the particle (i.e., the ratio of the density of the polymer particle (kg/m_S^3) and the molecular mass of the repeat unit (kg/mol)) and V_P stands for the volume of the particle.

According to the shrinking particle model eq. (2) can be written as:

$$C_P \times \frac{d\left(\frac{\pi}{6} \times d_p^3\right)}{dt} = -k_r \times \pi \times d_p^2 \times C_C \quad (3),$$

$$\frac{d(d_p)}{dt} = -\frac{2 \times k_r \times C_C}{C_P} \quad (4),$$

where d_p stands for the diameter of the particle.

The conversion of the polymer can be described as:

$$X = 1 - \frac{V_p}{V_{p,0}} = 1 - \frac{\frac{\pi}{6} \times d_p^3}{\frac{\pi}{6} \times d_{p,0}^3} \quad (5),$$

$$d_p = (1 - X)^{1/3} \times d_{p,0} \quad (6).$$

Substitution of eq. (6) into eq. (4) leads after rearrangement to eq. (7):

$$\frac{d(1-X)}{dt} = -\frac{2 \times k_r \times C_C}{C_P \times d_{p,0}} \times (1 - X)^{2/3} \quad (7).$$

Integration gives:

$$(1-X)^{1/3}-1=-k_{obs}\times t \quad (8),$$

where:

$$k_{obs}=\frac{2\times k_r\times C_C}{3\times C_P\times d_{p,0}}\,[1/s] \quad (9).$$

When depolymerization takes place at the surface of the solid polymer particle, the particle size will be of great importance in these reactions, because of the effective surface area per unit reaction volume. To investigate the influence of the particle size on the rate of the hydrolysis of PET, poly-H, poly-G, and poly-S experiments have been carried out using particles with different particle size classes. Virgin PET granules were ground and sieved with woven wire mesh sieves with different mesh sizes (180, 250, 355, and 500 µm). Each of these fractions was used separately in the depolymerization of PET. The depolymerization was carried out under reflux in 10 mL 1-butanol and 10 mmol sodium hydroxide to accelerate the molecular recycling of PET.

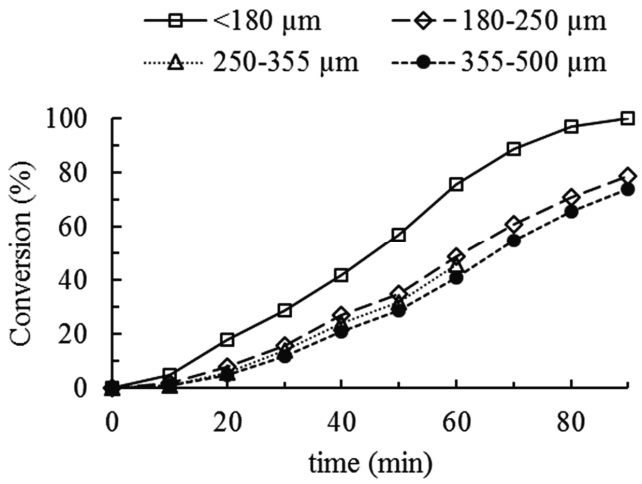

Figure 6.1: Conversion time history of the depolymerization of PET particles at 118 °C in 1-butanol and 1 M sodium hydroxide for different particle size classes, solid content: 10% w/w.

In this way and according to HPLC measurements, a complete conversion of PET is reached after 90 minutes at a temperature of 118 °C. Unfortunately, no further analysis was performed to investigate possible alcoholysis with 1-butanol. The results collected in Figure 6.1 show that smaller particles of PET lead to a shorter depolymerization time. Smaller PET particles have a larger specific surface area (m_S^2/m_S^3) available for reaction. As a consequence, the reaction rate per unit of mass (volume) of the particle phase increases with decreasing particle size, and higher conversions are obtained. After 90 minutes of reaction-time, conversion of 100% is reached for the smallest fraction (<180 µm) against 74-79% for larger particles (180-500 µm). The results in Figure 6.1 further demonstrate that conversion times histories for particle sizes above 180 µm are not significantly different. It is recommendable that both PET and semi-aromatic polyesters are ground and sieved. So particles with sizes ≤ 180 µm can be obtained with mesh no. 80. In all further experiments, only the fraction with particle sizes ≤ 180 µm has been used to get higher depolymerization rates than for larger particles.

The hydrolysis of Virgin PET granules and PET waste bottle crap in demineralized water at room temperature did not result in any breakdown of PET. Nevertheless, it is possible to depolymerize PET by neutral or acid hydrolysis, but much higher temperatures and pressures are required.[22-24] Also, the hydrolysis of poly-H, poly-G, and poly-S in demineralized water did not result in any breakdown of the polymer after 48 hours of reaction time at temperatures of 25 °C, 50 °C, or 80 °C. For comparing the semi-aromatic polyesters with PET polyesters, it has been decided to use only base-catalyzed hydrolysis. Base-catalyzed hydrolysis of PET is usually carried out in an aqueous NaOH solution with a concentration of 4 - 20 wt%.[5,25,26] The reaction products are ethylene glycol and the disodium terephthalate, see Scheme 6.2.

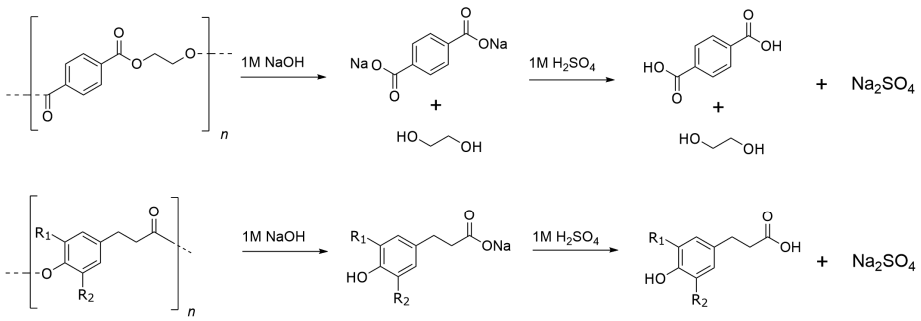

a Poly H: $R_1 = H$, $R_2 = H$
b Poly G: $R_1 = H$, $R_2 = OCH_3$
c Poly S: $R_1 = OCH_3$, $R_2 = OCH_3$

Scheme 6.2: Base-catalyzed hydrolysis of PET and the semi-aromatic polyesters (poly-H, poly-G, and poly-S). The reaction products of PET are ethylene glycol and the disodium terephthalate salt, and the reaction products of poly-H, poly-G, and poly-S are the dihydrocinnamic carboxylates.

After neutralization with H_2SO_4 to a pH of 3, terephthalic acid is recovered together with ethylene glycol. The results of the base-catalyzed hydrolysis of PET and molecularly recyclable polyesters poly-H, poly-G, and poly-S are presented in Figure 6.2. After 48 hours of reaction, the conversion reached for PET waste particles was 50% at a temperature of 80 °C. Note that for the same reaction time, the conversion of virgin PET particles is significantly lower. This lower conversion can be attributed to the fact that PET waste bottles are mostly in the amorphous state, contrary to virgin PET, which is more crystalline. Also, the attendance of additives like isophthalic acid and 2-methyl-1,3-propanediol[27-29] to enhance the amorphous state of PET bottles may have an influence on the rate of depolymerization. Note that for the depolymerization of the semi-aromatic polyesters, the time in Figure 6.2 is given in minutes. At a temperature of 80 °C, all three semi-aromatic polyesters are completely converted into monomer in about 15 minutes. The temperature has a significant influence on depolymerization time. A higher temperature leads to a considerable increase in the reaction rates, which reveals that the resistance against reaction is much larger than the resistance of mass transfer of NaOH to and the reaction products for the reactive surface.

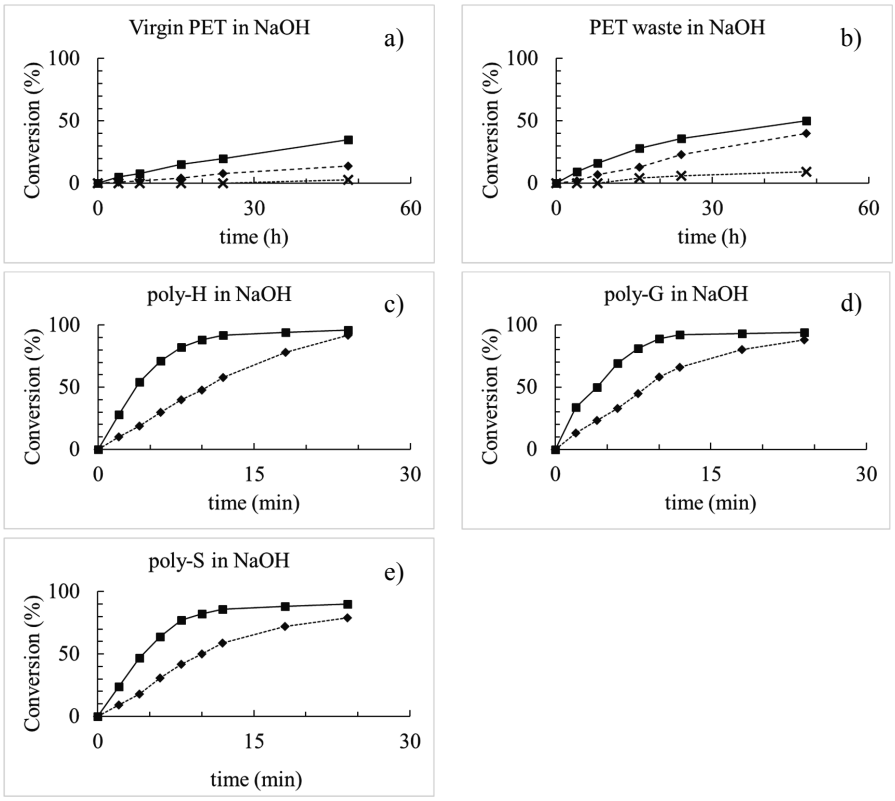

Figure 6.2: Conversion time history of the depolymerization of virgin PET (a), PET waste particles (b), poly-H (c), poly-G (d), and poly-S (e) in an 1 M aqueous sodium hydroxide solution at: 25 °C (×); 50 °C (♦) and : 80 °C (■), $d_{p,0} \leq 180$ μm, solid content: 5% w/w. Reported conversions are based on a calibration curve of the monomer with toluene as an internal standard at 254 nm.

The mathematical model developed has been applied to the experimental data. Because at 25 °C hardly any conversion has been observed for PET, this temperature has not been taken into account. In Figure 6.3 the observed values of $\left[1-(1-X)^{1/3}\right]$ have been plotted against t. According to eq. (8) the slope of the linear relation between $\left[1-(1-X)^{1/3}\right]$ and t is equal to k_{obs}. The rate coefficient k_r has been calculated from k_{obs} by eq. (9). Note that the concentration of repeat units (C_P) for PET is equal to the ratio of the density of PET (1370 kg/m_S^3)[30,31] and the molecular weight of the repeat unit (0.1922 kg/mol), so C_P for PET is 7130 mol/m_S^3.

Assuming the same density for the semi-aromatic polyesters as for PET and using the molecular weights of the repeat units 0.148, 0.178, and 0.208 kg/mol for poly-H, poly-G and poly-S, respectively, the C_P-values for poly-H, poly-G and poly-S are 9257, 7697 and 6587 mol/m_S^3, correspondingly. Also, the following values have been entered for the constants in eq. (9): C_C = 1000 mol/m^3 and $d_{p,0}$ = 180 μm. Table 6.1 presents the reaction rate constants k_{obs} and k_r at 50 °C and 80 °C, which have been found, including their correlation coefficient (R^2>0.99).

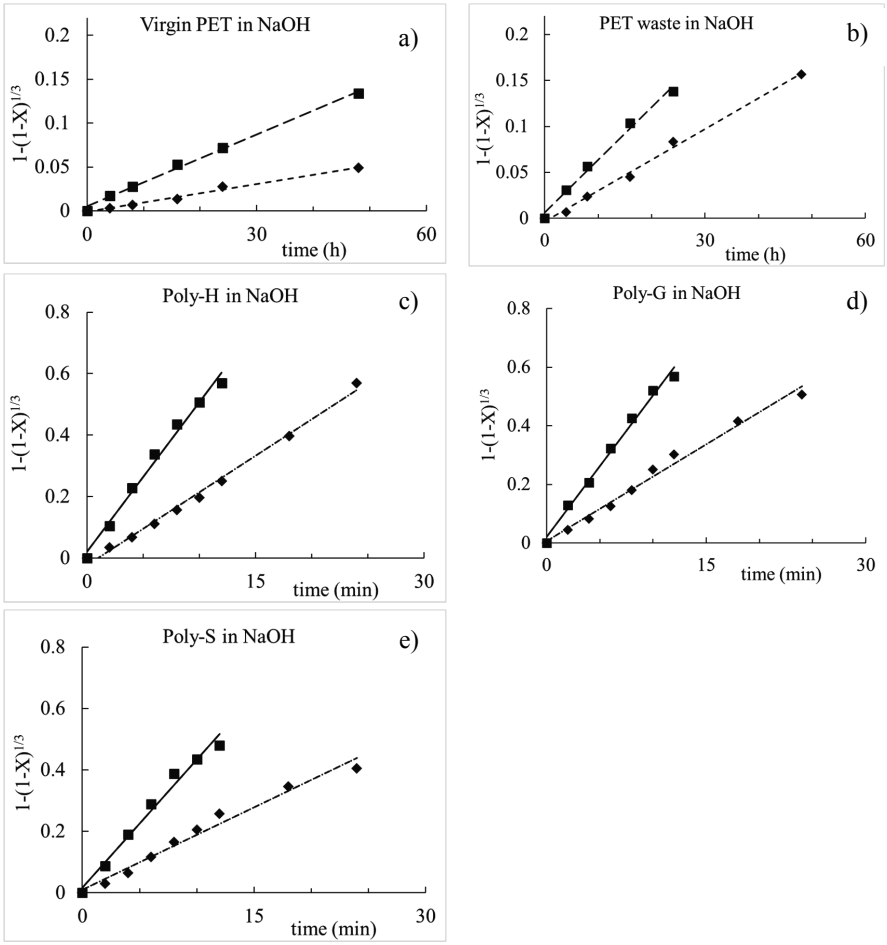

Figure 6.3: Evaluation of the kinetics of alkaline catalyzed depolymerization of virgin PET (a), PET waste particles (b), poly-H (c), poly-G (d), and poly-S (e) according to Eq.(8). ♦: 50 °C, and ■: 80 °C Kelvin, $d_{p,0} \leq 180$ µm.

Table 6.1: Reaction rate constants k_{obs} and k_r for the base-catalyzed depolymerization of virgin PET, PET waste particles, poly-H, poly-G, and poly-S at 50 °C and 80 °C.

	k_{obs} (323K) s^{-1}	R^2	k_r (323K) $m_w^3 m_s^{-2} s^{-1}$	rate relative to Arnite®	k_{obs} (353K) s^{-1}	R^2	k_r (353K) $m_w^3 m_s^{-2} s^{-1}$	rate relative to Arnite®
Virgin PET Arnite®	292 10^{-9}	0.990	562 10^{-12}	1	758 10^{-9}	0.996	1.46 10^{-9}	1
PET waste	931 10^{-9}	0.994	1.79 10^{-9}	3	1590 10^{-9}	0.989	3.06 10^{-9}	2
poly-H	395 10^{-6}	0.993	1.04 10^{-6}	1850	712 10^{-6}	0.982	1.87 10^{-6}	1280
poly-G	367 10^{-6}	0.988	765 10^{-9}	1360	707 10^{-6}	0.988	1.47 10^{-6}	1005
poly-S	298 10^{-6}	0.978	530 10^{-9}	945	575 10^{-6}	0.977	1.03 10^{-6}	702

k_r calculated from k_{obs} using eq. (9) with C_P = 7130, 9757, 7697 and 6587 mol/m_S^3 for PET, poly-H, poly-G, and poly-S. C_C = 1000 mol/m_L^3 and $d_{p,0} = 180 \times 10^{-6}$ m.

Given the experimental results, it appears the reaction times for complete depolymerization of semi-aromatic polyesters poly-H, poly-G, and poly-S are much shorter than those for PET. Compared to the reaction rate constants of PET, the rate constants (k_r) for depolymerization of poly-H, poly-G, and poly-S are between two and three orders of magnitude larger than those for PET. However, it must be pointed out that the chain length and the crystallinity of the polymer may have a considerable influence on the rate of depolymerization.

After hydrolysis, the monomers have to be separated from the solvent. First, the unreacted PET was separated by filtration. The remaining solution contains disodium terephthalate (TPA-Na) and ethylene glycol (EG). To end-up with terephthalic acid (TPA), instead of its disodium salt, the solution was acidified to a pH of 3 with a 1 M aqueous sulfuric acid solution. TPA precipitated and was separated by filtration. After drying, the isolated yield of the monomer TPA was 38% for the hydrolysis reaction of virgin PET at 80 °C. The filtrate contains ethylene glycol (EG), water, and dissolved salt (Na_2SO_4). Separation of ethylene glycol has to deal with the removal of the salt. Ethylene glycol (boiling point = 197.3 °C) and water can be easily separated by distillation. However, the salt remains in the EG fraction and moderately precipitates. In this project, the salt was removed by filtration, which led to an isolated yield of 28% of EG. Some improvement in this separation technique is required.

Previously in chapter 5, the recovery of the monomers of poly-H, poly-G, and poly-S was described with the acidifying step in a comparable way as the recovery of the monomers of PET. Because the monomers of the semi-aromatic polyesters are moderately soluble in water, extraction turned out to be a proper separation technique. Toluene, ethyl acetate, methyl-*tert*-butyl-ether (MTBE), n-heptane, and n-pentane were tested as solvents. Toluene, n-heptane, and n-pentane are not suitable because the monomers of the semi-aromatic polyesters are not soluble in any of these solvents. Phloretic acid dissolves in ethyl acetate and in MTBE. The partition coefficient for the system ethyl acetate/water was determined to be approximately 40 $\left[\frac{dm^3_{water}}{dm^3_{ethyl\ acetate}}\right]$. However, it must be pointed out that ethyl acetate and MTBE are also slightly soluble in water, so a ternary phase diagram is required for an accurate design of the extraction process. A ternary phase diagram has not been taken into account in this study. Also, there is no knowledge yet about the activities of phloretic acid in water, ethyl acetate, or MTBE. So further thermodynamic research on the separation of the monomers of the semi-aromatic polyesters is required.

Acid hydrolysis of PET is performed most frequently using concentrated sulfuric acid, although other mineral acids like nitric acid or phosphoric acid also have been used.[32] A substantial drawback of PET hydrolysis in concentrated sulfuric acid is the strong corrosive nature of the reaction system and the generation of aqueous waste. The hydrolysis of PET in 1 M sulfuric acid did not show any breakdown after 48 hours. The acid-catalyzed hydrolysis in a 4 M aqueous sulfuric acid solution of poly-H, poly-G, and poly-S looks very promising, as shown in Figure 6.4. Note that acid-catalyzed depolymerization does not deal with the problem of producing salt during workup. So it is recommended to investigate the depolymerization of the semi-aromatic polyesters with acid-catalyzed hydrolysis.

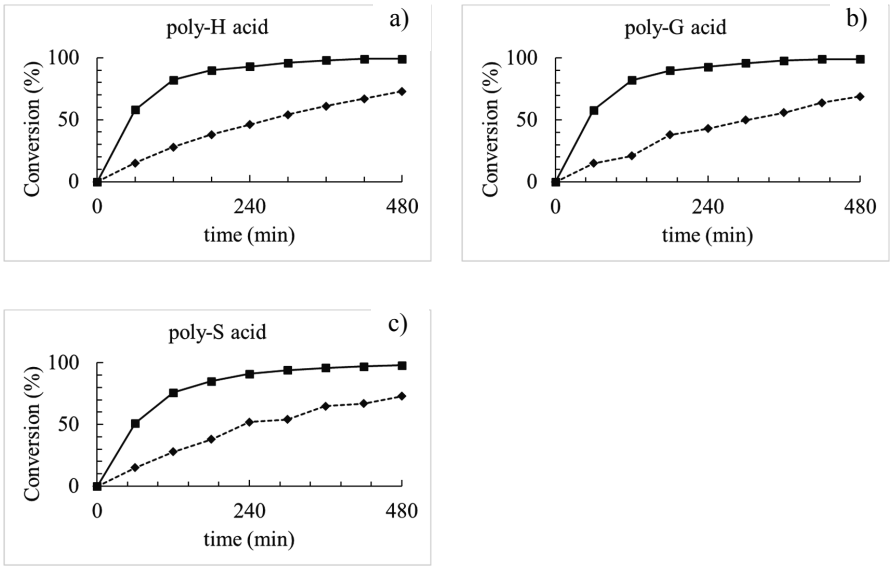

Figure 6.4: Conversion time history of the depolymerization of poly-H (a), poly-G (b), and poly-S (c) in an 4 M aqueous sulfuric acid solution at 50 °C (♦) and 80 °C (■), $d_{p,0}$ ≤ 180 µm, solid content = 5% w/w. Reported conversions are based on a calibration curve of the monomer with toluene as an internal standard at 254 nm.

6.3 Conclusions

The molecular recycling of PET and the semi-aromatic polyesters poly-H, poly-G, and poly-S have been studied. The hydrolysis of virgin PET granules and PET waste bottle crap in demineralized water did not result in any breakdown. Also, the hydrolysis of the semi-aromatic polyesters poly-H, poly-G, and poly-S in demineralized water did not result in any depolymerization after 48 hours of reaction time at temperatures of 25 °C, 50 °C and 80 °C.

Base catalyzed depolymerization of virgin PET leads to a low conversion after 48 hours reaction at 80 °C. The isolation of the monomer terephthalic acid can easily be performed by acidification and precipitation, which leads to an isolated yield of 38% TPA. The recovery of the monomer ethylene glycol has to deal with the salt formation, and only an isolated yield of 28% was reached, so further research on the recovering of EG is required.

Opposite to these results, the monomers of the semi-aromatic polyesters poly-H, poly-G, and poly-S can be recovered easily and in high isolated yields (>90%). A shrinking particle model has valued the intrinsic reaction rate constants.

It has been demonstrated that the rate coefficients of the depolymerization of the semi-aromatic polyesters poly-H, poly-G and poly-S are between 2 and 3 orders of magnitude larger than those for PET.

Hydrolysis of PET in aqueous sulfuric acid is very slow, and no depolymerization was observed after 48 hours of reaction. Next to PET, the semi-aromatic polyesters poly-H, poly-G, and poly-S have also been hydrolyzed in aqueous sulfuric acid. These polyesters were completely depolymerized in a 4 M aqueous sulfuric acid solution after 4 hours at 80 °C. The advantage of acidic depolymerization is that no acidification is required after depolymerization, and there is no salt formation.

6.4 Experimental section

6.4.1 Materials

4-Hydroxy benzaldehyde (**1a**), vanillin (**1b**), and syringaldehyde (**1c**), and all other chemicals (99% purity) were purchased from Sigma-Aldrich and were used as received. DMSO-d_6 was purchased from Cambridge Isotope, with 99 atom% deuterated. Virgin PET granules (Arnite® A04 900) were purchased from DSM.

6.4.2 Methods

Instrumentation: ^{1}H NMR spectroscopy measurements were performed on an Agilent 400-MHz NMR system with DMSO-*d6* as a solvent. Chemical shifts are reported in ppm, relative to tetramethylsilane (TMS).

HPLC analysis was carried out using a reversed-phase liquid chromatographic system (Agilent 1100 series) equipped with a diode array detector operating at 300 nm (Agilent 1100 series) and an autosampler injector with a 20 µL loop (Agilent 1100 series G1316A). The system was equipped with a Grace Alltima C18 5 µm column (250 mm × 4.6 mm). HPLC measurements were made with the following settings: Flowrate 1.0 mL/min at a temperature of 25 °C, eluent A = methanol, eluent B = acetic acid buffer (99% milliQ, 1% acetic acid). The samples were eluted using the following gradient: 40% A and 60% B set for 6 min, gradient to 100% A and 0% B in subsequent 10 min, 100% A and 0% B set for 5 min, followed by 40% A and 60% B set for 8 min.

LC-MS analysis was performed using a liquid chromatographic system (Agilent 1200 series) equipped with a Luna 3 µm C18 column (200 × 2.0 mm) and an ion trap (Agilent 6300 series).

The hydrogenation was conducted in 2 M aqueous NaOH-solution using Raney Nickel catalyst and was carried out at a temperature of 60 °C. A 450 ml Parr Series 3910 shaker type hydrogenation apparatus was employed.

Size exclusion chromatography (SEC-HFIP) was measured on a system equipped with a Waters 1515 Isocratic HPLC pump, a Waters 2414 refractive index detector (40 °C) , a Waters 2707 autosampler, a PSS PFG guard column followed by 2 PFG-linear-Xl (7μm, 8 × 300 mm) column in series at 40 ºC. 1,1,1,3,3,3-Hexafluoroisopropanol (HFIP, Biosolve) with potassium trifluoro acetate (20 mmol L^{-1}) was used as eluent at a flow rate of 0.8 mL min^{-1}. The molecular weights were calculated against poly(methyl methacrylate) standards (Polymer Laboratories, M_p = 580 g mol^{-1} up to $M_p = 7.1 \times 10^6$ g mol^{-1}). Samples were prepared in the eluent at a concentration of 2-3 mg mL^{-1}. Before GPC analysis was performed, the samples were filtered through a 0.2 μm PTFE filter (13 mm, PP housing, Alltech).

Size exclusion chromatography (SEC-DMF) was performed using a liquid chromatographic system (Agilent 1100 series G1362A) equipped with a Varian PLgel column (300 × 7.5 mm) at 70 °C, a refractive index detector (70 ºC) and an UV-vis absorbance detector. Dimethylformamide (DMF) was used as eluent at a flow rate of 1.0 mL/min. The molecular weights were calculated with respect to polystyrene standards (Polymer Laboratories, M_n = 500 g mol^{-1} up to $M_n = 2 \times 10^6$ g mol^{-1}). Before the GPC analysis, the samples were filtered through a 0.45 μm PTFE filter.

Differential scanning thermograms were obtained with a DSC Q20 from TA Instruments. About 5-10 mg of each sample was accurately weighed and transferred to a sealed pan that went through a heating/cooling/heating cycle at 10 °C/min. Reported data are from the second full cycle. The temperature range depends on the experiment but was limited to 300 °C by the instrument.

Thermogravimetric analysis (TGA) was performed on a Q50 TA Instruments TGA, using nitrogen as a purge gas, at a heating rate of 20 °C/min in the range of 0-600 °C.

Melting points were determined with the Hanon Automatic Video Melting Point apparatus MP450.

The depolymerization of polymers was performed in test tubes in an Eppendorf ThermoMixer C with a thermoblock.

6.4.3 Synthetic procedure

*Protocol for the Green Knoevenagel condensation towards **2a** with 5 mol% ammonium bicarbonate:*

Malonic acid (20.81 g, 200.0 mmol) together with 4-hydroxy benzaldehyde, (**1a**, 24.42 g, 200.0 mmol) was dissolved in 20.0 mL ethyl acetate, and ammonium bicarbonate NH_4HCO_3 (790.6 mg, 10.0 mmol) was subsequently added. The reaction mixture was kept for 1 hour at 90 °C for complete conversion to *p*-coumaric acid **2a**. Samples of 2.0 µL were taken for reversed-phase HPLC analysis and diluted in 7.5 mL methanol, filtered, and analyzed using the method described under "Methods." The calculated percentage of the peak area of the component of interest is in relation to the total area of peaks.

*Representative procedure for the hydrogenation of **2a** towards **3a** with Raney nickel:*

A 450 ml Parr® shaker type hydrogenation apparatus was charged with *p*-coumaric acid **2a** (24.62 gram, 150 mmol) dissolved in 300 mL 2 M NaOH solution and Raney Nickel™ slurry (1.5 gram, 18 mmol) was added. The reactor was pressurized with hydrogen (3 bar), and the reaction mixture was shaken at 80 °C for 3 hours. After this time, the reactor was cooled to room temperature and slowly depressurized. Most of the catalyst was retrieved with a magnet, and the solution was filtered through a 0.2 µm Whatman filter. Subsequently, the solution was acidified with 4 M HCl solution towards a pH of 2 and extracted with ethyl acetate (4 × 50 mL). After drying over $MgSO_4$, the solvent was removed under reduced pressure, and the solid product phloretic acid **3a** was subsequently dried at 40 °C in a vacuum oven.

*Protocol for the acetylation of **3a** with sodium acetate as a base towards acetylated monomers **4a** and oligomers (pre-polymer):*

Phloretic acid **3a** (16.62 g, 100 mmol) was dissolved in acetic anhydride (14.2 mL, 150 mmol) and the base sodium acetate (0.82 g, 10 mmol) was added, the solution was stirred and kept for 1 hour at 90 °C for complete conversion of **3a** towards 4-acetoxy dihydrocoumaric acid **4a** and acetylated oligomers. The solid was dissolved in 25 mL acetone, precipitated (solvent - nonsolvent) into 250 mL 0.1 M HCl and filtered under vacuum.

A typical procedure for the polymerization of acetylated monomers and oligomers:
To the monomers, **4a** and pre-polymer (20.8 g, 100 mmol) in a flask equipped with an overhead stirrer 10 mol% finely powdered NaOH (400 mg, 10.0 mmol) was added and heated for 3 hours at 140 °C. The reaction was stirred at ~100 rpm by the overhead stirrer. A solvent assisted polymerization was created by adding 25.0 mL of o-xylene and zinc(II)acetate (180 mg, 1 mmol). The mixture was refluxed at 144 °C for 3 hours. The reaction mixture was cooled down, and the o-xylene was removed by applying a vacuum (<10 mbar). During the final stage of the polymerization, the temperature was raised to 240 °C, and a high vacuum (<1 mmHg) was applied for 3 hours. The polymer poly-H **5a** was cooled to room temperature and washed with methanol to eliminate **4a** and oligomers.

Protocol for the depolymerization of PET in 1-butanol:
Virgin PET granules (Arnite®) (1.0 g, 5.0 mmol based on the repeating unit) together with NaOH (0.4 g, 10 mmol) were added to 10.0 mL 1-butanol. The reaction mixture was refluxed for 90 minutes at a temperature of 118 °C. Samples of 100 µL were taken every 10 minutes.

A typical procedure for the depolymerization of PET in 1 M NaOH:
To measure hydrolytic degradation, virgin PET granules (Arnite®) and PET waste bottle crap were finely ground (particles smaller than 180 µm). These PET particles were distributed over 8 test tubes in equal amounts of 20 mg, 1.0 mL of 1 M NaOH solution was added and incubated at three temperatures (25, 50, and 80 °C ± 1 °C) with agitation at 500 rpm using a controlled environment incubator shaker. At different time intervals (1, 2, 4, 8, 16, 24, and 48 hours after the start of the reaction), the content of a specific test tube was neutralized with 1.0 mL of 1 M H_2SO_4. 2.0 mL of methanol and 0.4% v/v toluene as internal standard was added and the content of the test tube was analyzed by high-performance liquid chromatography (HPLC). All samples were filtered using 0.45 µm PTFE syringe filters and subsequently injected (20 µL) using an autosampler. Absorbance was monitored at λ = 254 nm, and concentrations were calculated from a calibration curve of known terephthalic acid standard solutions relative to toluene as an internal standard.

In addition, 1.0 gram PET was hydrolyzed for 48 hours after the start of the reaction at a temperature of 80 °C ± 1 °C. After hydrolysis, the reaction mixture was filtered to separate the unreacted polymer from the monomers in solution. The unreacted polymer was dried in a vacuum oven at 50 °C for 24 hours and used as a confirmation of the total mass balance. The remaining solution contains disodium terephthalate (TPA-Na) and ethylene glycol (EG). To end-up with terephthalic acid (TPA), instead of its disodium salt, the solution was acidified to a pH of 3 with a 1 M aqueous sulfuric acid solution. TPA precipitated and was separated by filtration. After drying, the isolated yield of the monomer TPA was 38% (with a selectivity of 95% towards TPA verified by HPLC) for the hydrolysis reaction of virgin PET at 80 °C. The filtrate contains ethylene glycol (EG), water, and dissolved salt (Na_2SO_4). The salt was removed by filtration, which led to an isolated yield of 28% of EG.

A typical procedure for the depolymerization of poly-H in 1 M NaOH:
To measure hydrolytic degradation, poly-H **5a** was finely ground (particles smaller than 180 μm) and was distributed over 8 test tubes with equal amounts of 20 mg poly-H to which 1.0 mL of 1 M NaOH solution had been added and incubated at 80 °C with agitation at 500 rpm using a controlled environment incubator shaker. At different time intervals, the content of a specific test tube was neutralized with 1.0 mL of 1 M H_2SO_4. 2.0 mL of methanol and 0.4% v/v toluene as internal standard was added, and the content of the test tube was analyzed by high-performance liquid chromatography (HPLC). So for every depolymerization experiment, there were 8 samples for conversion measurement: one test tube gives one conversion. All samples were filtered using 0.45 μm PTFE syringe filters and subsequently injected (20 μL) using an autosampler. Absorbance was monitored at λ = 254 nm, and concentrations were calculated from a calibration curve of known phloretic acid **3a** standard solutions relative to toluene as an internal standard.

A typical procedure for the depolymerization of poly-H in 4 M H_2SO_4:

The release of phloretic acid **3a** from polymer poly-H **5a** was evaluated by molecular recycling in 4 M H_2SO_4. To measure hydrolytic degradation, poly-H **5a** was finely ground (particles smaller than 180 μm) and was distributed over 8 test tubes with equal amounts of 20 mg poly-H to which 1.0 mL of 4 M H_2SO_4 had been added and incubated at 80 °C with agitation at 500 rpm using a controlled environment incubator shaker. At different time intervals, 2.0 mL of methanol and 0.4% v/v toluene as internal standard was added to the content of a specific test tube and analyzed by high-performance liquid chromatography (HPLC). So for every depolymerization experiment, there were 8 samples for conversion measurement: one test tube gives one conversion. All samples were filtered using 0.45 μm PTFE syringe filters and subsequently injected (20 μL) using an autosampler. Absorbance was monitored at $\lambda = 254$ nm, and concentrations were calculated from a calibration curve of known phloretic acid **3a** standard solutions and 0.4% v/v toluene as an internal standard.

6.5 References

1. Ruvolo-Filho, A.; Curti, P. PET recycled and processed from flakes with different amount of water uptake: characterization by DSC, TG, and FTIR-ATR. *J Mater Sci* **2008**, *43*, 1406-1420.
2. Liu, B.; Lu, X.; Ju, Z.; Sun, P.; Xin, J.; Zhou, Q.; Zhang, S. Ultrafast Homogeneous Glycolysis of Waste Polyethylene Terephthalate via a Dissolution-Degradation Strategy. *Industrial & Engineering Chemistry Research* **2018**, *57*, 16239-16245.
3. Carta, D.; Cao, G.; d'Angeli, C. Chemical recycling of poly(ethylene terephthalate) (pet) by hydrolysis and glycolysis. *Environ Sci & Pollut Res* **2003**, *10*, 390-394.
4. Goje, A. S.; Thakur, S. A.; Diware, V. R.; Chauhan, Y. P.; Mishra, S. Chemical Recycling, Kinetics, and Thermodynamics of Hydrolysis of Poly(ethylene terephthalate) Waste with Nonaqueous Potassium Hydroxide Solution. *Polymer-Plastics Technology and Engineering* **2004**, *43*, 369-388.
5. Paszun, D.; Spychaj, T. Chemical Recycling of Poly(ethylene terephthalate). *Industrial & Engineering Chemistry Research* **1997**, *36*, 1373-1383.
6. Kawai, F.; Kawabata, T.; Oda, M. Current knowledge on enzymatic PET degradation and its possible application to waste stream management and other fields. *Applied microbiology and biotechnology* **2019**, *103*, 4253-4268.
7. Karayannidis, G. P.; Achilias, D. S. Chemical Recycling of Poly(ethylene terephthalate). *Macromolecular Materials and Engineering* **2007**, *292*, 128-146.
8. Chilton, T.; Burnley, S.; Nesaratnam, S. A life cycle assessment of the closed-loop recycling and thermal recovery of post-consumer PET. *Resources, Conservation & Recycling* **2010**, *54*, 1241-1249.
9. Awaja, F.; Pavel, D. Recycling of PET. *European Polymer Journal* **2005**, *41*, 1453-1477.
10. Lorenzetti, C.; Manaresi, P.; Berti, C.; Barbiroli, G. Chemical Recovery of Useful Chemicals from Polyester (PET) Waste for Resource Conservation: A Survey of State of the Art. *J Polym Environ* **2006**, *14*, 89-101.
11. Zenda, K.; Funazukuri, T. Depolymerization of poly(ethylene terephthalate) in dilute aqueous ammonia solution under hydrothermal conditions. *Journal of Chemical Technology & Biotechnology* **2008**, *83*, 1381-1386.
12. Zope, V. S.; Mishra, S. Kinetics of neutral hydrolytic depolymerization of PET (polyethylene terephthalate) waste at higher temperature and autogenious pressures. *Journal of Applied Polymer Science* **2008**, *110*, 2179-2183.
13. Yoshioka, T.; Motoki, T.; Okuwaki, A. Kinetics of Hydrolysis of Poly(ethylene terephthalate) Powder in Sulfuric Acid by a Modified Shrinking-Core Model. *Industrial & Engineering Chemistry Research* **2001**, *40*, 75-79.
14. Yoshioka, T.; Okayama, N.; Okuwaki, A. Kinetics of Hydrolysis of PET Powder in Nitric Acid by a Modified Shrinking-Core Model. *Industrial & Engineering Chemistry Research* **1998**, *37*, 336-340.
15. Karayannidis, G. P.; Chatziavgoustis, A. P.; Achilias, D. S. Poly(ethylene terephthalate) recycling and recovery of pure terephthalic acid by alkaline hydrolysis. *Advances in Polymer Technology* **2002**, *21*, 250-259.
16. Ruvolo-Filho, A.; Curti, P. S. Chemical Kinetic Model and Thermodynamic Compensation Effect of Alkaline Hydrolysis of Waste Poly(ethylene terephthalate) in Nonaqueous Ethylene Glycol Solution. *Industrial & Engineering Chemistry Research* **2006**, *45*, 7985-7996.
17. Tudela, I.; Bonete, P.; Fullana, A.; Conesa, J. A. Parameter Sensitivity Study of the Unreacted-Core Shrinking Model: A Computer Activity for Chemical Reaction Engineering Courses. *Journal of Chemical Education* **2011**, *88*, 56-58.
18. van Schijndel, J.; Canalle, L. A.; Molendijk, D.; Meuldijk, J. The Green Knoevenagel condensation: solvent-free condensation of benzaldehydes. *Green Chemistry Letters and Reviews* **2017**, *10*, 404-411.

19. van Schijndel, J.; Molendijk, D.; Spakman, H.; Knaven, E.; Canalle, L. A.; Meuldijk, J. Mechanistic considerations and characterization of ammonia-based catalytic active intermediates of the Green Knoevenagel reaction of various benzaldehydes. *Green Chemistry Letters and Reviews* **2019**, *12*, 323-331.
20. Naik, S. D.; Doraiswamy, L. K. Mathematical modeling of solid-liquid phase-transfer catalysis. *Chemical Engineering Science* **1997**, *52*, 4533-4546.
21. Fogler, H. S. *Essentials of Chemical Reaction Engineering;* Pearson Education: 2017
22. Campanelli, J. R.; Kamal, M. R.; Cooper, D. G. A kinetic study of the hydrolytic degradation of polyethylene terephthalate at high temperatures. *Journal of Applied Polymer Science* **1993**, *48*, 443-451.
23. Chen, J. Y.; Ou, C. F.; Lin, C. C. Depolymerization of poly(ethylene terephthalate) resin under pressure. *Journal of Applied Polymer Science* **1991**, *42*, 1501-1507.
24. Vaidya, U. R.; Nadkarni, V. M. Polyester polyols from glycolyzed PET waste: Effect of glycol type on kinetics of polyesterification. *Journal of Applied Polymer Science* **1989**, *38*, 1179-1190.
25. Ramsden, J. M.; Phillips, J. A. Factors Influencing the Kinetics of the Alkaline Depolymerisation of Poly(ethylene terephthalate): The Effect of Solvent. *Journal of Chemical Technology & Biotechnology* **1996**, *67*, 131-136.
26. Wan, B.; Kao, C.; Cheng, W. Kinetics of Depolymerization of Poly(ethylene terephthalate) in a Potassium Hydroxide Solution. *Industrial & Engineering Chemistry Research* **2001**, *40*, 509-514.
27. Holland, B. J.; Hay, J. N. The thermal degradation of PET and analogous polyesters measured by thermal analysis–Fourier transform infrared spectroscopy. *Polymer* **2002**, *43*, 1835-1847.
28. Lewis, C. L.; Spruiell, J. E. Crystallization of 2-methyl-1,3-propanediol substituted poly(ethylene terephthalate). Thermal behavior and isothermal crystallization. *Journal of Applied Polymer Science* **2006**, *100*, 2592-2603.
29. Wang, Q.; Zhang, F.; Qu, D.; Bai, Y. The effect of crystallization properties influenced by 2-methyl-1,3–propanediol units on the optical properties of modified poly(ethylene terephthalate). *High Performance Polymers* **2019**, *31*, 211-219.
30. Rahman, S. K.; Islam, M.; Ratul, S.; Dana, N.; Musa, S.; Hannan, M. Properties of flat-pressed wood plastic composites as a function of particle size and mixing ratio. *J Wood Sci* **2018**, *64*, 279-286.
31. Mishra, S.; Goje, A. S.; Zope, V. S. Chemical Recycling, Kinetics, and Thermodynamics of Poly (Ethylene Terephthalate) (PET) Waste Powder by Nitric Acid Hydrolysis. *Polymer Reaction Engineering* **2003**, *11*, 79-99.

7 Preparation of biobased styrene alternatives and their free radical polymerization

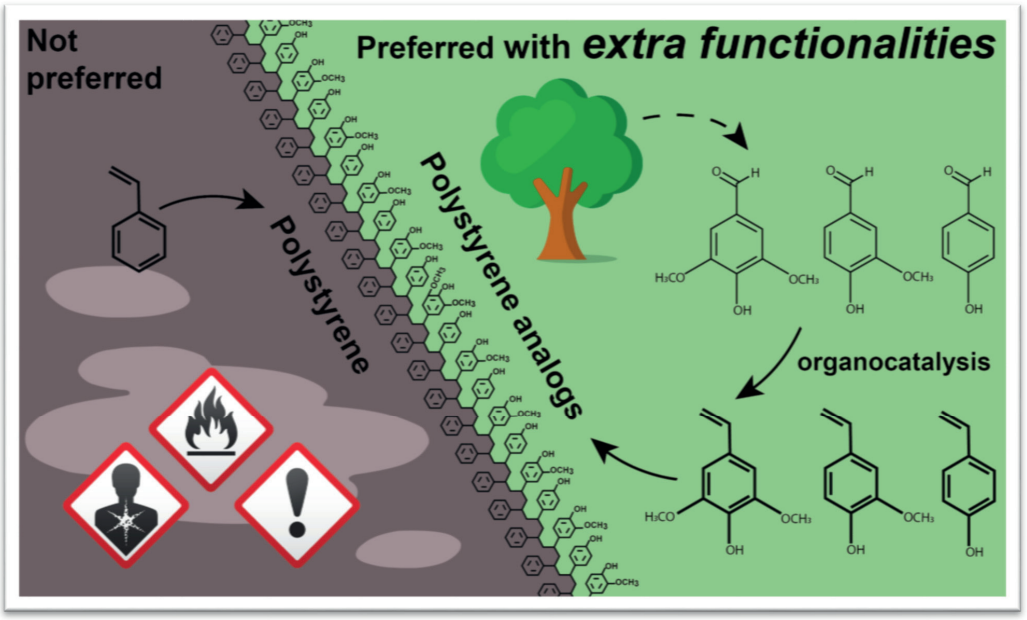

This chapter is based on:

van Schijndel, J.; European Polymer Journal **2020**
(DOI: 10.1016/j.eurpolymj.2020.109534)

Abstract

Three different biobased styrene monomer alternatives, i.e., 4-vinylphenol derivatives, were synthesized starting from lignin building blocks. The synthetic route encompassed a green Knoevenagel condensation followed by two decarboxylation steps and acetylation. High isolated yields for the decarboxylation were obtained in a polar aprotic solvent, which prevented oligomerization. The polymerization of the three acetylated 4-vinylphenols was performed by free radical polymerization. The chain transfer constants of styrene and 4-acetoxy styrene **4c** in toluene were evaluated in the Mayo procedure using the number-average molecular weight (M_n). After polymerization, the acetoxy group of the different polymers was efficiently hydrolyzed. The resulting phenol side groups of these polystyrene alternatives provide future opportunities to functionalize these biobased polymers further.

7.1 Introduction

Styrene was first isolated in 1839 from the American sweetgum tree by the German pharmacist Eduard Simon.[1] He noticed that when the tree's gum resin was exposed to air, light, or heat, it gradually transformed at room temperature into a hard, and with heating a rubber-like substance now known as polystyrene. Another component of the tree's resin, namely, cinnamic acid, could be decarboxylated in a laboratory resulting in styrene. However, after 1839, it took more than three decades before the Dutch chemist van 't Hoff discovered that these appearances of styrene were identical.[2]

Nowadays, styrene is no longer isolated from biomass. The modern method for styrene production is by dehydrogenation of the petrochemical ethylbenzene. Although this method is very cost-efficient, the production involves environmentally harmful procedures [3]. Also, styrene itself came with various health risks, like adverse effects on fertility and suspected carcinogenicity.[4,5] The interest in alternatives for fossil-based styrene is growing. Attention is increasingly focused on 4-vinylphenols due to the additional synthetic possibilities provided by the phenolic group. An example of this is the use of poly(4-vinylphenol)-based polyelectrolytes in CO_2 separation membrane applications.[6] Furthermore, the reduced toxicity of these biobased styrene alternatives only improves their prospects as alternatives for styrene.[7,8]

A few studies have been conducted towards the polymerization of these 4-vinylphenols resulting in polymers with suitable processing, as well as physico-chemical properties.[9-14] However, the application of the polymers is hampered by the lack of proper production of the necessary monomers.[15-19]

A possible alternative route to obtain 4-vinylphenols (**3**) is provided by the green Knoevenagel reaction followed by two decarboxylations (Scheme 1).[20-22] Several 4-hydroxybenzaldehydes (**1**) have been shown to react with malonic acid in a green Knoevenagel reaction with subsequent decarboxylation to give the corresponding α,β-unsaturated carboxylic acids known as 4-hydroxycinnamic acids (**2**). In nature, these 4-hydroxycinnamic acids can be found in the vegetable kingdom as secondary metabolites. [23] There are three familiar members of these ligno-phytochemicals (sinapinic acid **2a**, ferulic acid **2b**, and *p*-coumaric acid **2c**), which have been studied extensively, primarily due to their antioxidant properties.[24] A second decarboxylation should provide the corresponding 4-vinylphenol derivatives (**3**).[25]

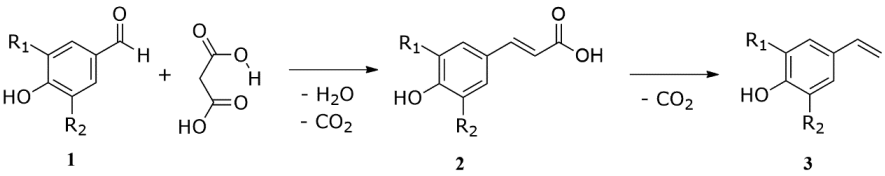

1 2 3

a $R_1 = OCH_3$, $R_2 = OCH_3$
b $R_1 = H$, $R_2 = OCH_3$
c $R_1 = H$, $R_2 = H$

Scheme 7.1: Knoevenagel reaction and subsequent decarboxylation of 4-hydroxybenzaldehydes towards 4-vinylphenols.

The present study explores a novel, green synthesis of three styrene alternatives starting from biobased building blocks with a focus on optimizing the second decarboxylation step. The route is applied for the synthesis of 4-hydroxy-3,5-dimethoxystyrene (HDMS) **3a**, 4-hydroxy-3-methoxystyrene (HMS) **3b**, and 4-hydroxystyrene (HS) **3c** and their acetylated derivatives 4-acetoxy-3,5-dimethoxystyrene (ADMS) **4a**, acetoxy-3-methoxystyrene (AMS) **4b**, and 4-acetoxystyrene (AS) **4c**. These acetylated biobased monomers will subsequently undergo a free-radical polymerization in bulk or solution, followed by hydrolysis of the acetoxy group, finally resulting in polystyrene alternatives with a phenolic functionality.

7.2 Results and discussion

The synthesis of the biobased styrene alternatives started with the derivatization of the ligno-phytochemicals **1a**–**1c**, using the previously reported Green Knoevenagel reaction using ammonium bicarbonate as catalyst under solvent-free conditions as shown in Table 7.1.[21] In line with earlier results, the condensation of benzaldehydes **1a**–**1c** and malonic acid proceeded very efficiently at 90 °C within 2 hours. The reaction resulted in high isolated yields of the corresponding α,β-unsaturated carboxylic acids **2a**–**2c**. For later comparison, benzaldehyde was also converted into cinnamic acid using the same protocol, with the exception that the reaction temperature had to be increased to 140 °C in order to get a complete conversion.

Table 7.1: Green Knoevenagel reaction of benzaldehyde and 4-hydroxybenzaldehydes **1** with malonic acid.

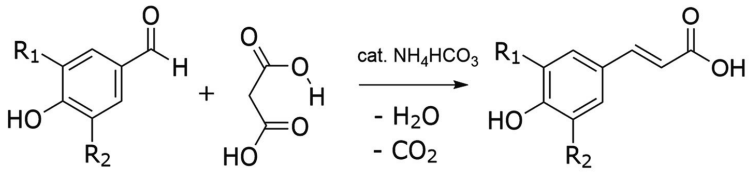

1 **2**

Entry	R_1	R_2	Conversion % **1** (HPLC)	Product	Yield % **2** (HPLC)	Yield % **2** Isolated
1	OCH_3	OCH_3	100	**2a**	98	93
2	H	OCH_3	100	**2b**	100	95
3	H	H	100	**2c**	100	94

Reaction conditions: 4-hydroxybenzaldehyde **1**, 1.1 eq. malonic acid and 0.1 eq. NH_4HCO_3 for 2h at 90 °C (benzaldehyde for 2h at 140 °C). Reported conversions and yields are based on the ratio of peaks of the HPLC chromatogram measured with a UV detector operating at 300 nm.

The subsequent decarboxylation of the four α,β-unsaturated carboxylic acids **2a**–**2c** and cinnamic acid towards the styrene alternatives **3a**–**3c** and styrene were initially performed using various nitrogen-containing catalysts (piperidine, pyridine, benzylamine, di-ethylamine, tri-ethylamine) under either solvent-free conditions or with ethylene glycol as solvent at 130 °C. In the case of cinnamic acid, no styrene formation could be detected. In the case of **2a**-**2c**, the desired styrene alternatives were found in the reaction mixture. Depending on the reaction conditions used, HPLC measurements indicated a yield between 20% and 60%. Upon further investigation, the yields appeared to be limited by the formation of dimers and trimers of the biobased styrene-like monomers. Column chromatography or distillation could be used to purify the styrene alternatives, but only with low isolated yields. These results correspond to previously reported observations under microwave conditions and are also in line with our previously reported investigations.[20,26]

One possible explanation for the formation of dimers and trimers can be found in the mechanism suggested by Cohen and Jones,[27] who studied the decarboxylation of 4-hydroxycinnamic acid in aqueous media. These authors propose that the carboxylate anion, formed after deprotonation of 4-hydroxycinnamic acid, tautomerizes to a quinomethine structure, which in turn

undergoes rapid decarboxylation (Scheme 7.2). This mechanism postulates an essential role for the 4-hydroxy group during the decarboxylation and explains why cinnamic acid did not react under the conditions mentioned above. It furthermore suggests the formation of an intermediate anion that can initiate an anionic oligomerization resulting in the observed oligomers during the decarboxylation of **2a**-**2c**.

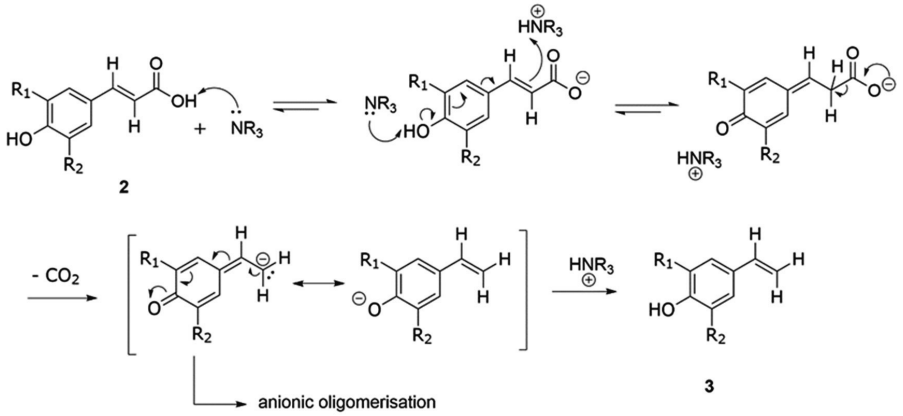

Scheme 7.2: Proposed mechanism from the base-catalyzed decarboxylation and subsequent anionic oligomerization.[27]

Alternative decarboxylation procedures of cinnamic acid derivatives have been reported using an in-situ complex of aromatic heterocyclic amines and Cu(I) in polyethylene glycol (PEG).[28,29] It has furthermore been reported that the toxic aromatic heterocyclic amines can be replaced with more benign ligands such as hexamethylenetetramine (HMTA).[30] Taking these procedures as a starting point for our synthesis, it turned out that Cu(I) was not a prerequisite for the decarboxylation of 4-hydroxycinnamic acids. In our case, HMTA was shown to catalyze the reaction single-handedly in PEG-400 at 130 ºC. Under these conditions, the decarboxylation of sinapinic acid **2a** produced a viscous yellow oil. This oil was purified using a silica column, resulting in highly pure HDMS **3a** as a white solid. Although the isolated yield was still below 20%, it was notable that in this case, no dimers or trimers were present in the reaction mixture.

The above results gave us insight to further optimize the decarboxylation reaction with a suitable solvent. PEG-400 ($\varepsilon = 12.4$) can be considered an aprotic semi-polar solvent, so we decided to investigate other aprotic polar solvents as a solvent for the decarboxylation of sinapinic acid **2a** with the catalyst HMTA. A list of solvents used is shown in Table 7.2.

Table 7.2: Various polar aprotic solvents to investigate the decarboxylation of sinapinic acid **2a**

Entry	Solvent	bp	dielectic constant	HPLC yield (%) of **3a**	Isolated yield (%) of **3a**
1	acetone, CH_3COCH_3	57	21	0	0
2	acetonitrile, CH_3CN	82	37.5	3	0
3	dimethylformamide (DMF), $HCON(CH_3)_2$	153	38	96	82
4	dimethyl sulfoxide (DMSO), CH_3SOCH_3	189	47	98	83
5	propylene carbonate (PC), $CH_3C_2H_3O_2CO$	242	64	80	75
6	ethylene carbonate (EC), $(CH_2O)_2CO$	243	90	93	90

Reaction conditions: sinapinic acid **2a** and 0.1 eq. HMTA in the selected solvent, for 2h at reflux or 130 °C; Reported HPLC yields are based on the ratio of peaks of the HPLC chromatogram measured with a UV detector operating at 300 nm.

The results collected in Table 7.2 demonstrate that a minimum reaction temperature between 90 and 130 °C is a prerequisite for the decarboxylation of sinapinic acid **2a** with HMTA as the catalyst. Furthermore, the dielectric constant seems to play a role in shielding the negatively charged phenol group, thereby preventing anionic oligomerization. The four aprotic polar solvents DMF, DMSO, EC, and PC all seem suitable. However, propylene carbonate is the only one that adheres to all the principles of Green Chemistry and was therefore selected for further optimization. For sinapinic acid **2a**, the temperature optimum was found to be 115 °C. At this temperature and with precipitation in toluene, the HDMS **3a** monomer is produced quantitively with an HPLC yield above 99% and with an isolated yield above 95%.

The styrene alternative HMS **3b** could be produced from ferulic acid **2b** with a similar procedure at a temperature of 120 °C and also with an HPLC yield above 99% with an isolated yield above 95%. HS **3c**, however, could only be produced from *p*-coumaric acid **2c** at a temperature of 115 °C in DMF as the solvent instead of PC. Subsequently, precipitation in ethyl acetate produced the desired product HS **3c** with an HPLC yield above 99% and with an isolated yield above 95%. It should furthermore be noted that it was difficult to prevent oligomerization of pure HS **3c** in the subsequent isolation procedures. All three styrene alternatives, **3a- 3c**, proved unstable for extended periods. As shown in Scheme 7.3, the phenolic group needs to be acetylated in order to obtain suitable monomers for radical polymerization anyhow. For these reasons, 4-vinyl phenols **3a-c** were directly acetylated with acetic anhydride without intermediated purification, providing the stable acetylated biobased styrene-like monomers **4a**–**4c**.

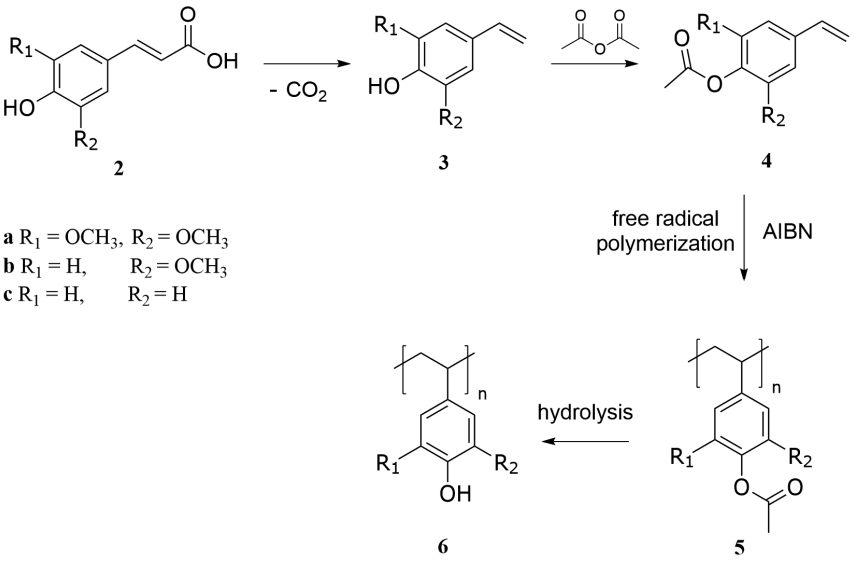

Scheme 7.3: Pathway from α–β unsaturated carboxylic acids **2** towards biobased styrene derivatives **3** and **4** and subsequent polymerizations towards **5** and hydrolysis to functional polystyrene **6**.

Important to emphasize is that despite the three 4-vinyl phenols **3a-c** are often described in the literature as a liquid or oil[24,26-28], we have established that these three biobased styrene-like monomers are solids with melting points above 60 °C. This also applies to the acetylated versions of HDMS **3a** and HMS **3b**. Only the acetylation of solid 4-hydroxy styrene **3c** yielded at room temperature the liquid 4-acetoxy styrene **4c**. Table 7.3 provides an overview of the total yields of the acetylated biobased styrene-like monomers **4a**–**4c**. In the applied conditions, the reactions are now almost quantitative.

Table 7.3: Decarboxylation reaction of cinnamic acids **2**.

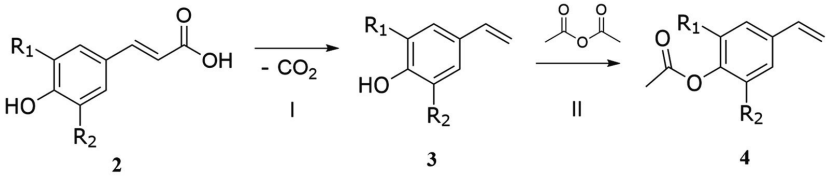

2 **3** **4**

Entry	R_1	R_2	Product	M_0[a]	Yield % **3** Isolated	Product	M_0[a]	Yield % **4** Isolated
1	OCH_3	OCH_3	**3a**	180	98	**4a**	222	98
2	H	OCH_3	**3b**	150	97	**4b**	192	99
3	H	H	**3c**	120	96	**4c**	162	99

[a] M_0 is the molecular weight of the monomer
Reaction conditions I: **2a** and **2b** with 0.1 eq. HMTA in PC, for 2h at 115 °C; **2c** with 0.1 eq. HMTA in DMSO, for 2h at 115 °C; II: crude 4-vinylphenol **3**, 1.5 eq. acetic anhydride and 0.05 eq. sodium acetate for 1h at 90 °C. Reported HPLC yields are based on the ratio of peaks of the HPLC chromatogram measured with a DAD operating at 300 nm.

Most commercial polystyrene (PS) is produced by free-radical bulk polymerization. Study of the bulk polymerization of the acetylated biobased styrene-like monomers **4a**–**4c** was, however, limited due to the high melting point of monomers ADMS **4a** and AMS **4b** and the high viscosity of the reaction mixture of AS **4c** above conversion of 30%. Therefore solution polymerization has opted for these exploratory studies. Styrene and the acetylated biobased analogs **4a**–**4c** were dissolved in toluene, which makes temperature control more straightforward but generally reduces the molecular weight. Using 2,2'-azobis(isobutyronitrile) (AIBN) as initiator at 60 °C for 24 hours, all these polymerizations produced off-white polymers in moderate isolated yields (>50% for ADMS **4a** and AMS **4b**) to high isolated yields (>80% for AS **4c** and styrene).

After purification by solvent/non-solvent precipitation from cold methanol, the molecular weights were measured using gel permeation chromatography (GPC). The molecular weights obtained for the biobased polystyrene alternatives **5a-5c** appear significantly higher than those for polystyrene with relatively low polydispersity indexes (PDI) as listed in Figure 7.2, together with the measured glass transition temperatures T_g of the polymers. Yet, the GPC data was recorded with polystyrene standards (to calculate M_n), which is possibly not an optimal standard for the biobased polystyrene alternatives **5a-5c** as it presumably gives an

overestimation of the molecular weights. As noticed by Hatakeyama[12] before, the influence of the methoxy substituent groups on the T_g is not easily recognized. If one methoxy-group is present at the position on the aromatic ring adjacent to the acetoxy-group at the para-position, the T_g decreases.[31]

The thermal stability of the samples was determined by thermogravimetry. Samples were stable up to 300-350 °C and the temperatures where degradation starts are similar to polystyrene (which has a $T_{50\%}$ of approximately 410 °C).

In order to get the extra phenol-functionality of the biobased polystyrenes available for further functionalization, hydrolysis of the acetylated polystyrenes was carried out in a hydroxide solution in acetone. This reaction is efficient and proceeds to conversion above 95% in all cases, as demonstrated by the ^{1}H NMR spectra of PAS **5c** and PHS **6c** in Figure 7.1. After hydrolysis, the characteristic signal of the acetyl CH_3 group at approximately 2.3 ppm in PAS **5c** disappeared entirely in the hydrolysis product PHS **6c**. Additionally, a new peak appeared at approximately 9.0 ppm, which can be assigned to the phenolic proton in PHS **6c**. After a while, the phenolic proton is exchanged by deuterium and declines.

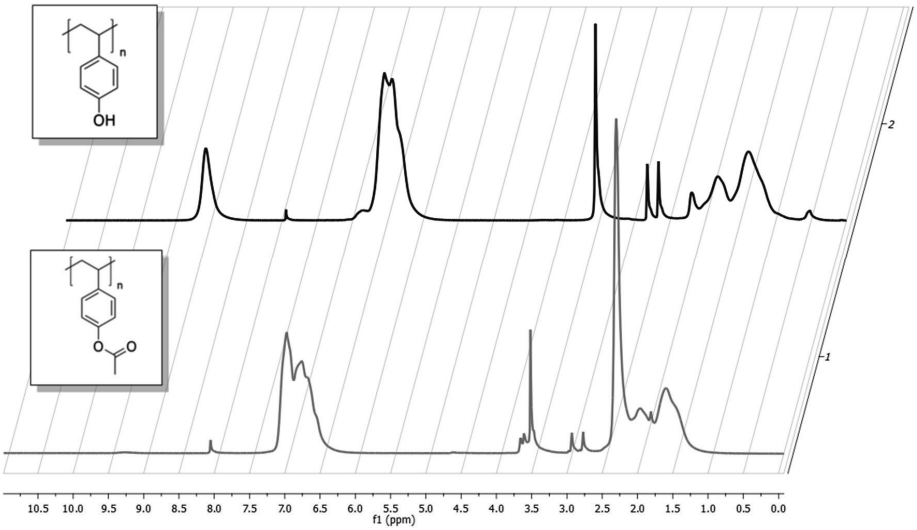

Figure 7.1: ^{1}H NMR-spectra (DMF-*d7*) of PAS **5c** and PHS **6c** after hydrolysis.

The results collected in Figure 7.2 show that the T_g values for PHDMS **6a**, PHMS **6b**, and PHS **6c** are higher than those of (commercially available) polystyrene. Moreover, the T_g values are also 30-50 °C higher than the corresponding acetylated biobased polystyrene-like polymers **5**. This can be understood by the added intermolecular interactions between phenol groups by hydrogen bonds, which restrict the molecular motion of the polymeric chain [32-34].

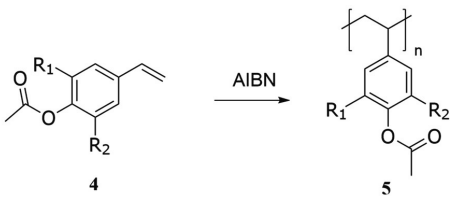

			M_n[a] (kDa)	M_w[a] (kDa)	DP_n	PDI[a]	T_g[b] (°C)	$T_{50\%}$[c] (°C)
5a	PADMS	Poly(4-acetoxy-3,5-dimethoxystyrene)	22.1	30.1	100	1.4	121	353
5b	PAMS	Poly(4-acetoxy-3-methoxystyrene)	28.3	45.1	147	1.6	104	370
5c	PAS	Poly(4-acetoxystyrene)	47.0	66.9	290	1.4	130	385
	PS	Polystyrene	14.2	23.4	137	1.6	107	406

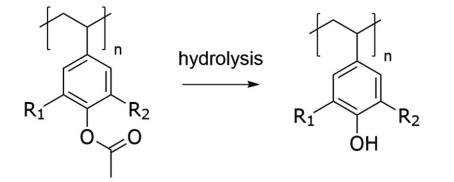

			M_n[a] (kDa)	M_w[a] (kDa)	DP_n	PDI[a]	T_g[b] (°C)	$T_{50\%}$[c] (°C)
6a	PHDMS	Poly(4-hydroxy-3,5-dimethoxystyrene)	18.2	25.5	101	1.4	146	365
6b	PHMS	Poly(4-hydroxy-3-methoxystyrene)	21.8	34.2	145	1.6	130	380
6c	PHS	Poly(4-hydroxystyrene)	34.3	48.0	286	1.4	188	390

Figure 7.2: Polymerization of acetylated biobased styrene-like monomers **4a**–**4c** and styrene towards biobased polystyrene alternatives **5** using free-radical solution polymerization and subsequent hydrolysis towards hydrolyzed biobased polystyrene **6**.

[a] Obtained by GPC in DMF at 70 °C versus polystyrene (PS) standards.
[b] Determined by DSC.
[c] Determined by TGA.

Limiting the molecular weight of polymers is essential for materials properties of, e.g., detergents, dispersants, and paints. A reduction in molecular weight can be realized by various approaches. Increasing the initiator amount is one way to promote a decrease in the molecular weight of the polymer. However, this procedure has its limits, is uneconomical, and is hardly applied in commercial polymerizations.

Another possibility is to carry out the polymerization in solution, especially with solid monomers like ADMS **4a** and AMS **4b**. The reduction of the molecular weight of the polymer formed in solution polymerization is caused by chain transfer to the solvent.

The influence of chain transfer to the solvent on the number-average degree of polymerization can be described by the classical Mayo equation:[35-37]

$$\frac{1}{DP_n} = \frac{1}{DP_{n,0}} + C_{tr,Sol}\frac{[\mathrm{Sol}]}{[\mathrm{M}]}$$

where DP_n and $DP_{n,0}$ are the number-average degree of polymerization in the presence or absence of solvent, respectively, and $C_{tr,Sol}$ (= $k_{tr,Sol}/k_p$) is the chain transfer constant of the solvent (Sol).

Free-radical solution polymerization of either styrene or the acetylated biobased styrene-like monomers **4a-4c** were carried out in several binary mixtures of the monomer and toluene[a] at 60 °C using 2,2'-azobis(isobutyronitrile) (AIBN) as initiator. The chain transfer constants $C_{tr,Sol}$ and $DP_{n,0}$ were determined with the Mayo procedure using the number-average molecular weight (M_n). The value of chain transfer constant in toluene is obtained as the slope of the line resulting from plotting $1/DP_n$ against the solvent concentration, as shown in Figure 7.3. In case of styrene $C_{tr,Tol} = 0.17 \times 10^{-3}$ and in case of AS **4c** $C_{tr,Tol} = 0.81 \times 10^{-3}$ which is about 5 times higher. The number-average degree of polymerization in the absence of solvent, i.e., $DP_{n,0}$ was 652 for styrene, and 2172 for AS **4c** under the conditions are shown in Figure 7.3. Note that GPC data was recorded with polystyrene standards (to calculate M_n), which is possibly not an optimal standard for PAS **5c** as it presumably gives an overestimation of the molecular weights. Chain transfer to the solvent toluene is shown to influence the maximum obtainable molecular weight in the conventional free radical polymerization of styrene with AIBN and likewise of the acetylated biobased styrene-like monomer AS **4c**.

When performing the Mayo procedure on the acetylated biobased styrene-like monomers, ADMS **4a** and AMS **4b,** almost constant DP_n's were obtained, as

[a] Solution polymerization of AS **4c** in ethyl acetate and DMF often produced a non-polymeric product. A possible explanation can be found in the formation of HS **3c** by hydrolysis of AS **4c**. Because the solubility of HS **3c** in toluene is minimal, a Mayo plot could be made with the solvent toluene.

shown in Figure 7.3. Probably, the molecular weight of these two biobased polystyrene-like polymers is defined predominantly by chain transfer to the monomer, resulting in a very low chain transfer constants $C_{tr,Tol}$ to the solvent toluene. The number-average degree of polymerization in the absence of solvent, i.e., $DP_{n,0}$ was 205 for ADMS **4a** and 215 for AMS **4b** under the conditions shown in Figure 7.3. In conclusion, the presence of methoxy groups on the aromatic ring appears to influence the chain transfer to the monomer and thereby substantially change the polymerization kinetics.

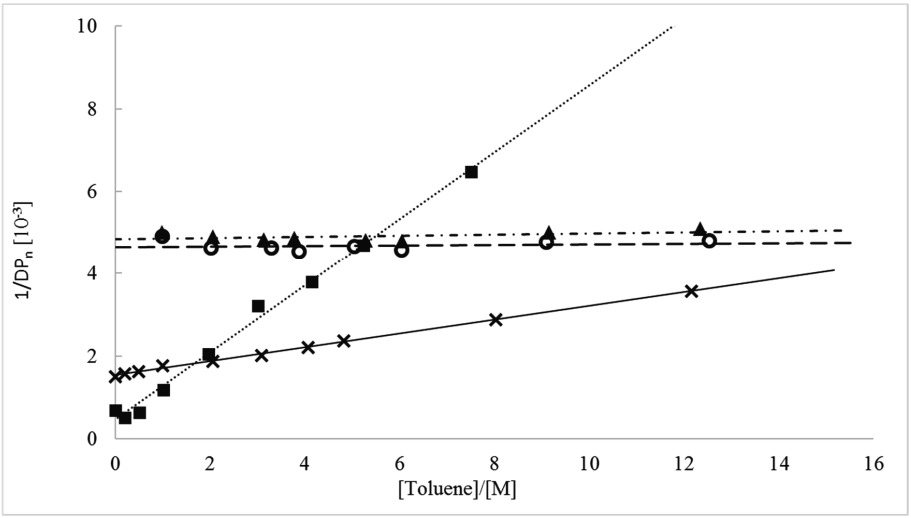

Figure 7.3: Mayo plots for conventional radical polymerizations of ADMS **4a** (▲, dash-dotted line), AMS **4b** (○, broken line), AS **4c** (■, dashed line), and styrene (×, solid line) initiated by AIBN (0.15 mol%) at 60 °C in toluene.

This study proves that various biobased functional styrene-like monomers can be obtained in an efficient and environmentally friendly way. There are essential differences between styrene and the biobased styrene alternatives relative to the different chain transfer pathways that take place. However, free-radical bulk polymerization with AIBN as an initiator is possible with all biobased styrene alternatives. Also, it demonstrates that it is possible to produce various biobased polystyrene-like polymers with a predefined M_n by carrying out the polymerization in solution. Because the role of the methoxy groups in the free radical polymerizations of the biobased styrene-like monomers has remained underexposed, further investigation is recommendable to investigate the role of these methoxy groups.

7.3 Conclusions

In this chapter, we have provided an easy procedure for producing biobased functional styrene-like monomers. A Green Knoevenagel reaction gives high isolated yields of α,β-unsaturated carboxylic acids from 4-hydroxybenzaldehydes. During the subsequent decarboxylation, aprotic polar solvents appear to stabilize the negatively charged 4-vinylphenols formed and therefore prevent unwanted anionic oligomerization. The free radical polymerization protocol developed is suitable for producing diverse and various acetylated biobased polystyrene on various scales. The polymeric materials are isolated in high yields with T_g values, as reported before. Thermogravimetry was used to check thermal stability, and this also corresponded with previously reported values. Finally, the value of the chain transfer constant of 4-acetoxy styrene **4c** in toluene was determined to be about 5 times as high as that of styrene.

7.4 Experimental section

7.4.1 General remarks

Reagents: Syringaldehyde (**1a**), vanillin (**1b**), 4-hydroxybenzaldehyde (**1c**), and all other chemicals (99% purity) were purchased from Merck and were used as received. DMSO-d_6 was purchased from Cambridge Isotope, with 99 atom% deuterated and used as received.

Instrumentation: ^{1}H NMR measurements were performed on an Agilent 400-MHz NMR system with DMSO-d_6 as a solvent. Chemical shifts are reported in ppm, relative to tetramethylsilane (TMS).

HPLC analysis was carried out using a reversed-phase liquid chromatographic system (Agilent 1100 series) equipped with a diode array detector operating at 300 nm (Agilent 1100 series) and an autosampler injector with a 20 µL loop (Agilent 1100 series G1316A). The system was equipped with a Grace Alltima C18 5 µm column (250 mm × 4.6 mm). The determination of the concentration of the components in the reaction mixtures was carried out by the external standard method and was based on peak areas. HPLC measurements were made with the following settings: Flow rate 1.0 mL/min at a temperature of 25 °C, eluent A = methanol, eluent B = acetic acid buffer (99% milliQ, 1% acetic acid). The samples were eluted using the following gradient: 40% A and 60% B set for 6 min, gradient

to 100% A and 0% B in subsequent 10 min, 100% A and 0% B set for 5 min, followed by 40% A and 60% B set for 8 min.

LC-MS analysis was performed using a liquid chromatographic system (Agilent 1200 series) equipped with a Luna 3 μm C18 column (200 × 2.0 mm) and an ion trap (Agilent 6300 series).

Size exclusion chromatography (SEC) was performed using a liquid chromatographic system (Agilent 1100 series G1362A) equipped with a Varian PLgel column (300 × 7.5 mm) at 70 °C, a refractive index detector (70 ºC) and an UV-vis absorbance detector. Dimethylformamide (DMF) was used as eluent at a flow rate of 1.0 mL/min. The molecular weights were calculated with respect to polystyrene standards (Polymer Laboratories, M_n = 500 g mol^{-1} up to $M_n = 2 \times 10^6$ g mol^{-1}). Before the GPC analysis, the samples were filtered through a 0.45 μm PTFE filter. The use of polystyrene standards inevitably leads to an error in molecular weights, so the $C_{tr,Sol}$ data reported also contains a comparable error.

The glass transition temperature (T_g) of the polymeric samples was measured using a TA Q200 differential scanning calorimeter from TA Instruments. The DSC runs were conducted over a temperature range between -30 °C and 230 °C, with a three-part sequence that included heating, cooling, and reheating. The heating rate and cooling rate were set at 20 °C/min. The T_g was determined using the second heating curve by measuring the peak in the first derivative graph of the enthalpy vs. temperature curve.

Thermogravimetric analyses (TGA) were performed in a nitrogen atmosphere with a TGA Q50 from TA Instruments. About 5–10 mg of each sample was heated at 20 °C/min from 25 °C to 600 °C.

The melting points of the low molecular materials were determined with the Hanon Automatic Video Melting Point apparatus MP450.

7.4.2 Experimental procedures

*Protocol for the Green Knoevenagel condensation towards sinapinic acid **2a** with 10 mol% ammonium bicarbonate:*

Malonic acid (10 mmol, 1.0 g) was dissolved in a minimum amount (e.g., 2.5 mL) of ethyl acetate. Syringaldehyde (**1a**, 10 mmol, 1.8 g) and ammonium bicarbonate (1.0 mmol, 79 mg) were subsequently added. The solvent (ethyl acetate) was removed by distillation under reduced pressure at 40 °C. The reaction mixture was kept for 2 hours at 90 °C for complete conversion of syringaldehyde according to HPLC analysis. Samples were taken for reversed-phase HPLC analysis and diluted in 7.5 mL methanol, filtered, and analyzed using the method described in section 2.2. The calculated percentage of the peak area of the component of interest is in relation to the total area of peaks.

In the workup procedure of sinapinic acid **2a**, the residue was dissolved in 10 mL of a saturated aqueous sodium bicarbonate solution and subsequently acidified to a pH of 2 by using an aqueous 6 M HCl-solution. The resulting precipitate was separated by filtration and washed with (demineralized) water (3 × 5 mL). After recrystallization in a mixture of water-ethanol (4:1, v/v), the crystals were separated by filtration and dried at 50 °C in a vacuum oven overnight.

Optimized protocol for the synthesis of hexamethylenetetramine (HMTA):

A mixture of formaldehyde solution (37 wt. % in H_2O, 60 mmol, 4.8 g) and an ammonium hydroxide solution (20 wt. % in H_2O, 40 mmol, 7.0 g) was allowed to stand unstirred for 3 hours at room temperature (if necessary more ammonia can be added to keep the solution slightly alkaline). The solution was filtered and then concentrated in a vacuum to a thick paste. The crystals which were formed were separated by filtration, washed with 10 mL ethanol, and dried in the air. The crude product was recrystallized from ethanol to obtain pure, white crystals.

*Optimized protocol for decarboxylation to HDMS (**3a**):*

Sinapinic acid **2a** (10 mmol, 2.24 g) and HMTA (1.0 mmol, 140 mg) were dissolved in propylene carbonate (30 mmol, 3.1 g) and transferred into a two-necked flask. The reaction mixture was deoxygenated by a series of three vacuum-nitrogen cycles while stirring and was subsequently kept for 2 hours at 105 °C. Pure HDMS **3a** was obtained by precipitation the reaction mixture in 10 mL toluene and the solid HDMS **3a** was kept herein to prevent oxidation.

*Optimized protocol for acetylation to ADMS (**4a**):*
A mixture of HDMS **3a** (10 mmol, 1.80 g) and sodium acetate (0.5 mmol, 41 mg) was dissolved in acetic anhydride (15 mmol, 1.53 g), and stirred at 90 °C for 30 minutes. In the workup procedure, 5 mL of ethyl acetate was added to the reaction mixture and washed with a saturated brine solution (3 × 5 mL). The organic layer was acidified with a 1.0 M HCl solution to a pH of 2, the layers were separated, and pure ADSM **4a** was obtained by precipitation in 5 mL of saturated brine solution. The precipitate was dried at 50 °C in a vacuum oven overnight.

*Protocol for solution polymerization to PADMS (**5a**):*
A mixture of solid ADMS **4a** (5 mmol, 1.11 g), toluene (2 mL), and 2,2'-azobisisobutyronitrile (0.05 mmol, 8.2 mg) was deoxygenated by a series of three vacuum-nitrogen cycles and stirred at a temperature of 60 °C for 24 hours. The resulting product was precipitated in 5 mL cold methanol, and the precipitate was washed with heptane (3 × 5 mL), followed by drying at 50 °C under reduced pressure for one day.

*Protocol for hydrolysis to PHDMS (**6a**):*
PADMS **5a** (0.155 g) was dissolved in 1.0 M NaOH solution in 10.0 mL acetone. The mixture was stirred for 24 hours at 60 °C and acidified with a 1.0 M HCl solution to a pH of 2. The precipitate was filtered, followed by drying at 40 °C under reduced pressure for one week.

Protocol for determination the chain transfer constants:
Toluene and monomer (styrene and 4-acetoxystyrene (AS) **4c**) were deoxygenated by a series of three vacuum-nitrogen cycles. For the series of experiments, the monomer was dissolved in toluene with concentrations ranging between x and y M. The initiator ratio was set at 1.5×10^{-3} mol of AIBN for 1 mol monomer in all experiments. Samples were prepared in small vials (1 mL) and placed at 60 ºC for a pre-determined time. Conversions were kept below 8% in all cases.

7.4.3 Characterization

Sinapinic acid (2a)

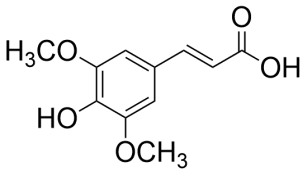

Light yellow solid, m.p. = 198 - 199 °C.
^{1}H NMR (400 MHz, DMSO) δ (ppm) = 12.11 (s, 1H), 8.90 (s, 1H), 7.49 (d, J = 15.9 Hz, 1H), 6.99 (s, 2H), 6.42 (d, J = 15.9 Hz, 1H), 3.80 (s, 6H).
^{13}C NMR (101 MHz, DMSO)
δ (ppm) = 168.50, 148.50, 145.32, 138.52, 125.11, 116.53, 106.48, 56.49. M calculated: 224.21 g/mol;
MS (ESI) *m/z* observed $[M+H]^+$: 225 $[M-H]^-$: 223

Ferulic acid (2b)

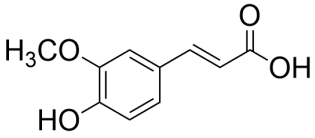

Light yellow solid, m.p. = 171 - 173 °C.
^{1}H NMR (400 MHz, DMSO) δ (ppm) = 12.12 (s, 1H), 9.54 (s, 1H), 7.49 (d, J = 15.9 Hz, 1H), 7.28 (d, J = 1.9 Hz, 1H), 7.08 (dd, J = 8.2, 1.9 Hz, 1H), 6.84 – 6.76 (m, 1H), 6.36 (d, J = 15.9 Hz, 1H), 3.82 (s, 3H).
^{13}C NMR (101 MHz, DMSO) δ (ppm) = 168.49, 149.54, 148.37, 144.99, 126.25, 123.28, 116.10, 116.00, 111.59, 56.12. M calculated: 194.18 g/mol;
MS (ESI) *m/z* observed $[M+H]^+$: 195 $[M-H]^-$: 193

***p*-Coumaric acid (2c)**

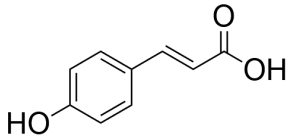

White solid, m.p. = 212 - 214 °C.
^{1}H NMR (400 MHz, DMSO) δ (ppm) = 12.11 (s, 1H), 9.91 (d, J = 84.3 Hz, 1H), 7.58 – 7.48 (m, 3H), 6.82 (d, J = 8.5 Hz, 2H), 6.32 (d, J = 16.0 Hz, 1H).
^{13}C NMR (101 MHz, DMSO) δ (ppm) = 168.47, 160.06, 144.66, 130.53, 125.75, 116.23, 115.80. M calculated: 164.16 g/mol;
MS (ESI) *m/z* observed $[M+H]^+$: 165 $[M-H]^-$: 163

cinnamic acid (2d)

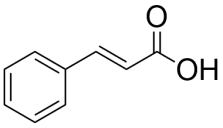

White solid, m.p. = 133 - 134 °C.

^{1}H NMR (400 MHz, DMSO) δ (ppm) = 12.41 (s, 1H), 7.73 – 7.65 (m, 2H), 7.60 (d, J = 16.0 Hz, 1H), 7.46 – 7.38 (m, 3H), 6.54 (d, J = 16.0 Hz, 1H).

^{13}C NMR (101 MHz, DMSO) δ (ppm) = 168.07, 144.38, 134.71, 130.63, 129.33, 128.62, 119.70. M calculated: 148.16 g/mol;

MS (ESI) *m/z* observed $[M+H]^+$: 149 $[M-H]^-$: 147

4-hydroxy-3,5-dimethoxystyrene = HDMS (3a)

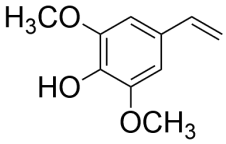

Off-white solid, m.p. = 53.1 – 54.0 °C.

^{1}H NMR (400 MHz, DMSO) δ (ppm) = 8.44 (s, 1H), 6.73 (s, 2H), 6.66 – 6.53 (m, 1H), 5.67 (dd, J = 17.6, 0.8 Hz, 1H), 5.09 (dd, J = 10.9, 0.7 Hz, 1H), 3.77 (s, 6H).

^{13}C NMR (101 MHz, DMSO) δ (ppm) = 148.51, 137.45, 136.29, 128.21, 111.78, 104.24, 56.40. M calculated: 180.20 g/mol;

MS (ESI) *m/z* observed $[M+H]^+$: 181 $[M-H]^-$: 179

4-hydroxy-3-methoxystyrene = HMS (3b)

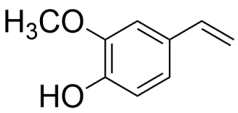

Off-white solid, m.p. = 45.1 – 46.2 °C.

^{1}H NMR (400 MHz, DMSO) δ (ppm) = 9.10 (s, 1H), 7.06 (d, J = 1.9 Hz, 1H), 6.87 (dd, J = 8.1, 1.9 Hz, 1H), 6.80 – 6.75 (m, 1H), 6.62 (dd, J = 17.6, 10.9 Hz, 1H), 5.64 (dd, J = 17.6, 0.9 Hz, 1H), 5.13 – 5.00 (m, 1H), 3.80 (s, 3H).

^{13}C NMR (101 MHz, DMSO) δ (ppm) = 148.19, 147.24, 137.17, 129.31, 119.99, 115.88, 111.33, 110.07, 56.00. M calculated: 150.16 g/mol;

MS (ESI) *m/z* observed $[M+H]^+$: 151 $[M-H]^-$: 149

4-hydroxystyrene = HS (3c)

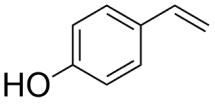

White solid, m.p. = 69.1 – 70.4 °C.

^{1}H NMR (400 MHz, MeOD) δ (ppm) = 7.94 (s, 1H), 7.28 – 7.22 (m, 2H), 6.78 – 6.71 (m, 2H), 6.61 (dd, J = 17.6, 10.9 Hz, 1H), 5.59 – 5.51 (d, J = 17.6 Hz, 1H), 5.02 (d, J = 10.9, 1H). M calculated: 120.12 g/mol;

MS (ESI) *m/z* observed $[M+H]^+$: 121 $[M-H]^-$: 119

4-acetoxy-3,5-dimethoxystyrene = ADMS (4a)

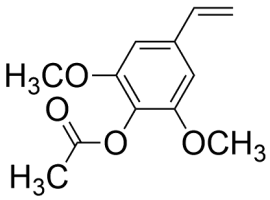

Yellow-white solid m.p. = 64.1 – 65.2 °C.

^{1}H NMR (400 MHz, DMSO) δ (ppm) = 6.85 (s, 2H), 6.76 – 6.63 (m, 1H), 5.89 (dd, J = 17.6, 0.5 Hz, 1H), 5.28 (d, J = 11.4 Hz, 1H), 3.78 (s, 6H), 2.24 (s, 3H).

^{13}C NMR (101 MHz, DMSO) δ (ppm) = 168.57, 152.31, 136.95, 136.04, 128.25, 115.19, 103.39, 56.39, 20.58. M calculated: 222.26 g/mol;

MS (ESI) *m/z* observed $[M+H]^+$: 223 $[M-H]^-$: 221

4-acetoxy-3-methoxystyrene = AMS (4b)

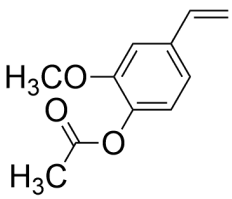

Yellow-white solid m.p. = 68.4 – 70.5 °C.

^{1}H NMR (400 MHz, DMSO) δ (ppm) = 7.23 (s, 1H), 7.04 (s, 2H), 6.72 (dd, J = 17.6, 11.0 Hz, 1H), 5.86 (d, J = 17.6 Hz, 1H), 5.27 (d, J = 11.0 Hz, 1H), 3.80 (s, 3H), 2.25 (s, 3H).

^{13}C NMR (100 MHz, DMSO) δ (ppm) = 169.00, 151.42, 139.49, 136.61, 136.55, 123.32, 119.08, 115.08 110.60, 56.22, 20.86. M calculated: 192.23 g/mol;

MS (ESI) *m/z* observed $[M+H]^+$: 193 $[M-H]^-$: 191

4-acetoxystyrene = AS (4c)

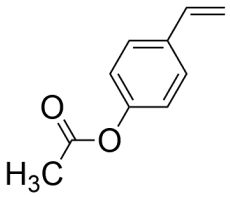

Liquid, m.p. = 7 - 8 °C.

^{1}H NMR (400 MHz, DMSO) δ (ppm) = 7.52 – 7.47 (m, 2H), 7.16 – 7.08 (m, 2H), 6.73 (dd, J = 17.7, 10.9 Hz, 1H), 5.79 (d, J = 17.7 Hz, 1H), 5.25 (d, J = 10.9 Hz, 1H), 2.25 (s, 3H).

^{13}C NMR (101 MHz, DMSO) δ (ppm) = 169.49, 150.68, 136.22, 135.29, 127.55, 122.39, 114.59, 21.14.

M calculated: 162.19 g/mol;

MS (ESI) *m/z* observed $[M+H]^+$: 163 $[M-H]^-$: 161

Poly(4-acetoxy-3,5-dimethoxystyrene) = PADMS (5a)

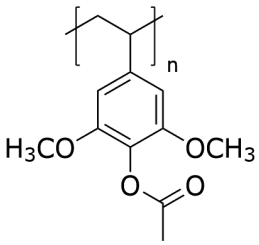

^{1}H NMR (400 MHz, DMF) δ (ppm) = 6.45 – 5.67 (m, 2H), 3.72 – 3.41 (m, 6H), 2.26 (s, 3H), 1.52 (m, 3H).

^{13}C NMR (101 MHz, DMF) δ (ppm) = 168.43, 151.94, 136.64, 135.94, 126.42, 113.96, 102.93, 56.03, 20.42.

T_g = 121 °C

$T_{50\%}$ = 353 °C

Poly(4-acetoxy-3-methoxystyrene) = PAMS (5b)

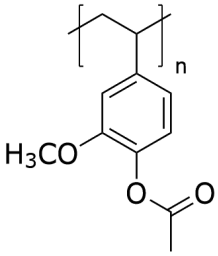

^{1}H NMR (400 MHz, DMF) δ (ppm) = 7.30 – 5.43 (m, 3H), 3.39 (s, 3H), 2.09 (s, 3H), 1.27 (m, 3H).

^{13}C NMR (101 MHz, DMF) δ (ppm) = 168.78, 150.82, 137.70, 122.34, 119.58, 55.73, 20.68.

T_g = 104 °C

$T_{50\%}$ = 370 °C

Poly(4-acetoxystyrene) = PAS (5c)

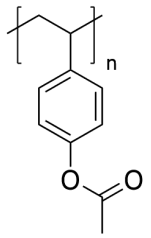

^{1}H NMR (400 MHz, DMF) δ (ppm) = 7.28 – 6.20 (m, 4H), 2.30 (s, 3H), 2.06 – 1.05 (m, 3H).

^{13}C NMR (100 MHz, $CDCl_3$) δ (ppm) = 169.24, 148.67, 135.89, 127.19, 121.36, 114.06, 21.20.

T_g = 130 °C

$T_{50\%}$ = 385 °C

Poly(4-hydroxy-3,5-dimethoxystyrene) = PHDMS (6a)

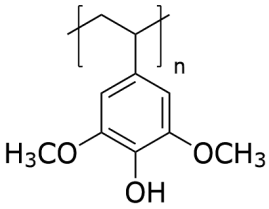

^{1}H NMR (400 MHz, DMF) δ (ppm) = 8.04 (s, 1H), 6.52 (m, 2H), 3.73 (s, 6H), 2.53 – 0.97 (m, 3H).

T_g = 146 °C

$T_{50\%}$ = 365 °C

Poly(4-hydroxy-3-methoxystyrene) = PHMS (6b)

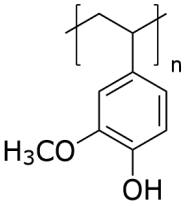

^{1}H NMR (400 MHz, DMF) δ (ppm) = 9.23 (s, 1H), 7.22 (m, 3H), 4.07 (s, 3H), 2.51 – 0.97 (m, 3H).

T_g = 130 °C

$T_{50\%}$ = 380 °C

Poly(4-hydroxystyrene) = PHS (6c)

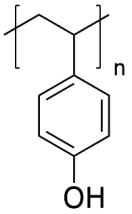

^{1}H NMR (400 MHz, DMF) δ (ppm) = 9.01 (s, 1H), 6.54 (m, 4H), 2.28 – 0.76 (m, 3H).

T_g = 188 °C

$T_{50\%}$ = 390 °C

7.5 References

1. Simon, E. Ueber den flussigen Storax (Styrax liquidus). *Annalen der Chemie* **1839**, *31*, 265-277.
2. van 't Hoff, J. H. Die Identität von Styrol und Cinnamol, ein neuer Körper aus Styrax. *Ber. Dtsch. Chem. Ges.* **1876**, *9*, 5-6.
3. Kolstad, H. A.; Juel, K.; Olsen, J.; Lynge, E. Exposure to Styrene and Chronic Health Effects: Mortality and Incidence of Solid Cancers in the Danish Reinforced Plastics Industry. *Occupational and Environmental Medicine* **1995**, *52*, 320-327.
4. Pleban, F. T.; Oketope, O.; Shrestha, L. Occupational Styrene Exposure on Auditory Function Among Adults: A Systematic Review of Selected Workers. *Safety and Health at Work* **2017**, *8*, 329-336.
5. Boffetta, P.; Adami, H.; Cole, P.; Trichopoulos, D.; Mandel, J. Epidemiologic Studies of Styrene and Cancer: A Review of the Literature. *Journal of Occupational and Environmental Medicine* **2009**, *51*, 1275-1287.
6. Hammann, M.; Castillo, D.; Anger, C.; Rieger, B. Highly selective CO_2 separation membranes through tunable poly(4-vinylphenolate)–CO_2 interactions. *J. Mater. Chem. A* **2014**, *2*, 16389-16396.
7. Bernini, R.; Mincione, E.; Barontini, M.; Provenzano, G.; Setti, L. Obtaining 4-vinylphenols by decarboxylation of natural 4-hydroxycinnamic acids under microwave irradiation. *Tetrahedron* **2007**, *63*, 9663-9667.
8. Shrestha, K.; Stevens, C. V.; De Meulenaer, B. Isolation and identification of a potent radical scavenger (canolol) from roasted high erucic mustard seed oil and its formation during roasting. *Journal of agricultural and food chemistry* **2012**, *60*, 7506-7512.
9. Takeshima, H.; Satoh, K.; Kamigaito, M. Biobased Functional Styrene Monomers Derived from Naturally Occurring Ferulic Acid for Poly(vinylcatechol) and Poly(vinylguaiacol) via Controlled Radical Polymerization. *Macromolecules* **2017**, *50*, 4206-4216.
10. Woo, D.; Kim, J.; Suh, M.; Zhou, H.; Nguyen, S. T.; Lee, S.; Torkelson, J. M. Styrene/4-hydroxystyrene random, block and gradient copolymers modified with an organic dye: Synthesis by controlled radical polymerization and characterization of electrorheological properties. *Polymer* **2006**, *47*, 3287-3291.
11. de Meftahi, M. V.; Fréchet, J. M. J. Study of the compatibility of blends of polymers and copolymers containing styrene, 4-hydroxystyrene and 4-vinylpyridine. *Polymer* **1988**, *29*, 477-482.
12. Hatakeyama, T.; Hatakeyama, H.; Nakamura, K. Differential thermal analysis of styrene derivatives related to lignin. *Polymer* **1978**, *19*, 593-594.
13. Hatakeyama, T.; Hatakeyama, H. Temperature dependence of X-ray diffractograms of amorphous lignins and polystyrenes. *Polymer* **1982**, *23*, 475-477.
14. Sun, H.; Young, Y. D.; Kanehashi, S.; Tsuchiya, K.; Ogino, K.; Sim, J. Radical Copolymerization of Ferulic Acid Derivatives with Ethylenic Monomers. *Journal of Fiber Science and Technology* **2016**, *72*, 74-79.
15. Hatakeyama, H.; Hatakeyama, T.; Nakamura, K. Determination of bound water content in polymers by DTA, DSC and TG. *Thermochimica Acta* **1988**, *123*, 153-161.
16. Hatakeyama, T.; Hatakeyama, H. Effect of chemical structure of amorphous polymers on heat capacity difference at glass transition temperature. *Thermochimica Acta* **1995**, *267*, 249-257.
17. Arichi, S.; Sakamoto, N.; Yoshida, M.; Himuro, S. Dilute solution properties of poly(4-hydroxystyrene). *Polymer* **1986**, *27*, 1761-1767.
18. Sanchis, A.; Masegosa, R. M.; Rubio, R. G.; Prolongo, M. G. Glass transition temperature for blends containing poly(4-hydroxystyrene). *European Polymer Journal* **1994**, *30*, 781-787.

19. Kratochvíl, J.; Šturcová, A.; Sikora, A.; Dybal, J. Note on the glass transition temperature of Poly(vinylphenol). *European Polymer Journal* **2009**, *45*, 1851-1856.
20. van Schijndel, J.; Canalle, L. A.; Smid, J.; Meuldijk, J. Conversion of Syringaldehyde to Sinapinic Acid through Knoevenagel-Doebner Condensation. *Open Journal of Physical Chemistry* **2016**, *6*, 101-108.
21. van Schijndel, J.; Canalle, L. A.; Molendijk, D.; Meuldijk, J. The green Knoevenagel condensation: solvent-free condensation of benzaldehydes. *Green Chemistry Letters and Reviews* **2017**, *10*, 404-411.
22. van Schijndel, J.; Canalle, L. A.; Molendijk, D.; Meuldijk, J. Exploration of the Role of Double Schiff Bases as Catalytic Intermediates in the Knoevenagel Reaction of Furanic Aldehydes: Mechanistic Considerations. *Synlett* **2018**, *29*, 1983-1988.
23. Manach, C.; Scalbert, A.; Morand, C.; Rémésy, C.; Jiménez, L. Polyphenols: food sources and bioavailability. *The American journal of clinical nutrition* **2004**, *79*, 727-747.
24. Menezes, J. C. J. M. D. S.; Kamat, S. P.; Cavaleiro, J. A. S.; Gaspar, A.; Garrido, J.; Borges, F. Synthesis and antioxidant activity of long chain alkyl hydroxycinnamates. *European Journal of Medicinal Chemistry* **2011**, *46*, 773-777.
25. Morley, K. L.; Grosse, S.; Leisch, H.; Lau, P. C. K. Antioxidant canolol production from a renewable feedstock via an engineered decarboxylase. *Green Chemistry* **2013**, *15*, 3312-3317.
26. Nomura, E.; Hosoda, A.; Mori, H.; Taniguchi, H. Rapid base-catalyzed decarboxylation and amide-forming reaction of substituted cinnamic acids via microwave heating. *Green Chemistry* **2005**, *7*, 863-866.
27. Cohen, L. A.; Jones, W. M. A Study of pH Dependence in the Decarboxylation of p-Hydroxycinnamic Acid. *Journal of the American Chemical Society* **1960**, *82*, 1907-1911.
28. Zou, Y.; Huang, Q.; Huang, T.; Ni, Q.; Zhang, E.; Xu, T.; Yuan, M.; Li, J. CuI/1,10-phen/PEG promoted decarboxylation of 2,3-diarylacrylic acids: synthesis of stilbenes under neutral and microwave conditions with an in situ generated recyclable catalyst. *Organic & biomolecular chemistry* **2013**, *11*, 6967-6974.
29. Cadot, S.; Rameau, N.; Mangematin, S.; Pinel, C.; Djakovitch, L. Preparation of functional styrenes from biosourced carboxylic acids by copper catalyzed decarboxylation in PEG. *Green Chemistry* **2014**, *16*, 3089-3097.
30. Cahiez, G.; Moyeux, A.; Gager, O.; Poizat, M. Copper-Catalyzed Decarboxylation of Aromatic Carboxylic Acids: En Route to Milder Reaction Conditions. *Advanced Synthesis & Catalysis* **2013**, *355*, 790-796.
31. Nakamura, K.; Hatakeyama, T.; Hatakeyama, H. DSC studies on hydrogen bonding of poly(4-hydroxy-3,5-dimethoxystyrene) and related derivatives. *Polymer Journal* **1986**, *18*, 219-225.
32. Kato, M. A Research on Polymerization of o-, m-, and p-Vinylphenol. *Journal of Photopolymer Science and Technology* **2008**, *21*, 711-717.
33. Nakamura, K.; Hatakeyama, H.; Hatakeyama, T. Differential scanning calorimetric studies on the glass transition temperature of polyhydroxystyrene derivatives containing sorbed water. *Polymer* **1981**, *22*, 473-476.
34. Nakamura, K.; Hatakeyama, T.; Hatakeyama, H. Effect of substituent groups on hydrogen bonding of polyhydroxystyrene derivatives. *Polymer Journal* **1983**, *15*, 361-366.
35. Mayo, F. R. Chain Transfer in the Polymerization of Styrene: The Reaction of Solvents with Free Radicals. *Journal of the American Chemical Society* **1943**, *65*, 2324-2329.
36. Gregg, R. A.; Mayo, F. R. Chain transfer in the polymerisation of styrene III. The reactivities of hydrocarbons toward the styrene radical. *Discussions of the Faraday Society* **1947**, *2*, 328-337.
37. Gregg, R. A.; Mayo, F. R. Chain Transfer in the Polymerization of Styrene VII. Compounds Containing Halogens, Oxygen and Nitrogen. *Journal of the American Chemical Society* **1953**, *75*, 3530-3533.

8 Epilogue

8.1 Highlights

The design, as well as the sustainable production of monomers, are crucial steps to realize molecularly recyclable polymers with high depolymerization selectivity and proper materials properties. The main objective of the work described in this thesis was to demonstrate the applicability of a set of renewable monomers in molecularly recyclable semi-aromatic polyesters. Moreover, an extensive effort was dedicated to synthesizing the selected monomers taking the principles of Green Chemistry into account. There are two main issues described in this thesis. The first one focuses on the synthesis of the three monomers phloretic acid, dihydroferulic acid, and dihydrosinapinic acid from benzaldehydes conceivably derived from lignin. The second one describes the polymerization, properties, and depolymerization of the intended polymers poly(phloretic acid) (poly-H), poly(dihydroferulic acid) (poly-G), and poly(dihydrosinapinic acid) (poly-S), see Scheme 8.1.

With the 12 principles of Green Chemistry[1] in mind, we are becoming increasingly aware that each step in the design of the monomer and polymer needs to be considered or reassessed with sustainability in mind. The envisioned monomers for the molecularly recyclable polyesters are already in small amounts present in plants and trees and occasionally also prevalent in significant quantities. Furthermore, the results of this study clearly demonstrate that it is also possible to produce the envisioned monomers sustainably from benzaldehyde-like compounds. Experts predict that soon, it will be possible to extract these benzaldehydes on a more substantial scale from lignin.[2,3] These benzaldehydes mainly involve molecules such as vanillin, syringaldehyde, and 4-hydroxybenzaldehyde. In the work described in this thesis, a scalable, sustainable route has been developed to produce the intended monomers from these benzaldehyde-like compounds.

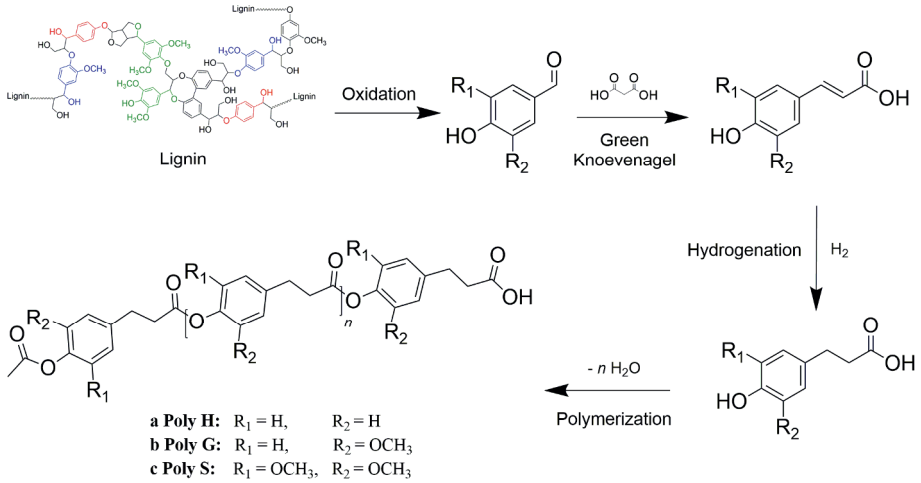

Scheme 8.1: Synthetic route towards the three monomers, followed by polymerization towards semi-aromatic polyesters. The benzaldehyde-analog undergoes a Green Knoevenagel reaction resulting in an α,β-unsaturated acid, which is subsequently hydrogenated to the intended monomer. Acetylation of the phenol-group is the first step towards polycondensation.

Ensuring that the core structure of these monomers is suitable to be molecularly recycled is the first step. This study provided valuable insights into the design and the application of renewable monomers in molecularly recyclable semi-aromatic polyesters. The most important outcome is that molecularly recyclable polyesters characteristically contain a high fraction of aliphatic ester groups. Note that derivatives of aliphatic carboxylic acids are several orders of magnitude more electrophilic than derivatives of aromatic carboxylic acids. Therefore, polyesters derived from aromatic carboxylic acids are far less sensitive to hydrolysis than aliphatic polyesters. However, complete aromatic polyesters have a higher melting temperature (T_m) and better mechanical properties as compared to aliphatic polyesters.[4]

Polyethylene terephthalate (PET), even though produced from two different monomers (ethylene glycol and terephthalic acid), is usually regarded as an AABB-type homopolymer because only one type of repeat unit is formed. Yet sometimes, it is suggested that the term monomers must be restricted to AB-type molecules, whereas AA- and BB-type ones should preferably be called reactants, the right monomer being the product of their first reaction. For molecular recycling, preference is given to AB-type monomers bearing two different functional groups (AB-type) that can react with each other. The envisioned

redesigned monomers phloretic acid, dihydroferulic acid, and dihydrosinapinic acid meet this requirement.

The redesigned and renewable monomers have been shown to polymerize to highly crystalline polyesters whose materials properties, e.g., degree of crystallinity, crystallization temperature, mode of extension, the Young modulus, still need to be investigated and optimized. The redesigned and renewable polymers can be returned to their building blocks under relatively favorable conditions. These building blocks can be repolymerized with limited material loss. Before-mentioned polymers avoid issues of quality loss, as observed with mechanical recycling[5,6], and show to possess the capacity to recover valuable products from these polymers. For the development of polyethylene terephthalate (PET), it took about four decades to turn PET from a highly crystalline polyester into the commodity polymeric material with which we are familiar today. PET crystallinity and, consequently, its physical and mechanical properties are highly dependent on processing conditions such as the temperature, the cooling rate, and the stretching process.[7]

The research work was conducted in small subprojects that were often embedded in the curriculum of Avans University of Applied Sciences. A significant advantage of working in such a manner with students is that many different ideas and principles can be investigated. The results of parallel research make specific paths visible, and certain general patterns become recognizable. Creating an applied research environment to stimulate the students' learning process can, therefore, be named as a highlight. Some examples of the above mentioned are given in the next paragraph.

Our students were one of the first who established that the studied styrene alternatives are in a solid-state. This observation has many advantages for polymerizations because it makes it easier to get the monomer more uncontaminated. Similarly, the observation that the catalyst of the second decarboxylation towards the styrene alternatives, hexamethylenetetramine (HMTA), is likewise a (catalytic) intermediate of (aliphatic) formaldehyde and ammonia (in the same ratio of 3:2!). Also, the idea that hydrobenzamide, as presented in Scheme 8.2, is an alternative for HMTA as the catalyst of the second decarboxylation turned out to be valuable (and is already applied). In this way, the entire conversion of, for example, vanillin to the styrene analog can be carried out using only ammonium bicarbonate as the catalyst. The desired production is optimized by just setting the temperature accurately.

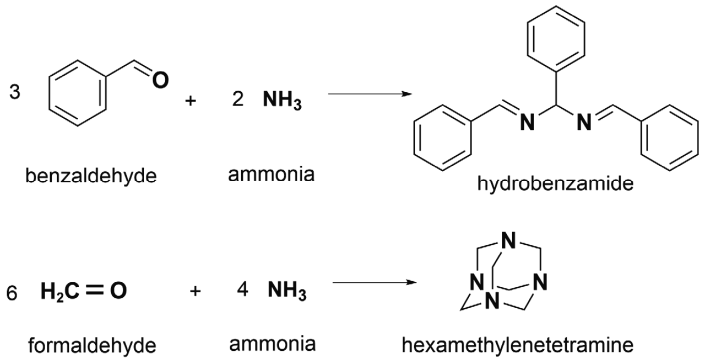

Scheme 8.2: The formation of the catalytic intermediate hydrobenzamide from benzaldehyde and ammonia in a ratio of 3:2 and the formation of hexamethylenetetramine (HMTA) from formaldehyde and ammonia in the same ratio.

8.2 Technology assessment

One of the problems of everyday polymeric materials is that they are blends of several polymer types. This is where molecular recycling could play a role in closing the loop back to the chemical feedstock again, enabling 'infinite' loops. Because the monomers developed in this study, can be recovered relatively efficient with molecular recycling, this quality can be used to transform the remaining part of the polymeric material to allow the additional recycling.

There is always a loss in every recycling procedure that ensures the release of the polymeric material in nature. In this situation, it is essential that the properties of the polymeric material are such that it composts adequately, including biodegrading at a rate comparable to known compostable materials. Further, the degradation of these materials must ensure that it will not diminish the value or utility of the compost resulting from the composting process. Because our designed polymers are often considered as "lignin"-like in all kinds of studies, we expect that these polymers will be broken down correspondingly as lignin by white-rot fungi.[8,9] These degradation mechanisms should be subject intended for further research.

This study has demonstrated that the rate coefficients of the depolymerization of the polyesters poly-H, poly-G, and poly-S in aqueous sodium hydroxide are between 2 and 3 orders of magnitude larger as compared to those for the depolymerization PET. A disadvantage of the current base-catalyzed depolymerization is the salt formation when the monomer is recovered. The semi-aromatic polyesters poly-H, poly-G, and poly-S also have been hydrolyzed in an aqueous 4 M sulfuric acid solution. These polyesters were completely depolymerized after 8 hours at 80 °C. The advantage of acid-catalyzed depolymerization over depolymerization in an alkaline medium is the absence of salt formation. The monomers could easily be re-acetylated after the removal of ethyl acetate and so re-introduced into the polymerization process. The molecular weight distribution (DP_n and PDI), as well as thermal properties (T_g and T_{melt}) of the 10th generation polymeric material, are identical to those of previous generations.

A possible molecular recycling process of acid-catalyzed hydrolysis for the recovery of the monomers is shown in Scheme 8.3. In such a process, the reaction mixture consists of the polymeric material poly-H, poly-G, or poly-S, water, and a catalyst, e.g., linear polystyrene sulfonic acid, which is water-soluble. After the hydrolysis, the solids (unreacted polymeric material, as well as in the water precipitated monomer) need to be separated from the aqueous phase by filtration. The aqueous phase contains the catalyst, which is recycled to the depolymerization reactor.

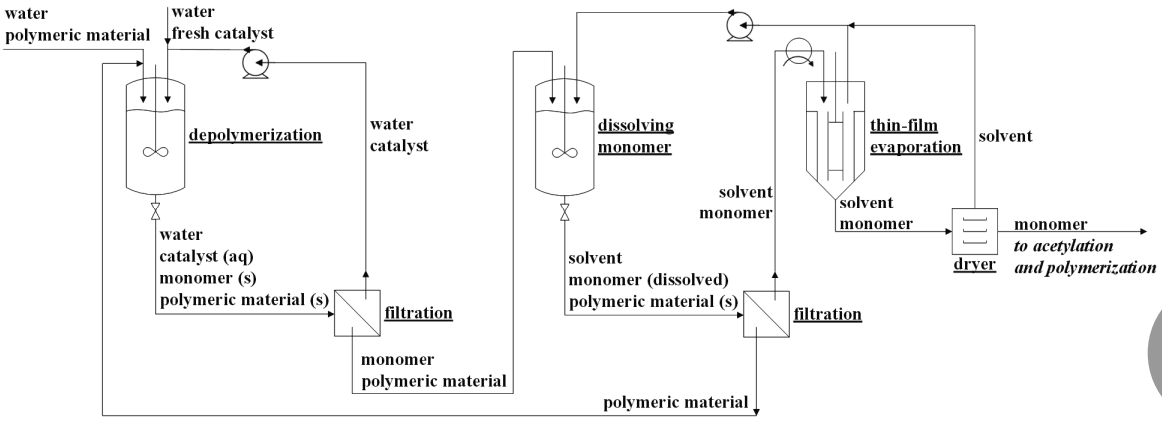

Scheme 8.3: Global representation of a possible process set-up of acid-catalyzed hydrolysis of the corresponding polyesters poly-H, poly-G, and poly-S.

Subsequently, the monomer needs to be separated from the polymeric material on the filter, and the smallest possible amount of solvent (e.g., ethyl acetate or methanol) is added as a solvent for the monomers. After this step, the solvent needs to be evaporated and is qualified for being reused subsequently. It is possible to choose for further purification of the monomer by recrystallization. However, the recovered monomers can as well be directly transferred to the acetylation reactor. The acetylated monomer is then transferred to the polymerization reactor. Even though this is a very global representation of the monomer recovery process, it is rather likely that the majority of the operational process costs will be governed by the heat consumption of the evaporation of the solvent. So it is of utmost importance to minimize the amount of solvent used to separate the monomer from the other (polymer-based) solids.

Emil Knoevenagel has already indicated that it can only be denoted as a Knoevenagel reaction if catalytic intermediates are demonstrated to be present.[10] Later, Knoevenagel remarks felt into oblivion and reverted in the nineties with the development of organocatalysis.[11] In this work, it has been demonstrated that with ammonia as a precursor, double-Schiff bases are formed as catalytic intermediates. The results of additional research have demonstrated that with primary amines, Schiff bases are formed as Knoevenagel catalytic intermediates, and with (as preferred by Knoevenagel) secondary amines, so-called “aminals” are formed as catalytic intermediates. Based on the principles of Emil Knoevenagel and the results of our research, one can conclude that there are three fundamental types of Knoevenagel reactions, i.e., with secondary amines, with primary amines, or with ammonia as a precursor. The Green Knoevenagel reaction with ammonia as a precursor meets the principles of Green Chemistry best.

8.3 Outlook

Molecularly recyclable polymers contribute significantly to a solution for the reduction of polymeric waste. Materials based on molecularly recyclable polymers may avoid topics of quality loss, as observed with mechanical recycling, and the inability to recover valuable products. Still, molecularly recyclable polymeric materials are still far away from commercial application. In addition to technological challenges, there are also economic issues. For manufacturers, it is usually more comfortable to use well known and trusted technology and materials than a novel technology and materials. Although the threshold for the introduction of novel technology and materials is high, it is not impossible.

The polymers synthesized, as part of the work summarized in this thesis, are still very crystalline, and, as a consequence, the processing of the polymeric material is complicated. The degree of polymer crystallinity depends on intrinsic as well as extrinsic factors. A narrow molecular weight distribution, a linear polymer chain structure, and a high molecular weight are essential pre-conditions to obtain materials with high crystallinity.[7] Crystallinity is also affected by extrinsic factors, like stretch ratio, mode of extension, and crystallization temperature in the preparation of polymer films.[13] By incorporating lactide and so introducing a flexible chain, one can influence the crystallinity. Experiments have already been carried out with this on a small scale, and it has undeniably been shown that crystallinity is decreasing.

8.4 References

1. Anastas, P. T., Warner, J. C. *Green chemistry: theory and practice;* Oxford University Press: New York, 1998; .
2. Fache, M.; Boutevin, B.; Caillol, S. Vanillin Production from Lignin and Its Use as a Renewable Chemical. *ACS Sustainable Chemistry & Engineering* **2016***, 4*, 35-46.
3. Sheldon, R. A. Green and sustainable manufacture of chemicals from biomass: state of the art. *Green Chemistry* **2014***, 16*, 950-963.
4. Graaf, A. Zin en onzin van bioafbreekbaar plastic. *C2W* **2015**, 18-19.
5. Awaja, F.; Pavel, D. Recycling of PET. *European Polymer Journal* **2005***, 41*, 1453-1477.
6. Karayannidis, G. P.; Achilias, D. S. Chemical Recycling of Poly(ethylene terephthalate). *Macromolecular Materials and Engineering* **2007***, 292*, 128-146.
7. Baldenegro-Perez, L.; Navarro-Rodriguez, D.; Medellin-Rodriguez, F.; Hsiao, B.; Avila-Orta, C.; Sics, I. Molecular Weight and Crystallization Temperature Effects on Poly(ethylene terephthalate) (PET) Homopolymers, an Isothermal Crystallization Analysis. *Polymers* **2014***, 6*, 583-600.
8. Bugg, T. D. H.; Ahmad, M.; Hardiman, E. M.; Rahmanpour, R. Pathways for degradation of lignin in bacteria and fungi. *Natural product reports* **2011***, 28*, 1883-1896.
9. Floudas, D.; Otillar, R.; Spatafora, J. W.; Coutinho, P. M.; Vries, R. P. D.; Ferreira, P.; Findley, K.; Foster, B.; Hibbett, D. S. The Paleozoic Origin of Enzymatic Lignin Decomposition Reconstructed from 31 Fungal Genomes. *Science* **2012***, 336*, 1715-1719.
10. Knoevenagel, E. Condensation von Malonsäure mit aromatischen Aldehyden durch Ammoniak und Amine. *Berichte der deutschen chemischen Gesellschaft* **1898***, 31*, 2596-2619.
11. List, B. Emil Knoevenagel and the roots of aminocatalysis. *Angewandte Chemie (International ed. in English)* **2010***, 49*, 1730-1734.
12. Gupta, K. C.; Sutar, A. K. Catalytic activities of Schiff base transition metal complexes. *Coordination Chemistry Reviews* **2008***, 252*, 1420-1450.
13. Yu, C.; Xie, Q.; Bao, Y.; Shan, G.; Pan, P. Crystalline and Spherulitic Morphology of Polymers Crystallized in Confined Systems. *Crystals* **2017***, 7*, 147.

Dankwoord

Op 1 april lijkt er serieus een einde te komen aan mijn promotieonderzoek, dat officieel de periode beslaat van 1 mei 2016 tot 1 april 2020. Het toekennen van het promotieonderzoek voelde in 2016 voor mij als een cadeau voor mijn 25-jarig dienstverband, maar bovenal als een prettige reis waarbij van alles op mijn pad kwam. Zo zijn er in dit onderzoek veel nieuwe, niet eerder gepubliceerde, moleculen gesynthetiseerd, katalytische mechanismen deels ontrafeld, eerder "vergeten" chemisch onderzoek weer in de schijnwerpers gezet en polymeren met bijzondere eigenschappen gemaakt. Als chemicus word ik van deze onderwerpen al blij en dat wordt nog vele malen versterkt doordat deze reis gemaakt kon worden samen met collega's en vooral met een groot aantal hbo-studenten.

Voorafgaand aan deze reis heb ik als docent-onderzoeker vanuit Avans het SIA RAAK-PRO project "Regie op Biopolymeren" richting mogen geven vanuit het lectoraat Biobased Products van lector Dorien Derksen. De prettige samenwerking met Guido Smets van Fontys Hogeschool, Gerald Schennink van Universiteit Wageningen en vooral met meerdere MKB-bedrijven (o.a. Alpha Enzymes, Appkuns, Bato, Colorex Master Batch, FabLab Breda, Modified Materials, Oerlemans Plastics, Onora, Rodenburg Biopolymers, Synbra, Top Tree Products, Tymag, Waterschap Brabantse Delta) bleek een springplank te zijn naar dit promotieonderzoek. De bijzondere samenwerking met Robert Lazeroms van Cosun leverde in de vele gefinancierde stage- en afstudeerprojecten steeds nieuwe puzzelstukjes in de furaanchemie op en over deze furaan-puzzel zou nog apart een proefschrift geschreven kunnen worden. In de aangename samenwerking met Nico Osse van HemCell werd duidelijk dat de ontwikkelde polyesters gekarakteriseerd kunnen worden als "polymelkzuur met een aromaatring in de keten" en verder onderzocht kunnen worden betreffende producteigenschappen, moleculaire recycling en microbiologische afbraak.

Paul van Hal, voormalig directeur van de Academie van de Technologie van Gezondheid en Milieu (ATGM) van Avans Hogeschool, bleef benadrukken hoe mooi het combineren van onderzoek en onderwijs zou kunnen zijn en bleef roepen hoe mijn invulling daarvan een voorbeeld is voor anderen. Paul, jij bent de drijvende kracht geweest achter de aanvraag van mijn promotiebeurs bij de Nederlandse Organisatie voor Wetenschappelijk Onderzoek (NWO). Bedankt

voor je aanhoudende steun en voor de mogelijkheid om dit promotieonderzoek onder de vlag van ATGM en in het bijzonder de opleiding Chemie uit te voeren. Zo werd deze reis meer een dienstreis en kon ik het promotietraject als onderdeel van mijn werk blijven zien. Natuurlijk gaat ook mijn dank uit naar de huidige directie die gezorgd heeft dat dit promotieonderzoek ook daadwerkelijk afgerond kon worden en mijn dienstreis tot het einde toe bleef supporteren**.**

Mijn promotor prof. dr. Jan Meuldijk wil ik bedanken voor het mogelijk maken van dit promotieonderzoek en de nodige sturing en adviezen op het juiste moment. Vanaf het begin voelde ik de betrokkenheid en onze gezamenlijke besprekingen heb ik altijd zeer gewaardeerd. De meest wilde ideeën werden subtiel teruggebracht naar werkbare, zinvolle onderzoeken. Tijdens onze gesprekken, waarvan ook een aantal samen met afstudeerder Sanne de Krom, kwamen veel onderwerpen aan de orde en was er altijd aandacht voor de menselijke maat. In het begin van het promotietraject was dr. ir. Bart Noordover bij de besprekingen betrokken en kwam duidelijk naar voren dat Bart anderen steeds het beste gunt. Aan het einde van het promotietraject nam dr. Timothy Noël de rol van 2e promotor op zich en werden de nodige aanwijzingen gegeven. Ik wens jullie nog een hele mooie en succesvolle carrière toe.

Graag dank ik de overige leden van de promotiecommissie, prof. dr. C. E. Koning, prof. dr. J. H. Bitter, prof. dr. ir. A. R. A. Palmans en prof. dr. ir. M. van Sint Annaland, voor de tijd en moeite voor zowel het lezen en beoordelen van het proefschrift als voor hun rol in de oppositie tijdens de promotieplechtigheid. In een inspirerende omgeving van de Technische Universiteit Eindhoven krijg je alle mogelijkheden om goed onderzoek te doen. Iedereen die op enigerlei wijze betrokken is geweest vanuit TU Eindhoven wil ik bedanken voor de ondersteuning.

Het management en de lectoren komen en gaan maar collega's blijven vaak langer betrokken bij je (loop)baan. Luiz Canalle en Arnold Nijhuis zijn betrokken collega's, die eveneens de overgang naar het lectoraat Biobased Building Blocks & Products van lector Han van Kasteren meemaakten en zeker ook de expertisegroep "Green Chemistry" mede vormgaven. Vanaf nu kan ook het antwoord gegeven worden aan de andere betrokken collega's (van A. D. tot Q. Z.), die regelmatig vroegen wanneer deze dienstreis beëindigd zou worden: 1 april.

Binnen Avans had ik verder het geluk om aan een intervisiegroep van buiten-promovendi te mogen deelnemen. Eefje Hendrikx, Ella Braat en Marieke Versteijlen, ik hoop dat ik binnenkort ook bij jullie verdediging aanwezig kan zijn.

Onderzoek kan niet plaatsvinden zonder de benodigde financiële en andere vormen van ondersteuning. Tijdens het promotietraject zijn deze middelen geleverd door Avans en NWO, onder andere in de vorm van Promotiebeurs voor Leraren. Ik ben natuurlijk iedereen erkentelijk en dankbaar voor deze steun.

Veel, heel erg veel studenten zijn direct of indirect betrokken geweest bij dit promotieproject. Via het watervalprincipe geven vierdejaars afstudeerders en stagiaires inhoud aan de minorprojecten van de derdejaars studenten en onderdelen hiervan zijn weer door tweedejaars en eerstejaars hbo-studenten onderzocht. Zelfs middelbare scholieren hebben voor hun profielwerkstuk onderzoek gedaan naar het maken van kleurstoffen op basis van curcumine-analogen uit de drie door ons geselecteerde bouwstenen van lignine.

De hbo-studenten die als afstudeerder of stagiaire minimaal een half jaar betrokken zijn geweest, hebben een plaats verdiend in mijn "periodiek systeem der studenten" en wil ik hierbij bedanken: *Koen van Beurden, Silvia Kockx, Thijs de Hoon, Erwin Korsten, Tim de Visser, Guy Erkelens, Stefan Jansen, Maxim Kooijman, Abdurrahman Citak, Rick Hagenaars, Jochum Smid, Lars Keijzer, Chris Barends, Arjan van Tiggelen, Wilco van den Oetelaar, Stef Bremen, Dennis Molendijk, Aukje Laurijssen, Miranda Schepers, Richard van Schie, Ruderik van Hierden, Liza Wilders, Ian Jansen, Omaid Shokouri, Kevin Evers, Rik Hellemons, William Janssen, Teis van Beurden, Jill Jansen, Steffijn de Koning, Nick Paassens, Thijs van Ostaden, Alex Huizinga, Dennis van der Leest, Sanne de Krom, Lydia 't Hardt, Lisette Konings, Rosemarie de Ruiter, Martijn Sterenborg, Juanita van Dongen, Linda Nijssen, Robbert Swinkels, Maarten Harijgens, Femke Kuijpers, Ian Jansen, Luc van der Elzen, Rik Mermans, Thijs Timmers, Nick van den Boomen, Mee Loke Lim, Frederik Kort, Harmen Spakman, Natasja Bos, Sanne Mol, Stefan Schapendonk, Marijn Kisters, Romy Vermeulen, Roland van Sprundel en Jasper van Vliet.*

Volgens typisch Nederlandse traditie wordt een promovendus begeleid door twee paranimfen tijdens de openbare verdediging. Koen van Beurden en Dennis Molendijk zijn de paranimfen, omdat ze belangrijk zijn in het onderzoek. Koen was de eerste hbo-student die succesvol afstudeerde bij de "Biopolymeren-club". Koen, ik ben je veel dank verschuldigd en ik wens je veel succes met het afronden van jouw studie aan de TU Eindhoven en met de onderzoeksplannen daarna. Dennis, ook jij bedankt. Het is uniek dat jij vaak aan een half woord genoeg hebt om te weten wat ik bedoel. In die zin is het overbodig om te benoemen waarvoor ik jou wil bedanken. Wat betreft het onderzoek geef ik graag aan beiden het stokje door.

Naast collega's en studenten is ook mijn familie belangrijk geweest om dit proefschrift af te ronden en met name mijn broer Ben en zussen Henny, Ria en Anita. Vrienden kun je kiezen, familie niet! Dat we elkaar tot steun kunnen zijn is al verschillende keren gebleken, zo ook bij het overlijden van onze moeder op 16 maart 2016. Een van haar zegswijzen was: je moet proberen af te maken waar je aan begonnen bent. Dat ik, vier jaar nadat ik de NWO-promotiebeurs heb gekregen, dit ook daadwerkelijk heb gedaan, zou haar trots hebben gemaakt en jullie hopelijk ook.

Lieve Enny, de laatste woorden zijn voor jou. Onze vier kinderen, Sebastian, Enja, Romee en Tessy, toonden op gezette tijden veel interesse, maar jij bent toch degene die dit promotieonderzoek mogelijk maakte door altijd een thuis te creëren. Je hebt zelf vaak niet in de gaten hoe belangrijk je voor me was, bent en zal blijven.

Jack van Schijndel, 2020

List of publications

So far, this thesis has resulted in the following peer-reviewed journal publications:

"Preparation of biobased styrene alternatives and their free radical polymerization",
van Schijndel, J.; Molendijk, D.; van Beurden, K.; Canalle, L.A.; Noël, T.; Meuldijk, J
European Polymer Journal **2020**, 109534

"Mechanistic Considerations and Characterization of Ammonia-based Catalytic Active Intermediates of the Green Knoevenagel Reaction of Various Benzaldehydes",
van Schijndel, J.; Molendijk, D.; Spakman, H.; Knaven, E., Canalle, L.A.; Meuldijk, J.
Green Chemistry Letters and Reviews **2019**, 12, 323-331.

"Temperature Dependent Green Synthesis of 3-Carboxycoumarins and 3,4-unsubstituted Coumarins",
van Schijndel, J.; Molendijk, D.; Canalle, L.A.; Rump, E.T.; Meuldijk, J.
Current Organic Synthesis **2019**, *16*, 130-135.

"Exploration of the Role of Double Schiff Bases as Catalytic Intermediates in the Knoevenagel Reaction of Furanic Aldehydes: Mechanistic Considerations",
van Schijndel, J.; Canalle, L.A.; Molendijk, D.; Meuldijk, J.
SynLett **2018**, *29*, 1983-1988.

"The Green Knoevenagel condensation: solvent-free condensation of benzaldehydes",
van Schijndel, J.; Canalle, L.A.; Molendijk, D.; Meuldijk, J.
Green Chemistry Letters and Reviews **2017**, *10*, 404-411.

"Conversion of Syringaldehyde to Sinapinic Acid through Knoevenagel-Doebner Condensation",
van Schijndel, J.; Canalle, L.A.; Smid, J.; Meuldijk, J.
Open Journal of Physical Chemistry **2016**, *6*, 101-108.

Patent application:

Luiz A. Canalle, Jack A.M. van Schijndel, Dennis Molendijk, Robert Lazeroms, Adeline Ranoux, Harry Raaijmakers, PRODUCTION AND USE OF FURAN COMPOUNDS, European patent, No. 161703553.3, **2016**

Other publications by the author:

"Temperature-Dependent Order-Disorder Phenomena in Crystal Structures: The Crystal and Molecular Structure of 3,5-Dinitrobenzoic Acid at Room and Liquid Nitrogen Temperature and Statistics of the Geometries of Hydrogen-Bonded Carboxyl Groups",
Kanters, J.A.; Kroon, J.; Hooft, R.; Schouten, A.; van Schijndel, J.A.M.; Brandsen J.
Croatica Chemica Acta **1991**, *64*, 353-370

"A convenient preparation of 3-carbethoxy-2, 4-dimethylquinoline hydrochloride",
Bastiaansen, L.A.M.; van Schijndel, J.A.M.; Buck, H.M.
Organic Preparations and Procedures International, **1988**, *20*, 102-103

About the Author



Jack van Schijndel was born in Terheijden on August 21, 1966. In 1987 he obtained his bachelor's degree in Applied Science (Organic Chemistry) at the Hogeschool West-Brabant. In 1990 he received his master's degree in Chemistry at the University of Utrecht with a major Structural Chemistry (prof. dr. J. Kroon) and a minor Chemistry Education (prof. dr. A.H. Verdonk).

As from September 1991, Jack has been teaching Chemistry at the tertiary level. He also supervised undergraduate as well as postgraduate research projects in chemistry at the Avans University of Applied Sciences, in Etten-Leur, and later in Breda and 's-Hertogenbosch. Jack is always looking to combine education and research with learning innovations and he has performed many projects with external partners.

In **May 2016** Jack received a "promotiebeurs voor leraren", and he started his PhD research in the Department of Chemical Engineering and Chemistry at Eindhoven University of Technology, under the supervision of prof. dr. J. Meuldijk. During his PhD project, he completed the advanced course "Molecular Affinity Separations" organized by OSPT. Besides this course, Jack successfully completed the postgraduate course Module A (Polymer Chemistry) of the National Dutch Graduate School of Polymer Science and Technology (PTN). The results of his PhD study are described in this thesis and published in peer-reviewed scientific journals.